REGULATION OF PROGRAMMED CELL DEATH AND LIPID DROPLET FORMATION BY CTP:PHOSPHOCHOLINE CYTIDYLYLTRANSFERASE ALPHA (CCTα)

by

Adam J. Aitchison

Submitted in partial fulfilment of the requirements
for the degree of Master of Science

at

Dalhousie University
Halifax, Nova Scotia
August 2014

DEDICATION PAGE

This work is dedicated to my parents, Anne and James and to my sister, Amanda for their unwavering support and encouragement after all these years. Thank you.

TABLE OF CONTENTS

LIST OF FIGURES

ABSTRACT

Phosphatidylcholine (PtdCho), the most abundant phospholipid in eukaryotic cell membranes, is synthesized by the CDP-choline pathway under the control of the rate-limiting nuclear enzyme CTP:phosphocholine cytidylyltransferase (CCT)α. Increased production of PtdCho is often observed in tumours and during the formation of lipid droplets (LDs). To understand how CCTα regulates PtdCho synthesis during LD formation and apoptosis, we examined its activity, cellular localization, phosphorylation and association with membranes. Using caspase 3-replete MCF7 cells, we showed that CCTα is cleaved by caspase 3 and released from the nucleus during apoptosis. However, inhibition of high-affinity choline transport was the mechanism for inhibition of PtdCho synthesis during apoptosis in MCF7 cells and during anoikis in intestinal epithelial cells (IEC-18). During detachment of anoikis-resistant Ras-transformed IEC-18 (IEC-Ras) from an extracellular matrix (ECM), CCTα activity and PtdCho synthesis were increased, with no change in enzyme localization. PtdCho synthesis is also required for LD biogenesis which involves targeting CCTα to the phospholipid surface. CCTα-GFP was previously shown to localize to the surface of expanding LDs in *Drosophila* S2 cells, but localization of endogenous CCTα in mammalian cells was not reported. In oleate-treated cells and differentiating 3T3-L1 preadipocytes, endogenous and V5-tagged CCTα localized to the nuclear envelope and cytoplasm, whereas CCTα-GFP localized to the surface of LDs in IEC-18. Silencing CCTα resulted in larger LDs and sensitized IEC-18 to oleate-induced toxicity, indicating an important role for cytoplasmic and nuclear CCTα in LD formation. I conclude that CCTα activity is regulated through changes in nuclear and cytosolic distribution that control PtdCho synthesis during apoptosis and LD formation.

LIST OF ABBREVIATIONS USED

ACL	ATP citrate lyase
APAF-1	Apoptosis protease activating factor-1
APC	Adenomatous polyposis coli
BHD	Bcl-2 homology domain
BSA	Bovine serum albumin
CARD	Caspase activation and recruitment domains
C/EPT	Choline/ethanolamine phosphotransferase
CCT	CTP:phosphocholine cytidylyltransferase
CHO	Chinese hamster ovary cells
CHO-MT58	CHO cells expressing thermolabile CCTα
CHT	High affinity choline transporter
CTL1	Choline-like transporters
CK	Choline kinase
CL	Cardiolipin
CMT	Camptothecin
CTP	Cytidine-5'-triphosphate
Cyt *c*	Cytochrome C
DAG	Diacylglycerol
DED	Death effector domain
DGAT	Diacylglycerol acyltransferase
DTT	Dithiothreitol
DMEM	Dulbecco's Modified Eagle's medium
DPH	Diphenylhexatriene
DPM	Disintegrations per minute
ECM	Extracellular matrix
EDTA	Ethylenediamine tetraacetic acid
EGFR	Epidermal growth factor receptor
ER	Endoplasmic reticulum
ERK	Extracellular signal regulated kinase
FADD	Fas-associated death domain
FAK	Focal adhesion kinase
FASN	Fatty acid synthase
FOH	Farnesol
GAP	GTPase activating protein
GDP	Guanosine 5'-diphosphate
GEF	Guanine nucleotide exchange factor
GFP	Green fluorescent protein
GPC	Glycerophosphocholine
GTP	Guanosine 5'-triphosphate
HC-3	Hemicholinium-3
HEK	Human embryonic kidney
IBMX	Isobutylmethylxanthine
IEC	Intestinal epithelial cell
IEC-Ras	Ras transformed intestinal epithelial cell
IMM	Inner mitochondrial membrane

INM	Inner nuclear membrane
IRE1α	Inositol Requiring Enzyme 1 alpha
LD	Lipid droplet
LSC	Liquid scintillation counter
MAPK	Mitogen activated protein kinase
mRNA	Messenger RNA
NA	No addition
NE	Nuclear envelope
NLS	Nuclear localization signal
NPC	Nuclear pore complex
NR	Nucleoplasmic reticulum
OCTs	Organic cationic transporters
OCTNs	Organic cationic/carnitine transporters
OMM	Outer mitochondrial membrane
ONM	Outer nuclear membrane
PBS	Phosphate-buffered saline
PDI	Protein disulfide isomerase
pChol	Phosphocholine
PtdCho	Phosphatidylcholine
PtdEtn	Phosphatidylethanolamine
PtdIns	Phosphatidylinositol
PtdOH	Phosphatidic acid
PtdSer	Phosphatidylserine
PEI	Polyethyleneimine
PEMT	Phosphatidylethanolamine-N-methyltransferase
PDGF	Platelet-derived growth factor
PKC	Protein kinase C
PLA/B/C/D	Phospholipase A/B/C/D
PM	Plasma membrane
PDI	Protein-disulfide isomerase
RTK	Receptor tyrosine kinase
SDS-PAGE	Sodium dodecyl sulfate polyacrylamide gel electrophoresis
SEM	Standard error of the mean
shNT	Non targeting short hairpin RNA
SP	Sea plaque agarose
Sp1/2/3	Specificity protein 1/2/3
SRE	Sterol response element
SREBP	Sterol regulatory element binding protein
TAG	Triacylglycerol
TBS	Tris-buffered saline
TNF	Tumour necrosis factor
TLC	Thin layer chromatography
UPR	Unfolded protein response
VLDL	Very low density lipoprotein
VSVG	Vesicular stomatitis virus glycoprotein
XBP	X-box protein

ACKNOWLEDGEMENTS

This work could not have been possible without the help and assistance of several groups. Specifically, I would first like to thank my supervisory members, Drs. Catherine Too and Kirill Rosen for their excellent comments, suggestions and criticisms towards my project. Additionally, I would like to thank all the members of the Atlantic Research Centre for their insightful comments and sharing of lab equipment. Particular mention goes towards Bob Zwicker and Rob Douglas for their excellent and consistent maintaining of cell cultures in addition to their technical expertise. To the members of the Ridgway Lab past and present: I thank you for your untiring support and enthusiasm (even though I probably annoyed you most of the time)!

This work was funded by an operating grant from the Canadian Institute for Health Research (CIHR).

Finally I would like to thank Dr. Neale Ridgway for consistently raising the bar and pushing me to do my very best. I truly appreciate the patience, input and criticisms over the last three years in the lab, which allowed me to develop a true appreciation for scientific research.

CHAPTER 1: INTRODUCTION

1.1 Phosphatidylcholine Synthesis and Function in Eukaryotes

1.1.1 Phospholipid Structure and Function

Lipid membranes are complex biological structures that separate intracellular compartments from one another and function as a barrier to the external environment [1]. Biological membranes are not rigid, rather existing as a fluid mosaic consisting of proteins, phospholipids, sphingolipids, glycolipids and cholesterol arranged in a bilayer structure [2]. The major phospholipids in eukaryotic membranes are phosphatidylcholine (PtdCho), phosphatidylethanolamine (PtdEtn), phosphatidylinositol (PtdIns), phosphatidylserine (PtdSer) and cardiolipin (CL), with the concentrations of each varying between membranes and each affecting membrane structure and function [3]. For example, PtdEtn, which composes up to 25% of total membrane mass, adopts a conical shape and induces negative curvature as a result of its small head group [4]. PtdSer, which composes less than 5% of total membrane mass, has an important role in apoptosis (discussed in Section 1.4.1) [5]. PtdIns, which composes 5 to 15% of total membrane mass, is phosphorylated at the 3', 4' or 5' positions of the inositol ring to give rise to a variety of PtdIns-derived phospholipids each with specialized functions [6]. For example, Golgi-localized phosphatidylinositol 4-phosphate (PI4P) recruits proteins involved in Golgi trafficking and promotes anterograde transport of secretory proteins [7]. In the inner mitochondrial membrane (IMM), CL composes up to 20% of total membrane mass and is required for oxidative phosphorylation [8]. Additionally, CL has a role in apoptosis (discussed in Section 1.4.1) [9].

PtdCho is the most abundant phospholipid in eukaryotic cell membranes, composing up to 40-60% of total membrane mass [10]. PtdCho is composed of two fatty acyl groups esterified at the *sn-1* and *sn-2* positions and a phosphocholine (pChol) head group esterified at the *sn-3* position of glycerol. The cylindrical shape of PtdCho promotes planar lateral packing, resulting in increased membrane stability and rigidity [11]. In addition, PtdCho is an important component of lung surfactant, lipoproteins and lipid droplets (LDs) (discussed in Section 1.5). PtdCho is also a source of signalling molecules released by different phospholipases. For example, PtdCho hydrolysis by phospholipase A_2 (PLA_2) yields arachidonic acid, an important precursor for the synthesis of proinflammatory leukotrienes and prostaglandins [12] and PtdCho hydrolysis by phospholipase C (PLC) yields diacylglycerol (DAG), a potent recruiter and activator of protein kinase C (PKC) [13]. Finally, PtdCho hydrolysis by phospholipase D (PLD) yields phosphatidic acid (PtdOH), a precursor for other bioactive lipids [14], a promoter of membrane curvature [15] and inducer of inflammation through activation of both mTOR and JAK/STAT pathways [16].

1.1.2 Phosphatidylcholine Synthesis

In eukaryotes, PtdCho is synthesized by the PtdEtn *N*-methyltransferase (PEMT) and CDP-choline pathways. The PEMT pathway is the major route for PtdCho synthesis in hepatocytes (30%) and involves three successive methylations of the amino head group of PtdEtn using S-adenosylmethionine (AdoMet) and is the only route for *de novo* synthesis of choline in eukaryotes [17]. As a result, *PEMT*$^{-/-}$ mice are unable to synthesize PtdCho via the PEMT pathway but are viable if the diet is supplemented with choline. On the other hand, *PEMT*$^{-/-}$ mice fed a choline-deficient diet had a 50%

decrease in very low density lipoprotein (VLDL) and bile secretion from the liver and the mice developed severe steatosis and steatohepatosis (fatty liver) followed by death after 5 days [18-20]. Other tissues have low PEMT activity relative to the liver (~2%); however, the role of PEMT in non-hepatic tissues is not clear [21]. Interestingly, PEMT expression and activity were increased in non-small-cell lung cancers and predicted a reduced median survival time [22].

The second pathway for PtdCho synthesis is by the CDP-choline pathway and is the only route for *de novo* synthesis of PtdCho in eukaryotic cells [23]. This pathway is predominant in all eukaryotic cells, including hepatocytes. The PtdCho produced by the PEMT and CDP-choline pathways is different with respect to length and saturation. For example, the PEMT pathway produces mainly PtdCho with long-chain unsaturated fatty acids, such as those found in secreted lipoproteins, whereas PtdCho synthesized through the CDP-choline pathway produces medium-chain length saturated fatty acids predominantly found in biological membranes [24]. Although the PEMT pathway is important, the focus of this thesis is on the CDP-choline pathway because it is the predominant pathway for *de novo* synthesis of PtdCho in mammalian cells. A schematic of the CDP-choline pathway, including the cofactors, enzymes and localization is shown in **Figure 1.1**. The role of each enzyme is described in Section 1.2

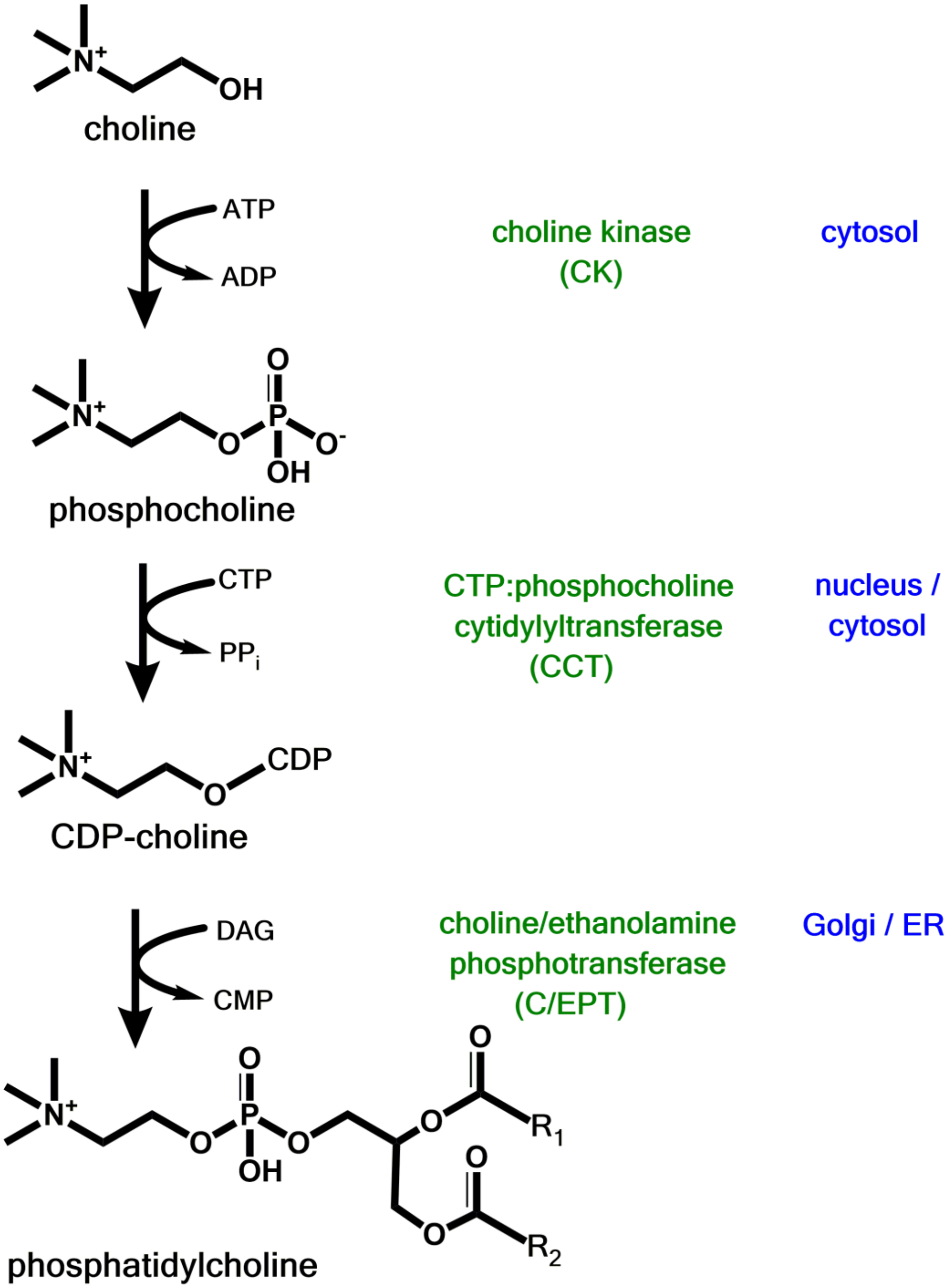

Figure 1.1. Synthesis of PtdCho by the CDP-choline pathway. Schematic of the CDP-choline pathway showing intermediates and products with enzymes and their subcellular localization indicated. Fatty acyl chains are indicated by R_1 and R_2.

.

1.2 Enzymes of the CDP-choline pathway

1.2.1 Choline Transporters

Eukaryotic cells (except hepatocytes) lack the capacity to synthesize choline *de novo* and therefore must absorb choline from the diet through facilitated transport [25]. There are three main types of choline transporters with a range of affinities. The first are the high-affinity choline transporters (CHT) that have a K_m for choline of less than 10 μM [26]. CHTs are sodium-dependent, sensitive to competitive inhibition by the choline analogue hemicholinium-3 (HC-3) and are highly expressed on pre-synaptic neurons where they mediate the uptake of choline for the synthesis of the neurotransmitter acetylcholine [27,28].

The second group of choline transporters are the low-affinity organic cation transporters (OCT) and organic cation/carnitine transporters (OCTNs). OCTs and OCTNs are sodium-independent and are insensitive to inhibition by HC-3 [29]. In terms of tissue distribution, OCT1 is expressed primarily in the liver, OCT2 is almost exclusively expressed in the kidneys and brain and OCT3 is highly expressed in the placenta, intestine, heart and, to a lesser extent the brain [30-32]. Whether or not the OCTs play a physiological role in the uptake of choline is not definitively known. In human embryonic kidney cells (HEK 293), OCT1 but not OCT2 transported choline [33]. OCT2 transports other polyamines involved in neurotransmission such as spermidine and may be involved in the modulation of inward-rectifier (Kir) potassium channels [34]. OCT3 is not a transporter of choline as incubation with increasing concentrations of choline did not inhibit transport of [^{14}C]guanidine into HeLa cells, but is required for histamine uptake into astrocytes [35,36].

As opposed to CHTs, choline-like transporters (CTLs) are the major transporters involved in PtdCho synthesis [29]. There are 5 known CTL genes with extensive alternative splicing, however the most prominent and well-characterized member with respect to choline uptake is CTL1 (SLC44A1) [37]. CTL1 has intermediate-affinity for choline (K_m of approximately 70 μM), is sodium-dependent and partially sensitive to inhibition by HC-3 [38]. CTL1 is ubiquitously expressed and is hypothesized to be the major CTL transporter involved in PtdCho synthesis. Overexpression of CTL1 in Cos-7 cells caused a 3-fold increase in choline uptake, however the effect on PtdCho synthesis was not investigated [39]. Additionally, treatment with glucocorticoids such as dexamethasone resulted in increased CTL1 mRNA expression accompanied by a concomitant increase in PtdCho synthesis [40]. Interestingly, treatment with the epidermal growth factor receptor (EGFR) antagonist gefitinib inhibited CTL1 directly in rat ATII alveolar cells, decreased PtdCho synthesis and compromised lung surfactant production [41]. Taken together, these results suggest that CTL1 is an important choline transporter and is indispensable for PtdCho synthesis.

1.2.2 Choline Kinase (CK)

The first committed step of the CDP-choline pathway is the phosphorylation of choline to form pChol by the cytosolic enzyme choline kinase (CK). There are two human CK genes (*CKA* and *CKB*) giving rise to three isoforms (CKα1, CKα2 and CKβ) [42]. The tissue distribution of all three isoforms is ubiquitous, but with significantly higher expression of murine CKα protein (both isoforms) in the liver and testes and higher expression of CKβ protein in the heart and liver [43]. In most tissues, CK is a dimer consisting of either α/α or β/β homodimers that contribute 40% of total CK activity or α/β heterodimers that contribute 60% of total CK activity [42].

In addition to its role in PtdCho synthesis, CK has been implicated in mitogenic signaling. Stimulation of cells with platelet-derived growth factor (PDGF) increased the expression and activity of CK, leading to an accumulation of pChol [44]. Moreover, addition of exogenous pChol in the absence of growth factors was sufficient in promoting DNA synthesis and subsequent cell division [44]. Since cancer cells have sustained mitogenic signalling, it is not surprising that CK expression and activity are often increased in a variety of tumour tissues and cells (Section 1.3.8) [45].

Although CK is not the rate-limiting step of the CDP-choline pathway, it is still unequivocally important for normal development and survival. Homozygous knockout of CKα was embryonic lethal in mice, while heterozygous knockout did not significantly affect PtdCho levels [46]. On the other hand, homozygous knockout of CKβ resulted in viable offspring, but caused a severe form of muscular dystrophy as well as bone deformities [47].

1.2.3 Choline/Ethanolamine Phosphotransferase

The last step of the CDP-choline pathway is catalyzed by the Golgi-localized choline phosphotransferase (CPT) or the ER-localized choline/ethanolamine phosphotransferase (CEPT), which are encoded by separate genes that share 60% sequence similarity [48]. CEPT and CPT are ubiquitously expressed; however CEPT is most abundant in the testis, colon, heart, intestine and spleen [49]. Both isoforms are predicted to contain 7 transmembrane segments and an α-helix near the catalytic domain that may function in DAG and CDP-alcohol recognition and binding [50]. Interestingly, although the catalytic domains of each isoform share near identical sequence similarity, CPT recognizes only CDP-choline, whereas CEPT recognizes CDP-ethanolamine and CDP-choline [51]. The reason for this dual specificity and redundant activity is not clear, but may involve generation of tissue-specific species of PtdCho. ER-localized CEPT is thought to be the main isoform involved in PtdCho synthesis since the rate-limiting enzyme of the CDP-choline pathway, catalyzed by CTP:phosphocholine cytidylyltransferase (CCT) translocates to ER membranes upon activation (discussed in Section 1.2.4). Interestingly, the production of sphingomyelin (SM) by SM synthase I in the Golgi produces DAG as a by-product and Golgi-localized CPT may function to attenuate DAG levels by converting it to PtdCho, preventing DAG-induced formation of COPI vesicles involved in the Golgi-to-ER secretory pathway [52]. Under normal circumstances, CEPT and CPT are not rate-limiting but have the potential if DAG is restricted [53]. In agreement to this, overexpression of CEPT and CPT did not increase total PtdCho mass [54].

1.2.4 CTP:Phosphocholine Cytidylyltransferase alpha (CCTα)

1.2.4.1 Domain Structure and Tissue Expression of CCTα

Two CCT isoforms (CCTα and CCTβ) are encoded by *Pcyt1a and Pcyt1b,* respectively [55]. CCTα has four distinct domains; a nuclear localization sequence (NLS), an α-helical membrane binding domain, a catalytic domain and a phosphorylation domain **(Fig 1.2)**. CCTα and CCTβ share high sequence similarity between amino acids 73 and 323, corresponding to the membrane binding and catalytic domains [56]. *Pcyt1b* is alternatively spliced, resulting in three major isoforms of CCTβ, all of which lack the

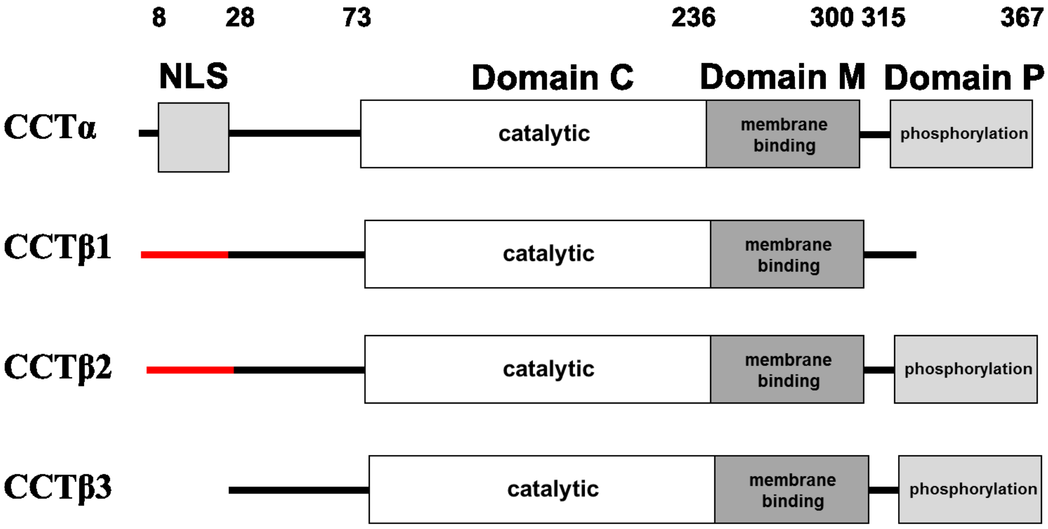

Figure 1.2: Domain structure of CCTα isoforms. CCTα isoforms have the following domains: nuclear localization signal (NLS), catalytic domain (Domain C), membrane binding domain (Domain M) and phosphorylation domain (Domain P). CCTβ isoforms lacks an NLS and CCTβ1 and CCTβ2 contain a unique N-terminal sequence compared to CCTα (denoted by red line). The position of amino acids within the structure are indicated.

N-terminal domain found in CCTα. CCTβ2 contains a unique N-terminal sequence and CCTβ3 is identical to CCTβ2 but lacks the first 28 amino acids [57]. Interestingly, hetereozygous CCTα knockout mice are viable and *Pcyt1b* transcript levels are increased suggesting that CCTβ may be able to compensate for loss of CCTα [55,58]. Decreased mRNA expression of CCTβ resulted in reduced growth and proliferation of rat adrenal medulla PC12 cells [59]. Moreover, *Pcyt1b*$^{-/-}$ mice had reduced fertility [60]. Although CCTβ is important for proper development, the remainder of this thesis is focused on CCTα.

CCTβ is expressed in certain tissues like the gonads and is developmentally regulated [57]. On the other hand, CCTα is required for PtdCho synthesis in all cells and has tissue specific functions in the lung and liver. In lung alveolar type II epithelial cells, CCTα is cytoplasmic and contributes to the production of dipalmitoyl-PtdCho that is incorporated into lung surfactant [61]. During murine fetal and neonatal lung development, both PtdCho synthesis and CCTα expression are upregulated to ensure adequate surfactant production [62]. Not surprisingly, the highest levels of CCTα mRNA were found in the alveolar cells and *Pcyt1a*$^{+/-}$ mice had decreased incorporation of PtdCho into lung surfactant [63]. Infection with *Pseudomonas aeruginosa* led to inhibition of CCTα activity directly and decreased PtdCho synthesis, resulting in compromised surfactant production and respiratory distress [64]. Lastly, inducible CCTα knockout resulted in normal epithelial cell development, but negatively impacted lung surfactant production, resulting in respiratory distress [64].

PtdCho is an important component of lipoproteins, such as VLDL and HDL, and CCTα is indispensable for assembly and secretion. Feeding mice a choline-deficient diet resulted in decreased VLDL secretion, suggesting that the PEMT pathway is unable to fully supply PtdCho for incorporation into lipoproteins [65]. Indeed, Cre/Lox-mediated deletion of CCTα resulted in a significant decrease in PtdCho synthesis with a concomitant decrease in both VLDL and HDL secretion [66]. Moreover, the plasma concentrations of triacylglycerides (TAG) and PtdCho were reduced, suggesting that PtdCho made by the CDP-choline pathway is required for proper delivery of TAG and cholesterol to peripheral tissues from hepatocytes [66].

1.2.4.2 The Nuclear Localization Sequence (NLS) of CCTα

The CCTα N-terminal domain (amino acids 8 to 28) contains a stretch of basic residues (RKRRK) that is sufficient to target reporter proteins, such as β-galactosidase to the nucleus [67]. In most cells, CCTα is localized to the nucleoplasm and is exported from the nucleus when activated by fatty acids such as oleate. However, CCTα is exclusively cytoplasmic in cells with high PtdCho demand such as differentiating B-cells where it is required for proliferation and class switch recombination [68]. The presence of an NLS increased affinity of CCTα for membranes, but did not contribute to CCTα activation [69]. Furthermore, Chinese hamster ovary (CHO) MT58 cells expressing a thermolabile CCTα (CHO-MT58) had decreased PtdCho synthesis and compromised growth when grown at the non-permissive temperature (40ºC), which was reverted upon re-expression of CCTα lacking an NLS [67]. The reason for nuclear localization of CCTα is unclear, as the NLS is not required for enzyme activity or PtdCho synthesis. It is possible that targeting CCTα to the nucleus is important for attenuating activity. This would suggest that export of CCTα from the nucleus is important for enzyme activation during periods of high PtdCho demand, such as during cell division.

The N-terminal domain of CCTα contains a putative caspase cleavage site at TEED↓G, the final residue of the NLS [70]. Induction of apoptosis with the isoprenoid farnesol (FOH) resulted in rapid activation of CCTα, characterized by translocation to the nuclear envelope, caspase cleavage to remove the NLS and export to the cytoplasm where it associated with cytoplasmic membranes [70,71]. Interestingly, caspase cleavage and removal of the NLS is not necessary for nuclear export of CCTα since mutagenesis of the TEED cleavage site still resulted in CCTα export upon FOH treatment [70]. There is a possibility that caspase cleavage of CCTα and nuclear export during apoptosis functions to exclude CCTα from the nucleus, where it may function independently of PtdCho synthesis, such as in formation of the nucleoplasmic reticulum (discussed in Section 1.3). Elucidating the role of caspase cleavage and export of CCTα from the nucleus during apoptosis and the resultant effect on PtdCho synthesis is one aim of my research and will be discussed in Section 1.4.10.

1.2.4.3 The Catalytic Domain of CCTα

The catalytic domain (amino acids 73 to 236) is highly conserved among mammalian CCTα [72]. CCTα is a homodimer and cross-linking experiments have mapped the site of dimerization to amino acids 139-145 [73]. Although the crystal structure of Domain C has not been solved, the tertiary structure was inferred by comparison to the related glycerol-3-phosphate cytidylyltransferase (GCT) found in bacteria, which has 60% sequence similarity to CCTα. Sequence comparison to GCT revealed a number of key motifs that are important for substrate binding and catalysis [74]. The conserved motif RTEGISTS is important since an R196K mutation significantly reduced both CTP binding and maximal activity (V_{max}) of the enzyme [75].

Also, the conserved motif HSGH is necessary for CTP binding as well as transition state stabilization [74]. Not surprisingly, mutations of either histidine in the HSGH motif resulted in ablation of CCTα activity. Lastly, the substrate pChol is recognized by Lys 122 and mutation to alanine resulted in an increased K_m for pChol [75].

1.2.4.4 The Membrane Binding Domain of CCTα

The membrane binding domain (amino acids 236 to 300) is a random coil that becomes α-helical when associated with membranes [76]. The 52 amino acid amphipathic α-helix contains primarily acidic residues on the polar face and 18 hydrophobic residues on the non-polar face that are hidden when the enzyme is inactive [77,78]. Upon CCTα association with membranes, the hydrophobic residues are exposed, which is facilitated by the relative composition of the membranes (**Fig 1.3)**. The insertion of domain M into membranes increases catalytic activity by approximately 80-fold, suggesting that binding of domain M to membranes results in a conformational change to the dimer interface that relieves autoinhibition of the catalytic domain [75]. The conformational changes resulting from membrane binding are thought to be the predominant mechanism for regulating CCTα activity. Domain M fused to a GFP reporter protein was sufficient for membrane recognition and binding in response to oleate treatment, suggesting that CCTα activity is modulated mostly through domain M interaction with membranes [79].

The binding of domain M to membranes is regulated by the composition and curvature of membranes. The many basic amino acids at the N-terminal section of domain M promotes electrostatic adsorption onto membranes enriched in anionic phospholipids or fatty acids [77]. On the other hand, DAG and unsaturated PtdEtn induce

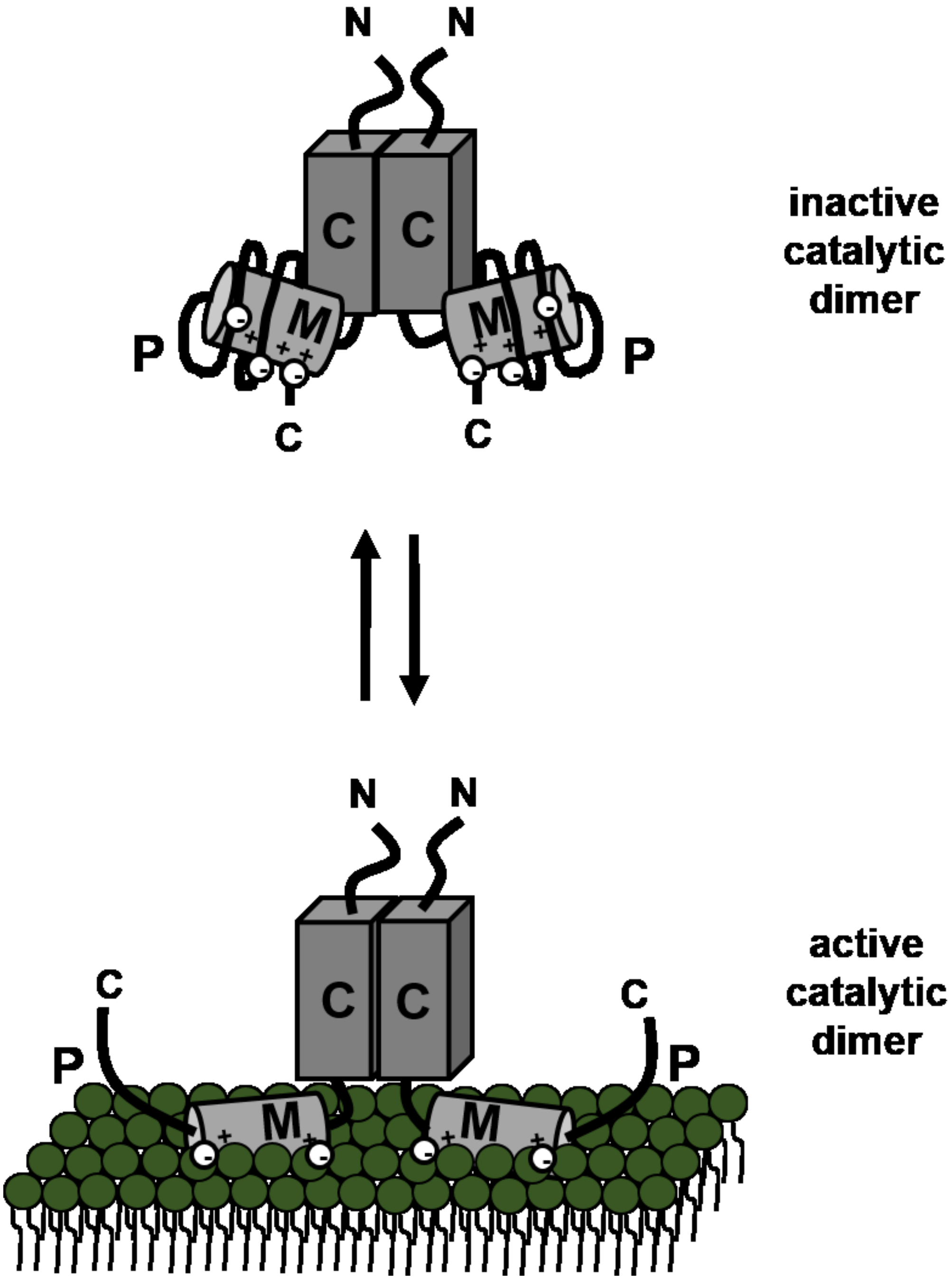

Figure 1.3: Mechanism for CCTα membrane binding and activation. CCTα exists as an inactive soluble form or a membrane bound active form. CCTα recognizes and preferentially binds via Domain M to membranes enriched in fatty acids, anionic phospholipids and negative curvature-inducing DAG and PtdEtn. Binding relieves auto-inhibition on the catalytic domain (C) activating the enzyme. In response to membrane translocation, domain P is dephosphorylated. Model is adapted from Northwood and Cornell [77].

negative curvature stress that is relieved upon domain M insertion into membranes [80]. DAG and fatty acids are generated through activation of phospholipases PLC and PLA_2, respectively, indicating an important role of phospholipases in mediating CCTα activation [53].

1.2.4.5 The Phosphorylation Domain of CCTα

The phosphorylation domain (amino acids 315 to 367) contains 16 putative serine phosphorylation sites [81]. Although it is not known exactly which kinases phosphorylate CCTα, it is a target for casein kinase II (CKII) and proline-directed kinases, such as cyclin dependent kinase 2 (cdk2) since 7 out of 16 serine residues are followed by a proline [82,83]. Other kinases, such as protein kinase C (PKC) and MAPK phosphorylate CCTα *in vitro* [84]. To coincide with the increased demand for PtdCho during S phase, CCTα is dephosphorylated during G1 phase and is more active. Conversely, when PtdCho demand is low during G0 and M phases, CCTα is heavily phosphorylated and is less active [85].

The correlation between phosphorylation status and membrane association of CCTα suggested that phosphorylation decreased the affinity of CCTα for membranes, however, dephosphorylation occurs after membrane binding [85]. To investigate the role of phosphorylation with respect to CCTα activity, different phosphomutants were analysed. A phosphomimetic mutant with all serines in Domain P mutated to glutamate associated with membranes suggesting that phosphorylation does not completely abolish membrane binding [81]. Moreover, a constitutively dephosphorylated mutant (16SA) had a 10-fold increase in membrane binding, but only a 2-fold increase in PtdCho synthesis suggesting that membrane binding does not result in full activation of the enzyme. The deletion of Domain P altogether resulted in a form of CCTα insensitive to lipid activators. However, phosphorylation may serve to increase the half-life of CCTα since the phosphomimetic mutant was more stable than the wild-type CCTα [81]. These results suggest that Domain P is involved in fine-tuning rather than dictating activity and in enzyme stability. An ‘electrostatic switching mechanism’ has been proposed where the negatively charged phosphates on Domain P compete with membrane anionic lipids for key interactions with the positively charged domain M and inhibit domain M insertion into membranes [86].

1.2.4.6 Transcriptional Regulation of CCTα

Changes in membrane composition and phosphorylation status are considered the predominant forms of CCTα regulation as these changes allow for rapid control of enzyme activity. On the other hand, CCTα is also regulated at the transcriptional level. For example, the transcription factors Sp1, Sp2 and Sp3 interact with cis elements in the promoter region of *Pcyt1a* [87]. Knockdown of Sp1 using siRNA resulted in decreased expression of CCTα [88] whereas phosphorylation of Sp1 by cAMP-dependent protein kinases and cdk2 during G1 and S phases of the cell cycle resulted in increased CCTα transcription and PtdCho synthesis [83]. Additionally, Sp1 is required for histone packaging of the *Pcyt1a* gene, as mutations in Sp1 decreased interaction with histone deacetylase (HDAC), repressing transcription of CCTα [89]. Sp3 increases CCTα expression in H-Ras transformed fibroblasts due to increased phosphorylation of Sp3 by p42/44 MAPK [90]. The connection between H-Ras transformation and increased CCTα expression is of particular interest in this study and will be discussed further in Section 1.4.8.

CCTα transcription is also activated by the sterol response element binding proteins (SREBPs). When sterols are depleted, SREBP is transported from the ER to the Golgi where it is cleaved by site 1 and site 2 proteases [91]. Proteolyzed SREBPs enter the nucleus where they activate many genes involved in lipid biosynthesis, such as fatty acid synthase (FASN), acetyl-CoA carboxylase and CCTα [92,93]. Although *Pcyt1a* has a sterol response element (SRE), SREBP is considered a poor activator of CCTα [93]. Rather, SREBPs are thought to increase CCTα expression and activity by the concurrent synthesis of anionic phospholipids and fatty acids, which are known potent activators of CCTα (discussed in Section 1.2.2.4).

Transcriptional regulation of CCTα is thought to provide a mechanism for responding to long-term changes in the demand for PtdCho, such as during growth and mitosis. During the G0 and G1 phases of the cell cycle, there is a rapid increase in PtdCho synthesis that is attributed to increased association of CCTα with membranes [94]. Moreover, increased PtdCho synthesis during G1 phase coincided with increased PtdCho turnover by activation of PLC and PLA_2, providing PtdCho-derived CCTα activators, such as fatty acids or DAG, necessary for progression through the cell cycle [94]. PtdCho synthesis continues to increase during S phase to ensure sufficient membranes for each daughter cell after mitosis. During further progression through the cell cycle, CCTα is phosphorylated and PtdCho synthesis is decreased during M phase [95].

It is thought that expression of CCTα is increased during the cell cycle to ensure sufficient CCTα for daughter cells rather than for increased PtdCho synthesis. Rather, changes in CCTα localization and membrane association during progression through the cell cycle is believed to be the main mechanism for CCTα activation and PtdCho synthesis. For example, during the G0 to G1 phase transition, CCTα is exported from the nucleus and binds to the NE and ER membranes and is dephosphorylated [94]. After rapid accumulation of PtdCho, the cell progresses through to the S and M phases and CCTα relocalizes completely to the nucleus and is phosphorylated [94]. Taken together, these results support a mechanism for controlling CCTα activity and PtdCho synthesis during cell cycle progression, mediated primarily by changes in localization and membrane association and fine-tuning of activity by changes in phosphorylation status.

1.3 The Role of CCTα in the Formation of the Nucleoplasmic Reticulum

The nuclear envelope (NE) is composed of an outer nuclear membrane (ONM) that is contiguous with the ER and an inner nuclear membrane (INM) with an underlying nuclear lamina enriched in intermediate filament proteins including lamin A/C [96]. Nuclear proteins, such as nucleoporins, and cytoskeletal components, such as actin are connected to the nuclear lamina and contribute to structural integrity and regulate DNA replication, cell division and chromatin organization [97,98]. Defects in lamina assembly are often caused by mutations in lamin-encoding genes and result in compromised nuclear stability, organization and function [99].

The NE contains a series of complex invaginations derived from ONM and INM called the nucleoplasmic reticulum (NR) and are found in almost all species [100]. There are two types of NR: type I involve invaginations of the INM, whereas type II involve invaginations of the INM and ONM [101]. Many proteins are found associated with the NR including lamins, nucleoporins and protein disulfide isomerase (PDI). The NR is thought to be involved in calcium signaling and to enhance the transport of material into the nucleus due to increased surface area [102,103]. During cell cycle progression, the NE changes in size and shape and is accompanied by expansion of the NR, extending the NE further into the nucleoplasm [104] and is coordinated with increased phospholipid synthesis for NE membranes.

Formation of the NR was shown to be dependent on CCTα activation. Activation of CCTα by oleate resulted in CCTα translocation to the NE followed by NR formation, whereas CHO-MT58 cells that express low levels of a temperature-sensitive CCTα had reduced NR formation [105]. Moreover, overexpression of CCTα resulted in increased production of type II NRs [106]. CCTα-dependent proliferation of the NR is thought to be the result of two mechanisms, either increased PtdCho synthesis or deformation of NR tubules by inducing positive membrane curvature. CCTα could be activated to supply PtdCho for NR proliferation, however catalytically dead CCTα mutants (H89G or K122A) still associated with the NE and caused proliferation of the NR [106]. CCTα-dependent proliferation of the NR also required expression of nuclear lamins. siRNA-mediated depletion of lamin A/C or lamin B1 disrupted NR formation but had no effect on PtdCho synthesis [107]. Additionally, CCTα mislocalized to non-NR structures in fibroblasts expressing a mutant form of lamin (progerin) and was associated with a 2-fold decrease in PtdCho synthesis. However, CCTα activity was unaffected, with the reduction in PtdCho synthesis attributed to inhibition of choline transporters [107].

These results implicate CCTα as having both catalytic and non-catalytic roles in the formation of NRs and expansion of the NE that requires cooperation with lamins.

1.4 Phosphatidylcholine and Apoptosis

1.4.1 Programmed Cell Death (Apoptosis) by Changes in Membrane Composition

Apoptosis is characterized by the coordinated targeting and cessation of key biochemical processes and is accomplished by a distinct family of cysteine-dependent aspartyl-specific proteases (caspases) that recognize a wide range of targets with crucial cellular functions (discussed in Section 1.4.2) [108]. An important determinant in the induction of apoptosis is the relative composition and distribution of membrane phospholipids. In non-apoptotic cells, the outer leaflet of the plasma membrane is largely composed of PtdCho and sphingomyelin [109] with the inner leaflet containing mostly PtdSer and PtdEtn [110]. This asymmetry relies on transport of PtdSer and other membrane phospholipids by glycerophospholipid transporters against a concentration gradient [109]. There are three major transporters: the flippases, the floppases, which are both ATP-dependent and the scramblases, which are ATP-independent. The flippases catalyze the movement of PtdSer from the outer to the inner leaflet, whereas floppases facilitate transport of PtdCho and PtdEtn from the inner to the outer leaflet [109]. The scramblases transport phospholipids between both bi-layers along a concentration gradient and are activated by increased intracellular calcium. As a result, PtdSer is externalized and acts as an “eat-me” signal for phagocytic cells [111]. PtdSer externalization precedes many other apoptotic events such as DNA fragmentation and membrane blebbing making it a good indicator of early apoptosis [112]. Additionally, thymocytes that do not recognize MHC class I or II or recognize self-antigens expose PtdSer on their surface and are subsequently targeted and destroyed indicating an important role for apoptosis in development [113].

Cardiolipin (CL) is enriched in the inner mitochondrial membrane (IMM) and regulates apoptosis by interaction with cyt *c* and facilitates electron transport between complexes III and IV [9]. One of the four acyl chains of CL is inserted into a hydrophobic channel within cyt *c* with the other acyl chains extending into the bilayer to anchor cyt *c* to the IMM [114]. Cyt *c* release from the mitochondria involves loss of CL interaction in addition to permeabilization of the outer mitochondrial membrane (OMM) by Bax or Bak [115]. This process is thought to involve CL peroxidation by reactive oxygen species (ROS) or by oxidative enzymes such as lipoxygenases [116]. In support of this, lipoxygenase activity was increased in response to ionizing radiation and growth factor withdrawal to induce apoptosis [117]. Additionally, it is suggested that Bcl-2 family members such as t-Bid may interact with CL directly for proper function affecting the release of cyt *c* from the mitochondria by a poorly defined mechanism [118]. Taken together, phospholipids such as PtdSer and CL have important regulatory roles in apoptosis by their effect on membrane composition.

1.4.2 Initiation and Execution of Apoptosis by Caspases

Caspases are a specific type of protease that once activated recognize a multitude of targets that proteolyze at specific residues to inhibit or activate the target [119]. There are two types of caspases, referred to as initiator and effector caspases that exist as inactive procaspases. The initiator caspases, which include caspases 2, 8, 9 and 10 contain two death effector domain (DED) repeats that are important for specific interactions with upstream activators and organizing scaffolds [120]. For example, activation of caspase 8 requires association with the upstream Fas-activating death domain (FADD) via the DED [120]. Initiator caspases also have a caspase activation and recruitment domain (CARD) that interacts with other CARD proteins. For example, activation of caspase 9 requires the formation of a complex with apoptosis protease activating factor (APAF)-1, mediated via CARD [121]. On the other hand, effector caspases, which include caspases 3, 6 and 7 cleave various cellular targets. Caspases 3 and 7 recognize regions of substrates, governed by the recognition site, and preferentially cleave after an aspartate residue [122]. However, specificity is not absolute, as effector caspases have broad specificity and recognize and cleave at many different cleavage sites with varying efficiencies [123].

Apoptosis can occur by intrinsic or extrinsic pathways. The intrinsic pathway is initiated in response to internal stimuli, such as DNA damage or toxins and is characterized by permeabilization of the mitochondria and release of cyt *c* [9]. The release of cyt *c* recruits APAF-1 and results in the formation of an apoptosome, which activates caspase 9, leading to activation of effector caspases, such as caspase 3 [121]. The extrinsic pathway is initiated in response to engagement of death receptors on the cell surface by death ligands, an example being FasL engaging with the Fas receptor. Activation of death receptors results in recruitment of FADD, which in turn recruits procaspase 8, forming the death-inducing signaling complex (DISC). This trimerization event results in caspase 8 activation, leading to activation of effector caspases [124].

Caspase activation is a tightly controlled process as unwarranted induction of apoptosis would be detrimental to otherwise healthy cells. To control these processes, anti-apoptotic proteins, such as Bcl-X_L, Bid and Bcl-2, interact with Bcl-2 homology domains (BHD) on proteins such as Bax and Bak, which are considered pro-apoptotic due to their ability to promote permeabilization of the mitochondria and release of cyt *c* [125,126]. It is not surprising that many tumours have increased expression and activity of anti-apoptotic proteins and decreased expression and activity of pro-apoptotic proteins. For example, expression of anti-apoptotic Bcl-2 is increased due to chromosomal rearrangement involving the enhancer region of the immunoglobulin heavy chain locus [127]. As a result, cancer cells do not readily undergo apoptosis in response to the appropriate stimuli, allowing them to proliferate and metastasize.

1.4.3 Mutations are a Driving Force in Tumour Formation

The transformation of a normal cell is a stepwise process that requires mutations in key signaling pathways involved in growth and survival. These mutations arise due to genomic instability, typically caused by a high rate of DNA damage which, if not repaired, leads to cellular transformation [128]. Mutations in genes that give rise to cancer can be classically divided into two types. Genes for which a gain-of-function mutation drives cancer formation are called proto-oncogenes and their constitutively active form are called oncogenes. Genes for which a loss-of-function mutation drives cancer formation are called tumour suppressor genes. Tumours are thought to arise through sequential accumulation of these oncogenic mutations [129]. For example, in colon cancer, an initial mutation in the adenomatous polyposis coli (APC) gene leads to hyperproliferation of epithelial cells, but is insufficient to cause tumour formation alone [130]. Rather, subsequent mutations in the proto-oncogene Ras (discussed in Section 1.4) and loss of the tumour suppressor p53 results in a hyperproliferative state characterized by aberrant growth and insensitivity to death signals [130,131]. As the cancer continues to grow, it destroys the basement membrane, leading to metastasis, a defining hallmark of aggressive cancers.

1.4.4 Anoikis: Detachment-Dependent Apoptosis

Epithelial cells grow as a monolayer attached to a complex network of proteins and polysaccharides called the extracellular matrix (ECM) also referred to as the basement membrane [132]. Moreover, when aged or damaged epithelial cells detach from the ECM, they undergo a type of apoptosis called anoikis (Greek for homelessness). Anoikis contributes to the maintenance of normal tissue architecture, allowing for the renewal of the epithelia [132].

There are many connections that occur between the cell and the ECM, with the most important being the integrins. Integrins are transmembrane adhesion receptors on epithelial cells that engage their ligand, such as fibronectin, laminin or vitronectin in a Ca^{2+} or Mg^{2+} dependent interaction [133]. Detachment of epithelial cells from the ECM results in disengagement of integrins, leading to changes in the activity of kinases such as Raf, MEKK3, p38, followed by changes in the expression and activity of downstream effectors involved in anoikis, such as Bax, Bcl-2 and FasL [134-136]. Overexpression of Bcl-2 blocked anoikis in detached cells, indicating that anoikis requires permeabilization of the mitochondria and release of cyt *c* [137]. In addition, loss of integrin interactions upon detachment triggers anoikis by upregulating Fas ligand in a p38 MAPK-dependent manner [134]. Since p38 is a downstream effector in the canonical Ras pathway, this implicates Ras in the anoikis response. Transformation of epithelial cells through constitutive activation of proto-oncogenes such as Ras results in a carcinogenic phenotype, characterized by insensitivity to anoikis, uncontrolled growth and proliferation and eventually metastasis [138].

1.4.5 Ras Proteins and Anoikis-Resistance

The proto-oncogene Ras (rat sarcoma) protein belongs to a superfamily of over 150 related proteins that share a similar function [139]. All Ras proteins are small GTPases whose activity is determined by whether GTP (active) or GDP (inactive) are bound. GTP or GDP binding is controlled by GTPase activating proteins (GAPs), which stimulate the hydrolysis of GTP and guanine exchange factors (GEFs), which stimulate the release of GDP to allow GTP to bind [140]. This cycle of activation and inactivation creates a molecular switch that regulates downstream proliferative signalling via Ras proteins. If a cell harbours mutations in Ras that prevent GTP hydrolysis, then proliferative signalling will persist even in the absence of a stimulus [141].

Three major H-Ras, K-Ras and N-Ras isoforms share the same overall functions, but differ in their tissue distribution [142,143]. For example, H-Ras protein expression is high in the brain, whereas K-Ras and N-Ras protein expression are high in the gut and thymus [144]. Homozygous knockout of K-Ras in mice was embryonic lethal, whereas N-Ras, or H-Ras knockout did not affect viability [145]. Not surprisingly, rat intestinal epithelial cells (IEC) that were transfected with a constitutively active form of H-Ras (IEC-Ras) acquired many hallmark characteristics of cancer cells, such as loss of contact inhibition, increased proliferation and resistance to anoikis [146].

Oncogenic H-Ras is known to block anoikis via several pathways involved in apoptosis and cell growth, including the phosphatidylinositol 3-kinase (PI3K)/AKT, focal adhesion kinase (FAK) and MAPK pathways [147,148]. The end result of H-Ras transformation is downregulation of pro-apoptotic proteins, such as Bim and upregulation of anti-apoptotic proteins, such as Bcl-X_L [149-151]. Additionally, cIAP2 and XIAP, which inhibit caspase activation are upregulated [152]. Finally, oncogenic Ras promotes proliferation of detached cancer cells by downregulating Beclin-1, which has been shown to block autophagy, leading to enhanced proliferation [153].

1.4.6 The Lipogenic Phenotype of Tumour Cells

A well-known perturbation of metabolism in cancer cells is the switch from oxidative phosphorylation of glycolysis-derived pyruvate to fermentation of pyruvate to sustain ATP production and regenerate NADH [154]. This phenomenon identified in 1956 is known as the Warburg effect and is characterized by a high rate of glucose uptake, followed by glycolysis and fermentation [154]. Tumours often rely on fermentation when they have outgrown their oxygen diffusion limit, and therefore must adapt to hypoxic conditions. To meet the increased glycolytic demand, cancer cells often have increased expression and activity of glycolytic enzymes, such as hexokinase and pyruvate kinase, which results from constitutive activation of the PI3K/AKT and Myc signalling pathways [155-157]. Pyruvate is decarboxylated to form acetyl-CoA and then condensed with oxaloacetate to form citrate in the mitochondria. Since citrate cannot enter the tricarboxylic acid cycle and undergo oxidative phosphorylation due to decreased oxygen availability or mitochondrial damage, it is shuttled into the cytoplasm and converted into cytosolic acetyl-CoA by the enzyme ATP-citrate lyase (ACL) [158,159]. This excess acetyl-CoA is a substrate for fatty acid synthase (FASN) the rate-limiting enzyme in fatty acid synthesis.

FASN catalyzes the formation of palmitate from acetyl-CoA and malonyl-CoA which is further modified by elongation, desaturation and acylation to form a wide range of lipids, including TAG, CL, PtdEtn and PtdCho [160-162]. Cancer cells have upregulation of key lipogenic enzymes involved in the synthesis of these complex lipids. For example, increased expression and activity of FASN is a direct result of activation by SREBP 1a and c, which are upregulated in certain cancers [163,164]. Inhibition of FASN with the pharmacological agent cerulenin (inhibits keto-acyl-ACP synthase moiety of FASN) resulted in the induction of apoptosis in human breast cancer cells either due to increased malonyl-CoA mass or decreased fatty acid oxidation [165]. FASN has many downstream targets, so it is imperative to determine whether apoptosis was a result of reduced incorporation of fatty acids into more complex lipids or an off-target effect.

1.4.7 The Role of PtdCho and Choline Metabolites in Cancer

Synthesis of phospholipids such as PtdCho is often increased in response to elevated levels of fatty acids as a result of higher FASN activity [166,167]. However, increased synthesis of PtdCho is often met with increased PtdCho degradation making comparison between PtdCho synthesis and increased FASN activity difficult. It follows that ablation of FASN activity would decrease the availability of fatty acids for incorporation into PtdCho and as a result total PtdCho mass would decrease. Silencing FASN by RNAi in human prostate adenocarcinoma LNCaP cells decreased PtdCho synthesis and total phospholipid mass [168]. Moreover, treatment of human breast ductal carcinoma MCF7 cells with cerulenin inhibited PtdCho synthesis [169]. These results suggest that increased PtdCho synthesis, due to increased activity of FASN is a determinant in the malignancy of cancer cells and tumours. Moreover, cerulenin-induced apoptosis could not be reversed by addition of exogenous fatty acids in human breast cancers, suggesting that these cancers rely heavily on *de novo* fatty acid synthesis [170].

The CDP-choline pathway is thought to play an important role in cancer cell biology, as cancer cells have increased demand of PtdCho for membranes and as a source of PtdCho-derived second messengers such as PtdOH [159,171,172]. To support this increased demand, levels of choline, pChol and PtdCho were found to be dramatically elevated in a variety of tumours as evidenced by NMR spectroscopy studies [173,174]. Increased synthesis of PtdCho in cancer cells is often coupled with increased degradation by phospholipases A_2 and C to sustain the production of DAG and PtdOH for mitogenic signalling [175-177]. Increased levels of choline metabolites in the CDP-choline pathway also suggests that the enzymes of the CDP-choline pathway are upregulated.

1.4.8 Enzymes of the CDP-Choline Pathway are Altered in Tumour Cells

Increased choline in cancer cells suggests potential upregulation of choline transporters to ensure a constant supply of choline for the CDP-choline pathway. CHT1 and OCT2 mRNA expression were increased in breast cancers, resulting in a 2-fold increase in saturable choline uptake [178]. Moreover, CTL1 and CTL2 mRNA expression were elevated in a wide range of other cancer cell lines, including MCF7 and SH-SY5Y [26,179]. Knockdown of *CTL1* in small-cell lung carcinoma was sufficient to block choline uptake and reduce cell growth, further suggesting the importance of choline transporters in cancer [179].

CK is universally upregulated in cancer cells as a direct result of oncogenic Ras signalling through the PI3K/AKT pathway [179]. In addition, the *CKA* promoter contains a hypoxia response element (HRE) that responds to HIF-1, a transcription factor that is active and binds under the low-oxygen conditions typically found in the tumour microenvironment [180]. Inhibition of the CK by pharmacological agents or lentiviral knockdown suppressed xenograft growth and induced apoptosis in breast cancer cells [181,182]. On the other hand, overexpression of CKα, but not the CKβ isoform, was sufficient to induce transcription of genes involved in the cell cycle, such as cyclins and those involved in proliferation in addition to downregulation of Bcl-2 [45,183]. The levels of pChol are increased in a wide variety of tumours, but whether the increased pChol is strictly required for PtdCho synthesis or has growth-regulating properties independent of PtdCho synthesis is still unclear [174]. For example, pChol has been shown to activate raf/MAPK and is indispensable for cell cycle progression [44].

The involvement of CEPT/CPT in cancer cell proliferation has not been extensively studied. However, CPT expression and activity are increased approximately 2-fold in breast carcinoma cells [184]. Depletion of CPT by RNAi resulted in the induction of apoptosis, but whether this was a result of reduced PtdCho is unknown [185]. Interestingly, treatment of MCF7 cells with the anti-mitotic drug docetaxel resulted in accumulation of CDP-choline and a concomitant decrease in PtdCho levels [186]. However, inhibition of the pathway was attributed to decreased levels of the substrate DAG, as opposed to direct inhibition of CPT.

CCTα protein expression is upregulated (up to 30-fold) in some cancer cells [187], however correlating an increase in CCTα protein expression with activity is difficult due to its complex post-transcriptional regulation. On the other hand, CCTα has been shown to have a non-catalytic function in establishing the architecture of the nuclear envelope in rapidly dividing cells and cancer cells have increased incidence of NRs [101,106]. Our lab has shown that IEC-18 cells stably transfected with oncogenic H-Ras (IEC-Ras) have increased expression of CCTα (30-fold) but with no change in activity when grown in monolayer [187]. However, IEC-Ras become resensitized to anoikis upon CCTα silencing, suggesting that CCTα plays a role in the anoikis response. Exactly *how* CCTα contributes to metastatic growth and anoikis-resistance of IEC-Ras is a focus of my research.

1.4.9 Disruption of PtdCho Metabolism During Apoptosis

The high demand for PtdCho by rapidly dividing cancer cells suggests that the CDP-choline pathway may be a target of apoptosis. Indeed, depriving PC12 cells of exogenous sources of choline, or inhibition of CKα by RNAi in HeLa cells resulted in reduced PtdCho synthesis and apoptosis [182,188]. Moreover, CPT inhibition by farnesol (FOH) through competing for DAG binding is sufficient to cause apoptosis [189-191]. However, overexpression of CPT does not rescue cells from apoptosis, bringing into question its exact role [191].

1.4.10 The Role of CCTα in Apoptosis

Ablation of the rate-limiting enzyme CCTα in CHO-MT58 cells resulted in reduced PtdCho synthesis and induction of apoptosis, which was preceded by growth arrest in G1 phase of the cell cycle [192]. Since the cell cycle is dependent on changes in CCTα localization and activity to sustain PtdCho synthesis, it makes sense that a reduction in CCTα expression could disrupt PtdCho homeostasis and cause apoptosis.

An early event in the induction of apoptosis is the recognition and cleavage of CCTα by caspases at the TEED motif resulting in the removal of the NLS [70]. Treatment with FOH resulted in caspase cleavage of CCTα, export from the nucleus, followed by binding to cytoplasmic membranes [70,192]. The contribution of NLS removal by caspases during apoptosis is unclear as a caspase-resistant form of CCTα was still exported and associated with membranes after FOH treatment [71]. Additionally, the cleaved and uncleaved forms of CCTα have similar *in vitro* activity suggesting that removal of the NLS may serve to prevent re-entry of CCTα into the nucleus during apoptosis [193]. siRNA silencing of caspases in HEK 293 cells showed that caspase 3 was involved in CCTα proteolysis. The first aim of my project investigated the role of caspase 3 in CCTα proteolysis and subsequent export of CCTα from the nucleus.

1.5 Phosphatidylcholine and the Formation of Lipid Droplets

1.5.1 Function and Composition of Lipid Droplets (LDs)

Fatty acids are highly reduced molecules that provide a source of energy when other energy sources have been depleted. However, fatty acids are hydrophobic and toxic, which necessitates a proper storage medium. This is accomplished by esterification of fatty acids to glycerol and cholesterol forming neutral TAG and cholesteryl esters (CE), respectively. Neutral lipids are then packaged into lipid droplets (LDs) which are surrounded by a phospholipid monolayer [194-196]. LDs are found in all eukaryotic cells, including yeast and some prokaryotes such as *Mycobacterium* sp [197]. In addition to providing a source of energy, LDs provide materials for membrane synthesis, are involved in protein trafficking and provide substrates for steroid hormone synthesis and other lipid-derived signaling molecules [198,199]. Although LDs are important for cell survival, accumulation has been linked to many metabolic diseases, such as type II diabetes, obesity and atherosclerosis [200].

1.5.2 Formation and Expansion of LDs

The basic processes that constitute LD formation are poorly understood but is thought to involve the ER. There are currently two proposed models for the synthesis of LDs. In the first model, accumulation of neutral lipids occurs between the luminal and cytosolic leaflets of the ER forming an oil 'lens' or a 'blister' [201]. Many of the enzymes involved in neutral lipid synthesis, such as diacylglycerol acyltransferase (DGAT) are ER-localized [202]. Further neutral lipid accumulation results in budding from the ER, forming a nascent LD comprised solely of the ER-cytosolic monolayer. The mechanism governing LD budding is thought to be a spontaneous process when sufficient neutral lipids have accumulated that surface tension is minimal [203]. In the second model, the entire lipid lens is excised from the ER membrane, with no budding event, forming a nascent LD comprised of the ER-cytosolic and -luminal bilayers [204]. However, this second model is inconsistent with ER integrity, as excision would result in the formation of a pore [205]. A point of contention is whether LDs completely detach from ER membranes or remain associated via specialized membrane contact sites. Freeze-fracture micrographs show that mature LDs surround and remain in close apposition with ER membranes similar to ER-mitochondria membrane contact sites [206]. The presence of these contact sites provides a potential route for protein and lipid transfer between the LDs and the ER. Additional routes for LD growth involve localized synthesis of lipids at nascent LDs or coalescence (fusion) of smaller LDs.

1.5.3 Protein Targeting to LDs

LDs are dynamic structures that recruit various proteins involved in both LD formation and maturation. For example, perilipins coat the LDs in adipocytes, acting as a protectant against hormone-sensitive lipases [207]. Phosphorylation of perilipin by protein kinase A causes the neutral lipid core to become exposed to lipases and to allow breakdown of TAGs [208]. Proteins typically involved in vesicle trafficking also localize to LDs. For example, Arf1/COP1 machinery localizes to LDs and is required for formation of ER membrane-LD contact sites and for budding, as well as subsequent recruitment of specific TAG synthesis enzymes, such as glycerol-3-phosphate acyltransferase 4 (GPAT4) [198,209,210]. Proteins involved in eicosanoid synthesis, such as 5-lipoxygenase were shown to localize to the surface of LDs. Production of eicosanoids results in inflammation, which is implicated in metabolic syndrome and cancer [211]. Since LDs contain a phospholipid monolayer instead of a bilayer typically found in other biological membranes, transmembrane proteins are suggested to not bind to LDs due to the potential orientation of hydrophilic loops in the hydrophobic core [194]. However, multi-pass proteins are present in the LD proteome, suggesting that these proteins may in fact bind to the surface of LDs or perhaps bind the adjacent ER membranes [212]. Moreover, proteins such as DGAT2 bind LDs via a hydrophobic hairpin domain [213]. Finally, proteins with amphipathic helices that bind to phospholipid bilayers may also bind monolayers [194]. Exactly how these proteins differentiate between mono- and bi-layers is unknown, but may involve changes in LD composition.

1.5.4 Phospholipid Synthesis for LDs

An increase in LD volume is met with expansion of the phospholipid monolayer. Although LDs are thought to originate from the ER, the fatty acid and phospholipid composition is unique [214]. The predominant phospholipids in mammalian LDs are PtdCho (60%) and PtdEtn (25%) and to a lesser extent, PtdOH and PtdIns, however in *Drosophila,* PtdEtn is the most abundant phospholipid in LD monolayers [202]. In addition to providing structure, LD phospholipids have other roles. For example, lipin-1 dephosphorylates PtdOH forming DAG, also localizes to the surface of LDs and is required for formation of mature LDs in 3T3-L1 preadipocytes by controlling ER budding [215,216]. Moreover, PtdCho is important for phase stabilization to prevent coalescence of smaller LDs [217,218]. Mature LDs do not readily exchange membrane phospholipids with other membranes via vesicular transport [219-221]. Therefore, growing LDs must rely on other pathways for phospholipid synthesis and remodelling during expansion of the surface monolayer. As previously suggested, formation of membrane contact sites with other organelles provides a potential source for newly synthesized phospholipids and for fast exchange of phospholipids by lateral diffusion [222]. Alternatively, protein-mediated transport could be involved in delivering phospholipids to LDs, but this route is hypothesized to be insufficient to meet the high demand for phospholipids by rapidly growing LDs [223]. Therefore, the likely pathway involved is localized synthesis of phospholipids at or in close proximity to growing LDs.

In support of this, enzymes involved in phospholipid synthesis and remodelling localize to the surface of growing LDs such as lysoPtdCho acyltransferase 1 (LPAT1) [214]. Moreover, PEMT localizes to the surface of LDs during adipocyte differentiation where it converts PtdEtn to PtdCho. PEMT knockdown in 3T3-L1 preadipocytes resulted in decreased LD formation and stability, suggesting that the PEMT pathway is necessary for expanding LDs [224]. However, PEMT expression is low in most non-hepatic tissues, suggesting that the PEMT pathway is insufficient to provide the bulk of PtdCho for expanding LD monolayers [21].

A previous genome-wide siRNA screen found that knockdown of many lipid biosynthetic enzymes resulted in aberrant LDs, characterized by increased LD size and coalescence [225]. Among the strongest phenotypes were knockdown of FASN and SREBP, which were previously discussed with respect to their role in fatty acid and sterol synthesis. Knockdown of either CK or CCTα resulted in coalescence of smaller LDs, suggesting that the CDP-choline pathway has an important role in providing PtdCho for LD membranes [225].

1.5.5 The Role of CCTα in LD Formation

In response to stimulation by fatty acids such as oleate, CCTα is exported from the nucleus where it activated upon association with cytoplasmic membranes. CEPT is the last step of the CDP-choline pathway and is ER-associated, suggesting that CCTα may also function at the ER to provide CDP-choline in close proximity to CEPT **(Fig 1.4**). On the other hand, CCTα may localize to the surface of LDs, but CDP-choline would still need to go to the ER for conversion to PtdCho. To support the idea that CCTα localizes to the surface of LDs, decreased levels of PtdCho would make domain M binding and insertion into the surface of the LD favourable, relieving the auto-inhibitory constraint on the catalytic domain. This would allow CCTα to respond to changes in

PtdCho composition of LDs independent of the ER or other membranes. Krahmer et al. showed that CCTα-GFP localizes to LDs and binds stably in response to oleate in *Drosophila* S2 cells, however, localization of endogenous CCTα in mammalian cell lines was not reported [218]. The third aim of my thesis investigates the role of endogenous CCTα during LD formation in mammalian cells.

1.6 Aims of This Study

Although my project seemingly involves different areas of focus, they are all related by the changes that occur with respect to CCTα expression, activity and localization during programmed cell death and LD formation.

1) How is the CDP-choline pathway targeted during camptothecin-induced apoptosis? Our lab has previously shown that caspase 3 is the major caspase involved in CCTα cleavage and export from the nucleus, however the functional significance of this event during apoptosis is still unclear. To address this, we monitored CCTα activity by the flux of choline through the CDP-choline pathway in MCF7 (which lack caspase 3) and MCF7 re-expressing caspase 3 (MCF7-C3) cells in order to compare caspase 3 –independent and –dependent apoptosis. In addition, choline transport and choline kinase activities were compared to investigate their role during apoptosis.

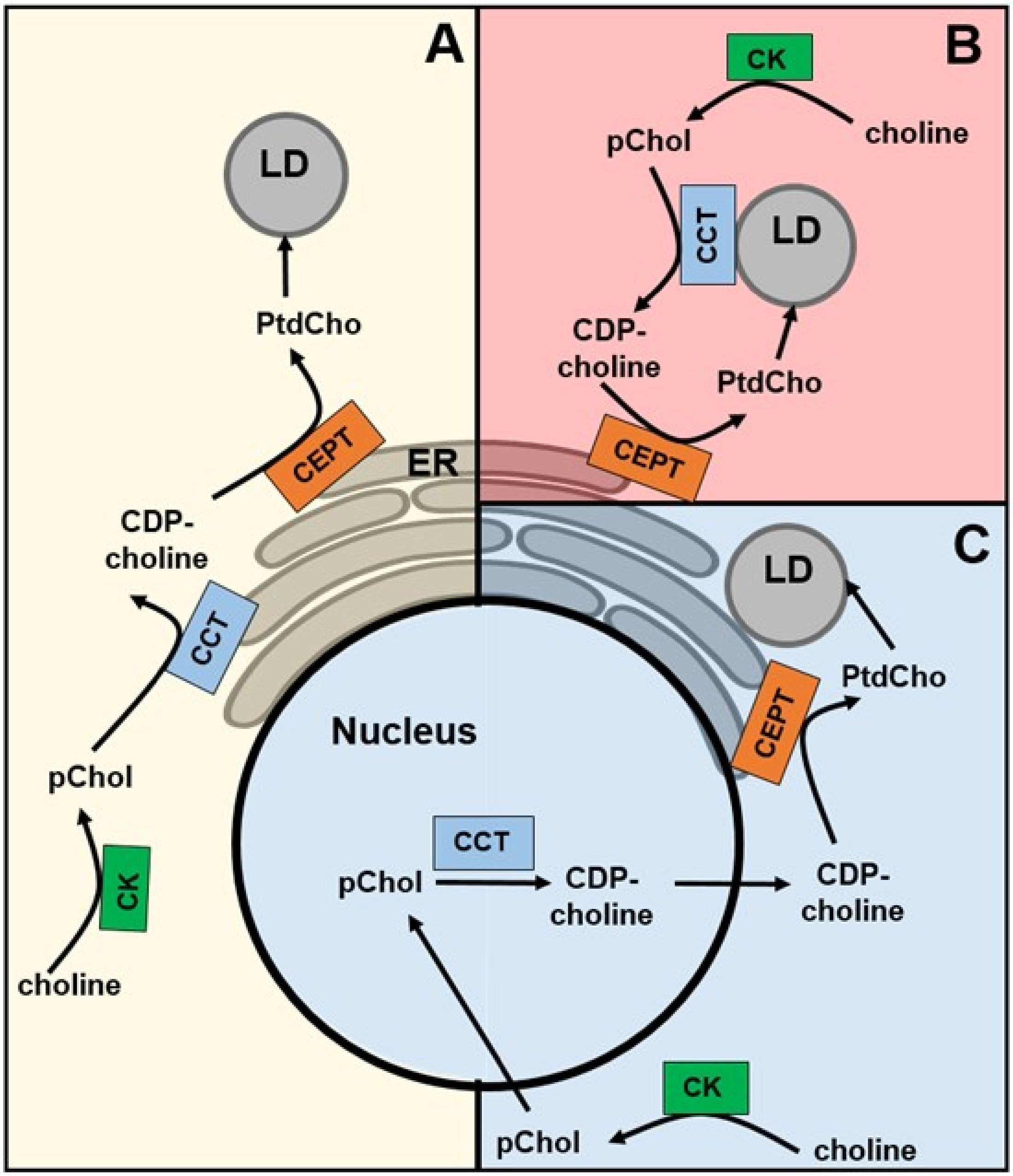

Figure 1.4 The role of the CDP-choline pathway, specifically CCTα, in the formation of LDs. LDs are thought to originate from within the ER bilayers and requires the synthesis of PtdCho for phospholipid monolayers. Choline is transported into the cell by choline transporters (not shown) and is phosphorylated by choline kinase (CK). The next step depends on the localization of CCTα. In one model, CCTα localizes to ER membranes, allowing coupling with CEPT **(A).** Conversely, CCTα may localize to LDs directly and function there **(B).** Alternatively, CCTα may function entirely within the nucleus, with substrates and products freely diffusing in and out of the nucleus **(C).** The last step is catalyzed by ER-associated CEPT. PtdCho can be added to forming LDs before or after budding from the ER.

2) How is CCTα involved in resistance to anoikis in IEC-Ras? Our lab has previously shown that CCTα expression is increased in IEC-Ras, but mostly as a nuclear inactive soluble form. CCTα silencing in IEC-Ras resulted in reduced clonogenicity when these cells were grown in detached conditions, suggesting that CCTα may be activated upon detachment in IEC-Ras, perhaps due to changes in localization and/or activity. My objective was to determine whether the localization of CCTα was changed in detached IEC-Ras and to find the cause of reduced clonogenicity in CCTα-silenced IEC-Ras. To investigate this, I looked at changes in caspase activation, as well as the induction of an ER stress response upon detachment from the ECM.

3) What is the role of CCTα during LD formation? The formation of an LD requires PtdCho in order to coat the enlarging phospholipid monolayer and requires the rate-limiting enzyme CCTα. Other labs have shown that CCTα localizes to the surface of LDs, but this phenomenon was not observed in preadipocytes or other mammalian cells. Possible explanations for this discrepancy include the use of fluorescently-labelled CCTα (GFP versus endogenous) and different host species (insect versus mammal). To investigate this, I looked for changes in endogenous CCTα localization in response to oleate treatment to induce LD formation in various cell lines. I also used tagged variants of CCTα (GFP, V5/His) to see whether this affected localization. Finally, I silenced CCTα in different cell lines and observed changes in LD formation and lipid dynamics.

CHAPTER 2: MATERIALS AND METHODS

2.1 Materials

Dulbecco's Modified Eagle Serum (DMEM), fetal bovine serum (FBS), Lipofectamine 2000 transfection reagent, Alexa-Fluor® 488 goat anti-rabbit, Alexa-Fluor® 594 goat anti-mouse secondary antibodies and antibiotics (carbenicillin, kanamycin, puromycin) were purchased from Invitrogen (Burlington, ON). Polybrene, diphenylhexatriene, poly-L-lysine, phosphomolybdate, stannous (II) chloride, mouse anti-β-actin monoclonal antibody, sodium oleate and lentiviral shRNA pLKO.1 plasmids (shNT and shCCTα) were purchased from Sigma-Aldrich (St. Louis, MO). Polyethyleneimine (PEI) was purchased from Polysciences (Warrington, PA). A rabbit polyclonal antibody against the C-terminal domain of CCTα was raised and purified by GenScript (Scotch Plains, NJ). [^{3}H]Choline chloride was purchased from Perkin-Elmer (Waltham, MA). Odyssey blocking buffer, nitrocellulose stripping buffer, IRDye® 800CW and 680LT secondary antibodies were purchased from LI-COR Biosciences (Lincoln, NE). Tween-20, TEMED, nitrocellulose membranes, glycine and acrylamide/bis solution (40%) were purchased from Bio-Rad (Hercules, CA). Bovine serum albumin (BSA) was purchased from Amresco (Solon, OH). Thin-layer chromatography (TLC) silica gel G plates were purchased from Analtech (Newark, NJ). Plasmid purification kits were purchased from Qiagen (Missisauga, ON). CellTiter 96 AQUEOUS Non-radioactive Cell Proliferation Assay was from Promega (Madison, WI). Complete EDTA-free protease inhibitor tablets were purchased from Roche Diagnostics (Indianapolis, IN). IRE1α, PDI primary antibodies were purchased from Cell Signalling

(Boston, MA). A Bip antibody was purchased from Enzo Life Sciences (Brockville, ON). Mowiol 4-88 was purchased from EMD Biosciences Inc (La Jolla, CA).

2.2 Cell Culture

All cells used in this study were maintained at 37ºC in a humidified 5% CO_2 atmosphere. IEC-18 and IEC-Ras34 were cultured in IEC-MEM (α-MEM containing FBS (5%), D-glucose (3.6 g/L), insulin (12.7 µg/mL), penicillin (600 µg/mL), streptomycin (100 µg/mL) and glutamine (2.9 mg/mL)). HEK 293, HEK 293T, J774A1 macrophages and 3T3-L1 preadipocytes were cultured in DMEM containing 10% FBS (CCL-107). MCF7 and MCF7 stably re-expressing caspase 3 (MCF7-C3) (provided by Dr. Daum Tang, McMaster University, ON) were cultured in CCL-107 containing puromycin (0.5 µg/mL)). Chinese hamster ovary (CHO) cells were cultured in CCL-107 containing proline (34 µg/mL). HepG2 cells were cultured in CCL-107 containing glutamine (2.0 mM).

2.3 Plasmid Transfection

CCTα-GFP and CCTα-V5/His were previously constructed in our lab. The V5/His-tagged CCTα was prepared by cloning the HindIII/XbaI fragment of rat CCTα cDNA from pCM5-CCT into HindIII/XbaI digested pCDNA3.1/V5His. The GFP-tagged CCTα was prepared by cloning the HindIII/SacII fragment from pCDNA3.1/V5His into pEGFP-N1 digested with HindIII/SacII. To prevent aggregation of GFP-fusion proteins, pEGFP-N1 had a single amino acid substitution (L221K) to create monomeric GFP.

Lipofectamine 2000 (3 µL) and plasmid DNA (1 µg) were combined in 400 µL of DMEM and incubated at room temperature for 30 min. The DNA mixture was added to

35 mm dishes of 70% confluent IEC-18 and IEC-Ras34 in 1.6 mL of IEC-MEM. The cells were incubated for 24 h prior to the start of experiments.

2.4 Lentiviral Production

Transient knockdown of CCTα was performed using lentivirus expressing an shRNA against the membrane binding domain of CCTα. The first step was to assemble viral particles containing the shRNA of interest in a replication suitable cell line, in this case HEK 293T cells expressing an SV40 invariant large T-antigen. The second step was to transduce target cells with these viral particles. Upon transduction, target cells take up the lentivirus, which then integrates into the host genome. The end result is expression of the desired shRNA which is processed by dicer and activates the RNA-induced silencing complex, leading to targeted gene silencing.

The assembly of viral particles requires co-transfection of plasmids encoding packaging factors (pCMV-Δ8.2), vesicular stomatitis virus glycoprotein envelope protein (pCMV-VSVG) and a pLKO.1-shRNA of interest. To 400 μL of DMEM, 5 μg pLKO.1-shRNA, 3 μg pCMV-Δ8.2, 0.5 μg pCMV-VSVG and 25 μL of polyethyleneimine (PEI) transfection reagent were added and incubated at room temperature for 15 min. This was then added to HEK293T (4 x 10^6 cells) in 3 mL of DMEM containing 5% FBS and the cells were allowed to produce viral particles for 48 h. CCTα was silenced with the following pLKO.1 shRNA (5’-CCGGCCTGTGAGAGTTTATGCGGATCTCGAGATC CGCATAAACTCTCACAGGTTTTTG-3’). Non-targetting shNT (5’-CCGGCAACAA GATGAAGAGCACCAACTCGAGTTGGTGCTCTTCATCTTGTTGT TTTT-3’) served as a control.

Viral particles were collected and filtered through a 0.45 µm cellulose-acetate filter. The media was brought up to 5 mL with α-MEM and polybrene (1 µg/mL) was added. The viral media was added to 100 mm dishes of 70% confluent IEC-18 or IEC-Ras34 for 4 h. Afterwards, 8 mL of IEC-MEM was added followed by incubation for 24 h. After infection, the media was changed to media containing puromycin (1 µg/mL for IEC-18 and 2 µg/mL for IEC-Ras34) to kill non-infected cells for 48 h. A dish containing an equal density of non-infected cells was also selected in puromycin as an indicator for non-infected cell death. Knockdown was confirmed by immunoblot for each knockdown experiment.

2.5 Immunofluorescence Microscopy

Cells were seeded on sterile coverslips (0.17 mm thickness) prior to the start of the experiment. For IEC-Ras34 grown in suspension, cells were collected and adhered to poly-L-lysine coated coverslips (0.1%, w/v) for 30 min at 4ºC prior to fixing in 4% paraformaldehyde for 15 min at room temperature. The coverslips were washed twice with 50 mM ammonium chloride to quench any remaining aldehyde. Cells were permeabilized with 0.5% Triton X-100 for 10 min at 4ºC. The Triton X-100 permeabilization step was not performed for experiments involving LD formation, with all following dilutions containing 0.1% saponin. After permeabilization, cells were blocked in PBS (10 mM sodium phosphate [pH 7.4], 225 mM NaCl and 2 mM $MgCl_2$) supplemented with 1% BSA for 1 h at room temperature. Primary antibodies were diluted as shown in the figure legends in PBS/BSA and 750 µL was applied to each coverslip and allowed to incubate for 1 h at room temperature. The coverslips were washed twice with PBS/BSA for 10 min each. Secondary antibodies were diluted 1:4500 in PBS/BSA and 750 µL was applied to each coverslip and allowed to incubate for 1 h at room temperature. Neutral lipid dyes (BODIPY 493/503 and DPH) were diluted 1:1000 and incubated with the secondary antibodies. After washing with PBS/BSA, the coverslips were rinsed once with distilled water and then mounted onto glass slides with 10 µL of Mowiol 4-88©.

Confocal microscopy was performed using a Zeiss LSM510 META confocal microscope scanned at 0.6 µm thickness, using either a 63X- or 100 X- oil-objective lens (1.4 NA) and analyzed using ZEN 2009 software. Wide-field microscopy was performed using an Zeiss Axiovert 300 M microscope equipped with a AxioCamHR camera and a 100 X oil-objective lens (1.4 NA).

2.6 Immunoblotting of Cell Lysates

Cells in monolayers were washed twice with ice-cold PBS before lysis with 2 X Laemmli buffer (12.5% SDS, 30 mM Tris-HCl [pH 6.8], 12.5% glycerol and 0.01% bromophenol blue). Cells grown on Sea-plaque agarose (1% in αMEM) were collected, subjected to centrifugation at 13,000 rpm for 15 seconds and the supernatant discarded. This was followed by two washes with PBS and lysis with Laemmli buffer as described before. The lysate was subjected to sonication (60 Hz) for 15 seconds, followed by heating at 95ºC for 5 min. Equal amounts of lysate were loaded on an SDS-PAGE acrylamide gel (8% to 12 %) and subjected to denaturing electrophoresis in SDS-running buffer (3 mM SDS, 200 mM glycine and 25 mM Tris-base) for 1 h at 120 V. After electrophoresis, proteins were transferred to nitrocellulose membranes (0.2 µm) in Towbin buffer (25 mM Tris-base, 192 mM glycine, 20% methanol) for 1 h at 100 V.

Proper protein loading and transfer were confirmed by Ponceau staining (0.1% Ponceau-S, 30% trichloroacetic acid, 5% sulfosalicylic acid). The membranes were incubated in a 1:5 Odyssey blocking buffer: TBS (20 mM Tris-HCl, [pH 7.4] 500 mM NaCl) solution for 1 h. In accordance to the figure legends, primary antibodies were diluted in the above blocking buffer supplemented with 0.5% Tween-20 and applied to the membranes for either 1 h at room temperature, or 4ºC overnight. The membranes were washed three times with TBS-Tween-20 for 5 min each, followed by application of diluted secondary antibodies (1:15000) in blocking buffer for 1 h at room temperature in accordance with the figure legends. After washing three times with TBS-Tween-20, followed by one wash with TBS, fluorescence was detected at either 680 nm or 800 nm using the Licor Odyssey scanner. Densitometry analysis was performed and quantified using Odyssey Application software (V 3.1).

2.7 Measurement of PtdCho and Metabolites by [^{3}H]Choline Incorporation

Activity of the CDP-choline pathway was measured by either [^{3}H]choline pulse or pulse-chase in IEC-18 or MCF7 cells, respectively. For pulse-chase experiments, cells were incubated in choline-free media supplemented with 2 µCi/mL [^{3}H]choline chloride at 37ºC for 1 h. The cells were washed once with CCL-107, followed by incubation in 2 mL of CCL-107 containing 50 µM unlabelled choline chloride. For pulse experiments with IEC-18 detached and attached cells were incubated in IEC-MEM containing 1 µCi/mL [^{3}H]choline chloride for the indicated times. Prior to harvesting, 200 µL of PBS supplemented with unlabelled choline chloride (10 mM) was added to each dish on ice to block further [^{3}H]choline uptake. Attached cells were rinsed twice with cold PBS and harvested in 1 mL of methanol:water (5:4 v/v). Detached cells were collected and subjected to centrifugation at 2000 rpm for 5 min, rinsed twice with PBS and harvested as before. An aliquot (200 μL) was taken for protein determination by the Lowry method. Chloroform (3 mL) was added and the samples were subjected to centrifugation at 2000 rpm for 5 min. The aqueous phase was collected and the organic phase was washed twice with 2 mL of ideal upper phase (chloroform:0.58% NaCl:methanol (45:47:3 v/v)) and dried under N_2. The organic phase was resuspended in 1 mL of chloroform and 200 μL was quantified for radioactivity using liquid scintillation counting (LSC). The aqueous phase was dried under N_2, resuspended in 100 μL of water and 20 μL was spotted onto TLC plates (Silica Gel G) along with unlabelled pChol, CDP-choline and GPC standards. Separation of the aqueous choline metabolites was performed using a water:ethanol:ammonium hydroxide (95:48:6) solvent system. The plates were subsequently sprayed with phosphomolybdate (1% in CH_3OH : $CHCl_3$) (1:1 v/v)) and stannous chloride (1% in HCl (3 M)). Samples were collected by scraping and radioactivity was quantified by LSC.

2.8 Choline Kinase Assay

MCF7 and MCF7-C3 cells treated with or without the topoisomerase inhibitor camptothecin (CMT) to induce DNA damage and induce apoptosis were grown to 80% confluence on 100 mm dishes prior to the start of the assay. Cells were rinsed twice with ice-cold PBS and collected by scraping followed by centrifugation at 2000 g for 5 min. The pellet was homogenized in 100 μL of Buffer A (Tris-HCl (20 mM; [pH 7.4]), NaF (10 mM), EDTA (1 mM), DTT (5 mM) and protease inhibitor) and subjected to 15 passes through a 25 gauge needle at 4ºC. Homogenates were subjected to centrifugation for 1 h at 125,000g. The supernatant was collected and assayed for CK activity in addition to an aliquot taken for protein determination using the Lowry method.

To assay choline kinase activity, 40 μg of protein was diluted to 100 μL with reaction buffer (Tris-HCl (100 mM; [pH 8.5]), $MgCl_2$ (10 mM), ATP (10 mM) and [methyl-^{3}H]choline chloride (2 μCi)). Each sample was incubated at 37ºC for 20 min followed by 2 min at 100ºC to terminate the reaction. An aliquot (50 μL) was applied to a silica gel G TLC plate and resolved using a water/ethanol/ammonium hydroxide (95/48/6, v/v) system in addition to a pChol standard. pChol was visualized by spraying the plate with sodium phosphomolybdate (1%, in 1:1 chloroform/methanol) followed by stannis chloride (1%, in 3 N HCl), scraped and radioactivity was measured by LSC.

2.9 Choline Transport Assay

MCF7 and MCF7-C3 cells treated with or without CMT or attached IEC-18 were 80% confluent prior to the start of the experiment. The cells were briefly rinsed in 0.5 mL of Krebs-Ringers buffer (NaCl (130 mM), KCl (1.3 mM), $CaCl_2$ (2.2 mM), $MgCl_2$ (1.5 mM), K_2HPO_4 (1.2 mM), HEPES (10 mM) and D-glucose (10 mM) [pH 7.4]) and incubated in 0.5 mL of this buffer for 30 min. The cells were then incubated with 500 μL of Krebs-Ringer buffer containing increasing concentrations of choline (1-25 μM) and 5 nM of [^{3}H]choline chloride for 10 min at 37ºC. To terminate the reaction, cells were immediately placed on ice and 1 mM of unlabelled choline chloride was added. The cells were washed three times with ice-cold Krebs-Ringer buffer and then solubilized in 250 μL of SDS (0.1%) / NaOH (0.2 N) for 10 min at room temperature. To determine specific activity, 125 μL of sample was measured for radioactivity by LSC. For protein determination using the Lowry method, untreated cells were washed three times with buffer and solubilized in 100 µL of NaOH (0.5 N) at room temperature.

The choline transport assay for detached IEC-18 was similar except for the following changes. IEC-18 cultured on Seaplaque were collected and subjected to centrifugation at 200g for 10 min at 4ºC. The cells were resuspended in Krebs-Ringers buffer and incubated for 30 min at 37ºC. The cells were then resuspended in 500 µL of buffer containing increasing concentrations of choline (1-25 µM) and uptake of [^{3}H]choline was measured as above.

2.10 Differentiation of 3T3-L1 preadipocytes

3T3-L1 preadipocytes were cultured to confluency in CCL-107 in 35 mm dishes before differentiation. The media was replaced with 2 mL of induction media (CCL-107 containing 3-isobutyl-1-methylxanthine (IBMX; 500 µM), dexamethasone (1 µM) and insulin (167 nM)) to induce differentiation. Two days after induction, the media was replaced with 2 mL of insulin media (CCL-107 supplemented with insulin).

2.11 MTT Cell Viability Assay

IEC-18 and IEC-Ras34 shNT and shCCTα were seeded at 5 x 10^3 cells/well in a 96 well plate. Increasing concentrations of 100 µL oleate (0 to 400 µM) were added to the wells in IEC-MEM and cell viability was measured after 24 h. Cell viability was determined using the CellTiter 96 AQUEOUS Non-radioactive Cell Proliferation Assay, which directly measures the conversion of a tetrazolium salt (MTS) to a coloured formazan product and is dependent on a functioning mitochondria, which correlates with cell viability. In brief, 15 μL of MTS/phenazine methosulfate (PMS) was added to each well and incubated for 4 h at 37ºC. The reaction was terminated/solubilized by addition of 100 μL stop solution and absorbance read at 490 nm.

2.12 Statistical Analysis

Unless otherwise stated, each experiment is the mean and standard error of the mean (SEM) of at least three experiments, performed in duplicate. Significance was determined using a two-tailed t-test assuming unequal variances. The significance is shown as a *P* value with <0.05 (*), <0.01 (**), <0.001 (***).

CHAPTER 3: RESULTS

3.1 A Mechanism for Suppression of the CDP-choline Pathway During Apoptosis

Induction of apoptosis results in caspase cleavage of CCTα and removal of the nuclear localization signal (NLS); however, the contribution of this event to suppression of the CDP-choline pathway remains poorly understood. It was previously shown that CCTα is recognized and proteolyzed *in vitro* by caspases 3, 6, 7 and 9. However, siRNA experiments implicated caspase 3 as the caspase that recognizes and proteolyzes CCTα in cells. To better understand how cleavage of CCTα by caspase 3 contributes to the apoptotic response, MCF7 cells (which are caspase 3-deficient) and MCF7 cells stably expressing caspase 3 (MCF7-C3) were used. This system is useful as it allows for the comparison between caspase 3 –independent (MCF7) and –dependent (MCF7-C3) suppression of the CDP-choline pathway during apoptosis. To confirm that CCTα is a caspase 3 substrate, MCF7 and MCF7-C3 cells were treated with CMT (inhibits topoisomerase and induces DNA damage) and TNFα (activates caspase 8) to induce apoptosis and immunoblotted for CCTα and poly ADP-ribose polymerase (PARP), a protein involved in DNA repair and acts as a suitable marker for apoptosis (**Fig 3.1.1)**. The appearance of a lower band (indicated by the black arrowhead) was indicative of cleavage. PARP was extensively proteolyzed in both MCF7 and MCF7-C3 cells during apoptosis **(Fig 3.1.1A)**. However CCTα proteolysis was only evident in the MCF7-C3 cells, indicating that CCTα is a caspase 3 substrate (**Fig 3.1.1B)**. In apoptotic MCF7-C3 cells 50% of CCTα was proteolyzed at 24 h, whereas with TNFα only 20% of CCTα was proteolyzed (**Fig 3.1.1C)**. CCTα and PARP protein expression was significantly lower in both cell lines after both CMT and TNFα treatment at longer time points compared to control. This is most likely due to inhibition of protein synthesis in late stages of apoptosis. Subsequent experiments use 24 h (CMT) or 12 h (TNFα) where total protein expression is similar to control.

Removal of the nuclear localization signal by caspase 3 during apoptosis would block the import of CCTα into the nucleus, resulting in increased cytoplasmic CCTα. Immunofluorescence microscopy was used to visualize changes in CCTα localization after treatment with CMT and TNFα (**Fig 3.1.2)**. Cells were counterstained with an antibody against the nuclear pore complex (NPC) to establish nuclear integrity and size. In MCF7 cells treated with either CMT or TNFα (**Fig 3.1.2A and B)**, there was a decrease in overall nuclear size (shrunken nuclei), the NPC antibody showed uniform staining (intact nuclear envelope) but CCTα was retained in the nucleus. On the other hand in MCF7-C3 cells treated with CMT and TNFα, there was a decrease in nuclear size, the NPC antibody showed weak nuclear staining and CCTα localized almost extensively to the cytoplasm. These results show that CCTα is a caspase 3 substrate and is excluded from the nucleus during apoptosis in caspase 3 expressing cells.

Proteolysis and exclusion of CCTα from the nucleus in MCF7-C3 cells provides one potential mechanism by which the CDP-choline pathway is inhibited during apoptosis. However, these results are insufficient to explain the reduced incorporation of [^{3}H]choline into pChol during a pulse-labelling experiment in both MCF7 and MCF7-C3 cells [192]. These results suggest additional inhibitory mechanisms independent of caspase 3 mediated proteolysis of CCTα. To monitor the activity of CCTα during apoptosis, nonapoptotic and apoptotic MCF7 and MCF7-C3 cells were pulse-labelled with [^{3}H]choline to allow for accumulation of the precursor phospho[^{3}H]choline,

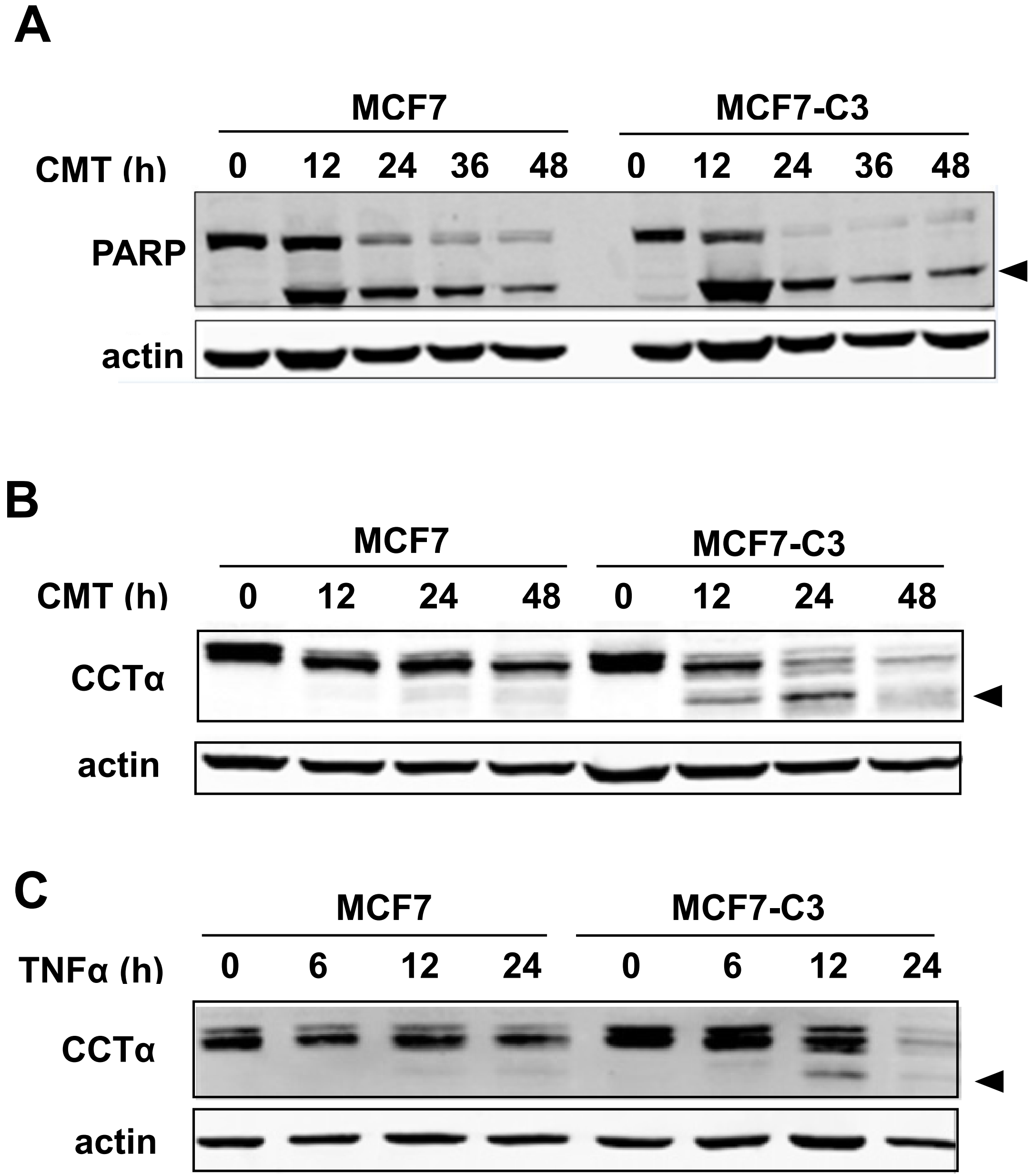

Figure 3.1.1. CCTα proteolysis is restored in MCF7 cells upon stable expression of caspase 3. MCF7 and MCF7-C3 cells were treated with either 15 μM CMT **(A and B)** or 10 ng/mL TNFα and 30 μg/mL cycloheximide **(C)** for the indicated times. Cells were lysed in an SDS-PAGE lysis buffer and total cell lysates were immunoblotted against PARP **(A)** or CCTα **(B and C)**. β-Actin was used as a loading control. Black arrowheads indicate the cleaved form. Immunoblots were visualized using the Odyssey Infrared Imaging System.

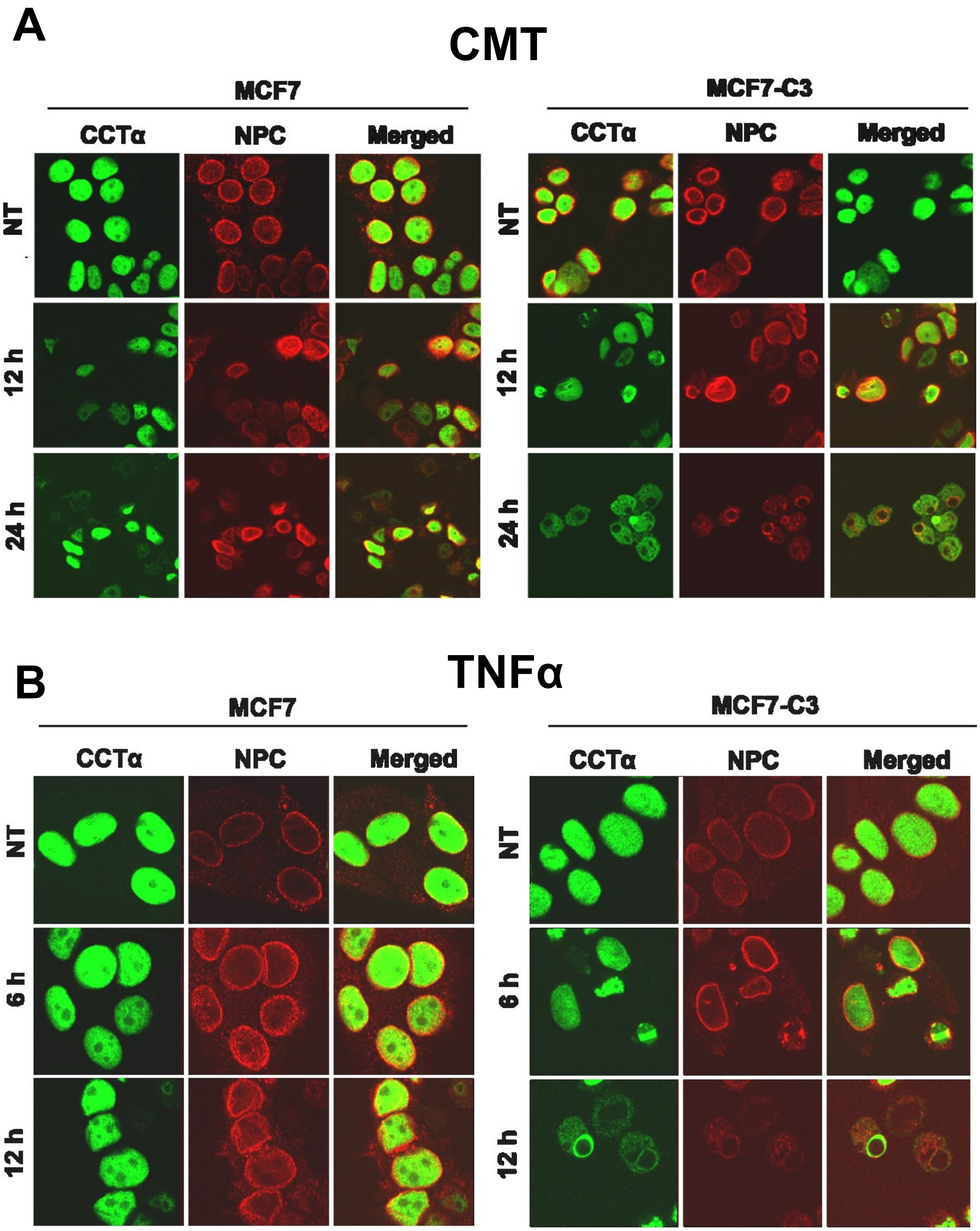

Figure 3.1.2. CCTα is excluded from the nucleus during camptothecin- and TNFα-induced apoptosis in MCF7-C3 cells. MCF7 and MCF7-C3 cells were treated with either 15 μM CMT **(A)** or 10 ng/mL TNFα and 30 μg/mL cycloheximide **(B)** for the indicated times. Cells were fixed, permeabilized and incubated with rabbit anti-CCTα (1:2500) and mouse anti-NUP62 (1:1500) and viewed using confocal microscopy.

followed by a 3 h chase period to allow for conversion to Ptd[^{3}H]Cho and other metabolites (**Fig 3.1.3)**. The rate of PtdCho synthesis in MCF7 cells (~27,000 dpm/h) was reduced by approximately 50% after treatment with CMT (~15,000 dpm/h) **(Fig 3.1.3A and B)**. The rate of pChol depletion was similar. The rate of PtdCho synthesis in MCF7-C3 cells (~12,000 dpm/h) was also reduced by approximately 50% after treatment with CMT (~6000 dpm /h) and this conversion was complete by 1 h **(Fig 3.1.3C and D)**. The rate of pChol depletion was similar in both cases. Incorporation of [^{3}H]choline into GPC and CDP-choline were low compared to PtdCho and pChol and remained relatively unchanged in apoptotic cells. Initial phospho[^{3}H]choline levels were lower in apoptotic versus nonapoptotic cells suggesting inhibition of an earlier step in the pathway. Additionally, based on the conversion of phospho[^{3}H]choline to Ptd[^{3}H]Cho, there is a 50% reduction in CCTα activity by CMT treatment in both MCF7 and MCF7-C3 cells, indicating a caspase 3-independent mechanism for CCTα inhibition.

Metabolic labelling experiments showed that pChol levels are reduced in both MCF7 and MCF7-C3 cells by CMT treatment, suggesting inhibition at an earlier step in the pathway, either at the choline transport and/or phosphorylation steps. CKα is overexpressed in many types of cancer and is the major isoform found in MCF7 cells, making it a putative target for inhibition during apoptosis. To investigate this, total CK activity was measured in both nonapoptotic and apoptotic MCF7 and MCF7-C3 cells. The cytosolic fraction (containing CK) was incubated with [^{3}H]choline and ATP and the amount of phospho[^{3}H]choline produced was measured (**Fig 3.1.4)**. Compared to their nonapoptotic MCF7 and MCF7-C3 counterparts, apoptotic MCF7 and MCF7-C3 cells had no change in CK activity, indicating that CK is not targeted during apoptosis.

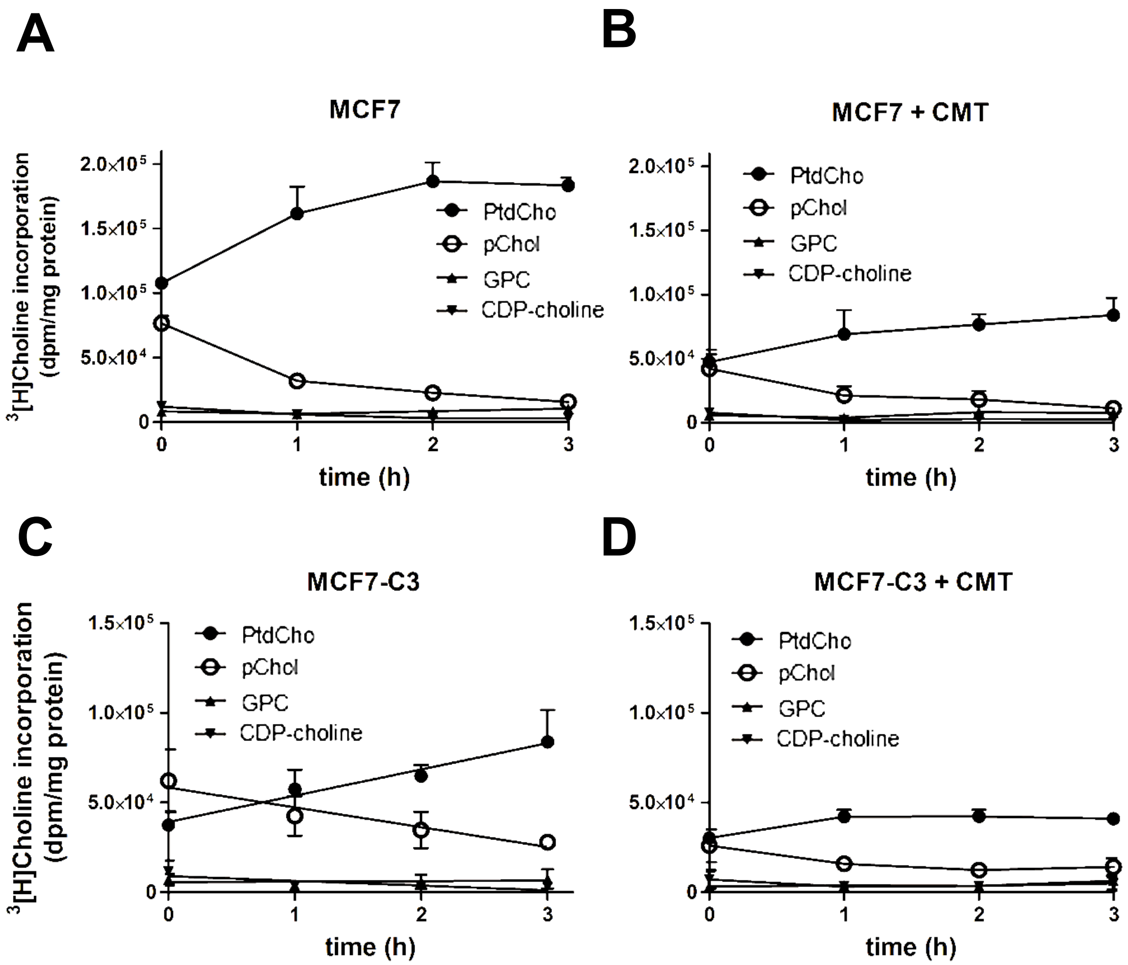

Figure 3.1.3. **MCF7 and MCF7-C3 cells have reduced incorporation of [^{3}H]choline into PtdCho and metabolites during camptothecin-induced apoptosis**. MCF7 cells (A and B) and MCF7-C3 cells (C and D) were treated without (A and C) or with 15 μM CMT (B and D) for 24 h. Cells were pulsed with 2 μCi/mL [^{3}H]choline for 1 h, followed by a media change containing choline-free DMEM supplemented with 50 μM unlabelled choline chloride. Cells were harvested at the indicated times and choline incorporation into PtdCho, pChol, GPC and CDP-choline was measured by liquid scintillation counting. Results are the mean and SEM of three independent experiments.

The conclusion that phosphorylation of choline is not affected during apoptosis suggests a potential defect in choline uptake. Indeed, a block in choline uptake would serve to limit the flux of choline into the cell, effectively starving the cell of choline resulting in inhibition of the CDP-choline pathway. To investigate whether choline transporters were inhibited during apoptosis, choline transport activity was measured based on uptake of choline (1-25 μM) into nonapoptotic and apoptotic MCF7 and MCF7-C3 cells (**Fig 3.1.5 A)**. Saturable choline transport (321 ± 82 pmol/min/mg and 340 ± 82 pmol/min/mg) and K_D values (23 ± 9 μM and 27 ± 11 μM) were found to be similar in nonapoptotic MCF7 and MCF7-C3 cells, respectively (**Fig 3.1.5 B)**. There was no change in the K_D value (18 ± 7 μM and 14 ± 7 μM) however, saturable choline transport (219 ± 51 pmol/min/mg and 163 ± 39 pmol/min/mg) was significantly reduced after CMT treatment in MCF7 and MCF7-C3 cells, respectively **(Fig 3.1.5 B)**. To determine the type(s) of choline transporter(s) that is/are inhibited during apoptosis, HC-3, a competitive inhibitor of high-affinity choline transporters was used. Nonapoptotic and apoptotic MCF7 and MCF7-C3 cells were incubated with increasing concentrations of HC-3 and choline uptake was measured as before (**Fig 3.1.6)**. To confirm expression of a high-affinity choline transporter, MCF7 and MCF7-C3 cells were incubated with increasing concentrations of HC-3, which resulted in a 70%-80% inhibition in choline uptake **(Fig 3.1.6A)**. To determine whether low- or intermediate- choline transporters were inhibited during apoptosis, nonapoptotic and apoptotic MCF7 and MCF7-C3 cells were treated with HC-3 and relative inhibition was measured. MCF7 cells treated with CMT resulted in reduced choline transport, however, HC-3 did not result in an additional reduction in choline uptake, indicating that inhibition of choline transport in apoptotic

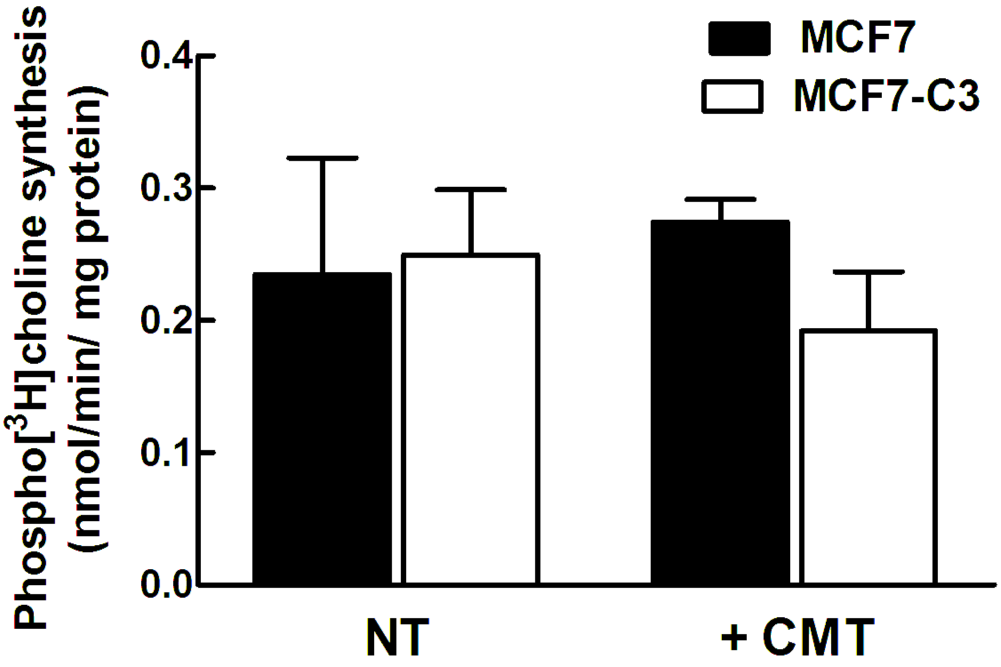

Figure 3.1.4. Choline kinase activity is unaffected during camptothecin-induced apoptosis in MCF7 and MCF7-C3 cells. MCF7 and MCF7-C3 cells were treated with or without 15 µM CMT for 24 h. CK activity was assayed in the cytosolic fraction (40 µg) in the presence of [^{3}H]choline and ATP for 10 min. [^{3}H]choline incorporation was determined using liquid scintillation counting. Results are the mean and SEM of three independent experiments.

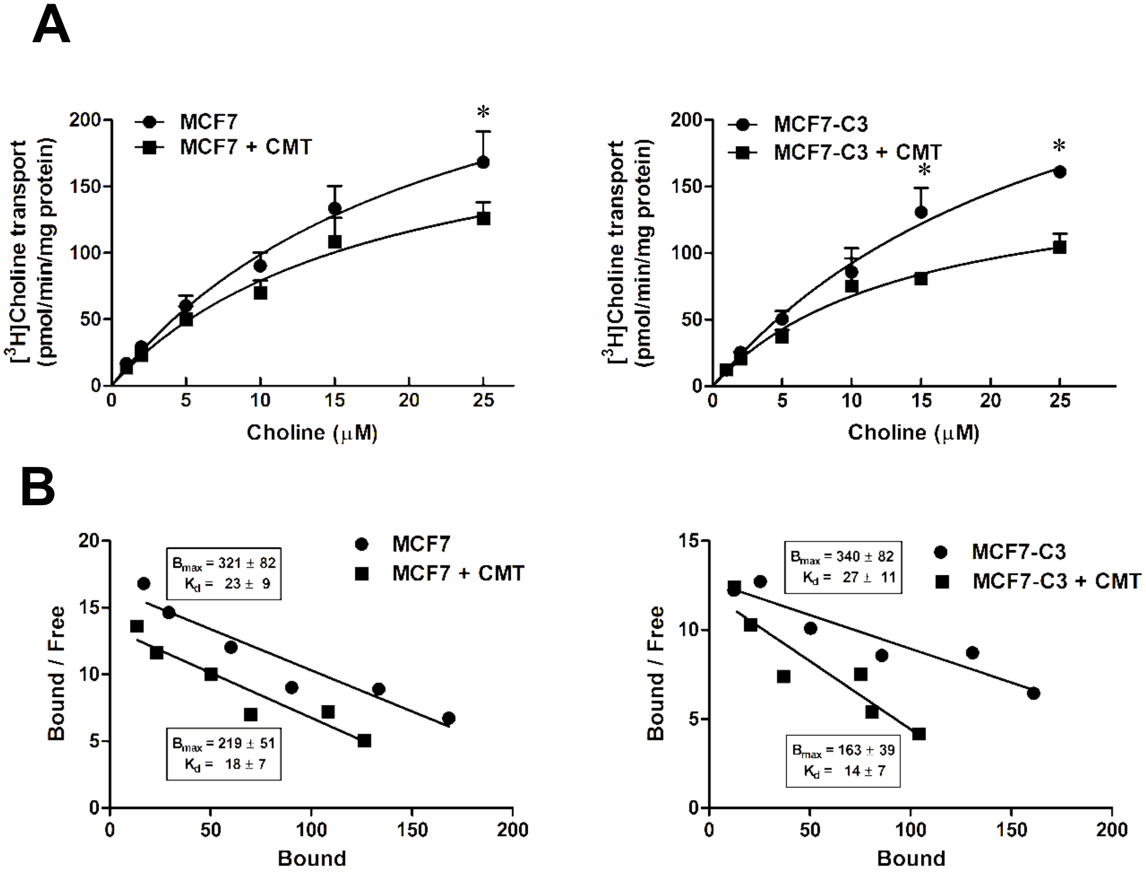

Figure 3.1.5. MCF7 and MCF7-C3 cells have reduced [^{3}H]choline uptake during camptothecin-induced apoptosis. MCF7 and MCF7-C3 cells were treated with or without 15 μM CMT for 24 h. Cells were incubated with increasing concentrations (1-25 μM) [^{3}H]choline chloride for 10 min at 37ºC and radioactivity was measured by liquid scintillation counting (**A**). B_{max} and K_d values were determined using a Scatchard fit analysis assuming a one-site binding model (**B**). Results are the mean and SEM of 3-5 independent experiments performed in triplicate. * $P < 0.05$ using a student's *t*-test assuming unequal variances.

MCF7 cells is through the inhibition of high-affinity choline transporters **(Fig 3.1.6B)**. On the other hand, HC-3 resulted in a further decrease in choline uptake in apoptotic MCF7-C3 cells compared to nonapoptotic MCF7-C3 cells, suggesting an additional low- or intermediate- affinity choline transporter component **(Fig 3.1.6C)**.

Rat intestinal epithelial cells (IEC-18) were used to test whether reduced choline uptake was observable in other forms of apoptosis. Upon detachment from the ECM, IEC-18 undergo anoikis due to disengagement of integrin receptors and loss of pro-survival signals through Ras and downstream kinases. However, very little is known about PtdCho metabolism after detachment in IEC-18. Therefore, experiments were undertaken to test whether the CDP-choline pathway was inhibited after detachment in IEC-18. Previously, Arsenault and colleagues showed that during longer periods of detachment (> 24 h), [^{3}H]choline incorporation into all metabolites of the CDP-choline pathway was dramatically reduced, suggesting that PtdCho synthesis is inhibited during anoikis. However, choline flux through the pathway was never measured during initial detachment and early induction of anoikis. To investigate this, attached and detached IEC-18 were radiolabelled with [^{3}H]choline and collected at 1, 3 and 6 h. Incorporation of [^{3}H]choline into PtdCho (**Fig 3.1.7A)**, pChol (**Fig 3.1.7B)** and GPC (**Fig 3.1.7C)** was significantly decreased in detached cells compared to an attached control indicating decreased flux of choline through the CDP-choline pathway. CDP-choline levels were not significantly affected, as this metabolite is short-lived and does not build up in cells (**Fig 3.1.7D)**. This data suggests that an early step in the pathway is potentially inhibited after cell detachment.

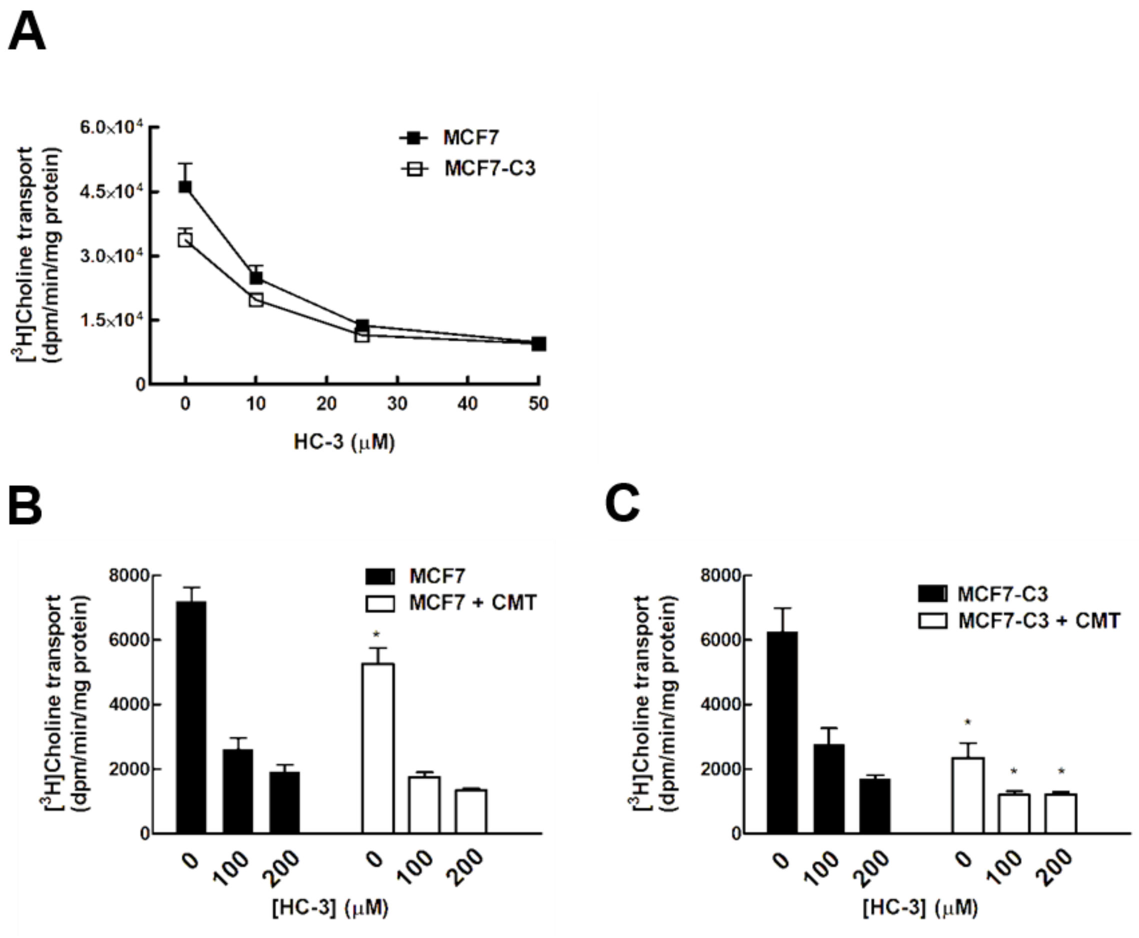

Figure 3.1.6. High-affinity choline transporters are inhibited in MCF7 and MCF7-C3 cells during camptothecin-induced apoptosis. MCF7 and MCF7-C3 cells were incubated with 10 nM [^{3}H]choline with increasing concentrations of hemicholinium-3 (HC-3) (A). Uptake of 20 µM choline into MCF7 cells (B) and MCF7-C3 cells (C) treated with or without 15 µM CMT for 24 h was assayed in the presence of increasing amounts of HC-3 for 10 min at 37ºC. Results are the mean and SEM of three independent experiments. * $P < 0.05$ using a student's *t*-test assuming unequal variances.

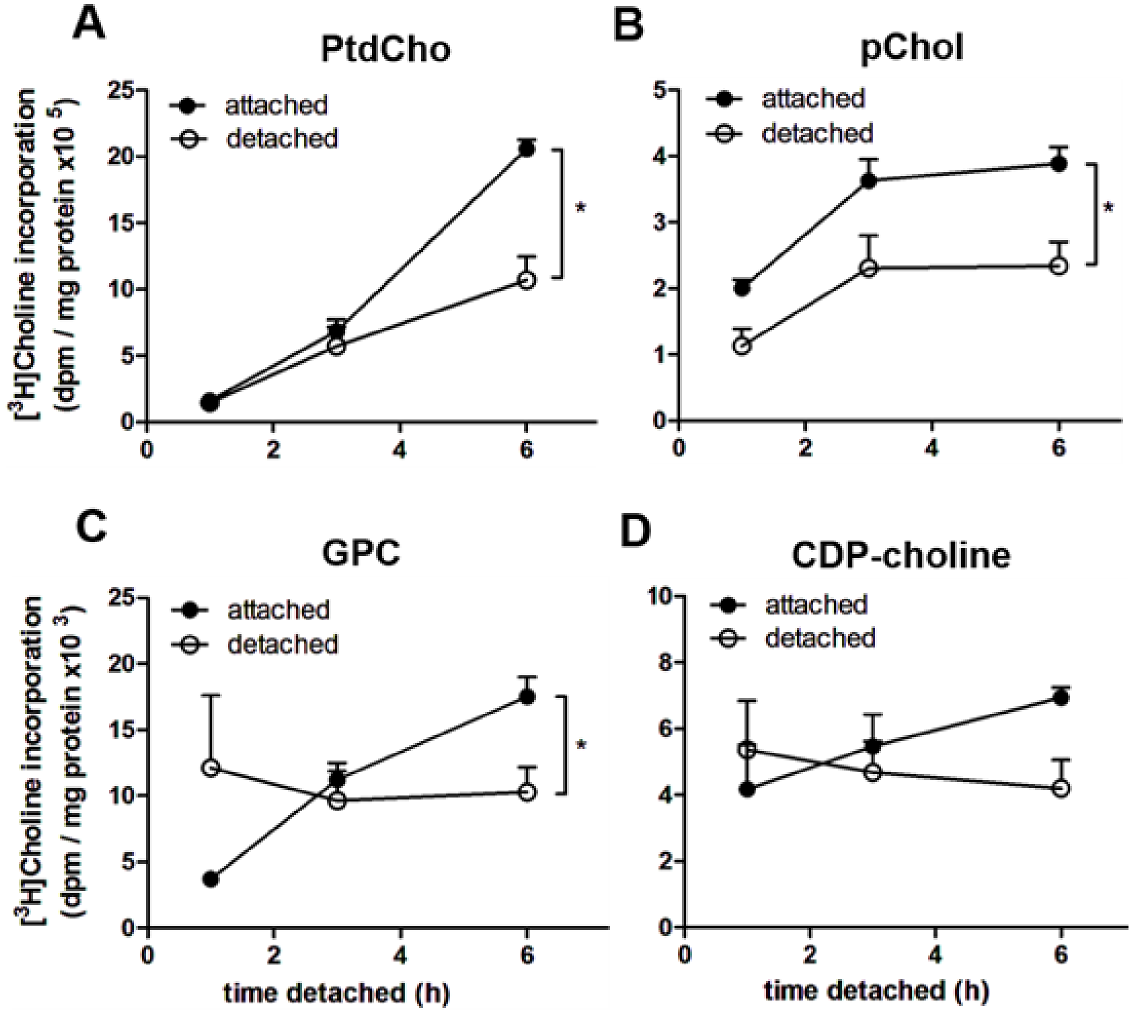

Figure 3.1.7: Detachment from the ECM causes reduced flux of [^{3}H]choline through the CDP-choline pathway in IEC-18. [^{3}H]Choline incorporation into PtdCho **(A)**, pChol **(B)**, GPC **(C)** and CDP-choline **(D)** were measured in detached IEC-18 and an attached counterpart. Isotope incorporation was measured after the specified times in accordance to Section 2.8. The values presented are the mean and SEM of three independent experiments. * $P < 0.05$ using a student's *t*-test assuming unequal variances.

The reduced incorporation of [^{3}H]choline into all CDP-choline pathway metabolites after detachment suggested inhibition of an earlier step, reminiscent of the experiments performed with MCF7 cells (**Fig 3.1.5)**. As such, choline transport activity was measured based on the uptake of [^{3}H]choline into detached and attached IEC-18 **(Fig 3.1.8)**. The K_D values were found to be similar (12 ± 3 μM and 16 ± 6 μM) for attached and detached IEC-18, respectively **(Fig 3.1.8B)**. However, saturable choline uptake was significantly reduced (302 ± 32 μM and 203 ± 40 μM) for attached and detached IEC-18, respectively, corresponding to about a 33% reduction (**Fig 3.1.8B)**. Taken together, these results suggest that inhibition of the CDP-choline pathway through a block in choline uptake is a common theme in different types of apoptosis.

3.2 The Role of CCTα in the Anoikis-Resistance of IEC-Ras

IEC-18 are susceptible to anoikis, however transformation with oncogenes such as Ras confers anoikis-resistance, allowing for uncontrolled growth, invasion of the surrounding tissue, leading to metastasis. This is a result of constitutive activation of pro-survival pathways that function downstream of Ras. It was previously shown in our lab that CCTα is required for anoikis-resistance in three IEC-Ras clones: (IEC-Ras-33, -34, -37), generated by transfection of IEC-18 with H-Ras cloned from an EJ human bladder carcinoma. CCTα is overexpressed in IEC-Ras, but is predominantly nucleoplasmic and relatively inactive when grown in monolayer. It is possible that detachment results in CCTα activation through increased association with membranes. To investigate this, I monitored localization of CCTα during detachment of on IEC-Ras clone (IEC-Ras34)

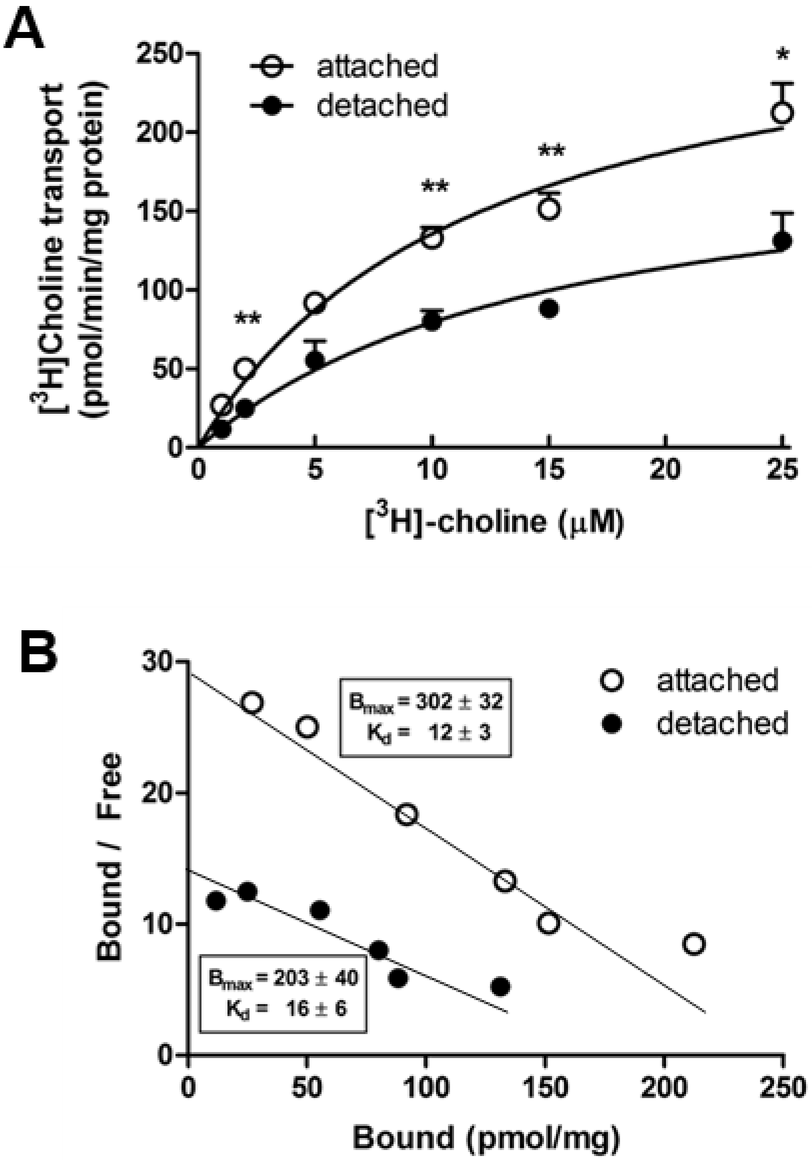

Figure 3.1.8: Detachment from the ECM causes a reduction in [^{3}H]choline uptake in IEC-18. IEC-18 cultured in monolayer (attached) or cultured on Seaplaque for 4 h (detached) were rinsed with Krebs-Ringer buffer and incubated with increasing concentrations of [^{3}H]choline (1-25 μM) for 10 min at 37ºC (**A**). B_{max} and K_d values were determined by Scatchard analysis using a one-site specific binding model (**B**). Results are the mean and SEM of triplicate measurements for 3-4 independent experiments. *$P < 0.05$, ** $P < 0.01$ using a student's *t*-test assuming unequal variances.

by immunofluorescence (**Fig 3.2.1)**. Cells were counterstained with the nuclear marker lamin A/C. In attached IEC-Ras34 (NT), CCTα was exclusively nucleoplasmic, with no detectable association with the nuclear envelope. IEC-Ras34 were detached for 6, 12 and 24 h and then seeded onto poly-L-lysine coated coverslips. At these time points, CCTα was also nucleoplasmic, with no apparent localization to the nuclear envelope or export from the nucleus. However, there was reduced nuclear integrity at 24 h detachment based on diminished lamin A/C staining, but the significance is not apparent. The control (0 h) was also used to ensure that any results obtained were a result of detachment and not off-target effects from the trypsinization process. Taken together, these findings suggest that CCTα localization does not change during detachment in IEC-Ras34.

Experiments implicating CCTα in anoikis-resistance are from shRNA knockdown experiments, which showed growth arrest and reduced clonogenicity of detached IEC-Ras [186]. Anoikis is largely caspase-dependent and induction of apoptosis through caspase activation may be sufficient to explain the reduced clonogenicity of CCTα-silenced IEC-Ras. To investigate this, activation of caspases 8 and 3 was measured using immunoblot in CCTα-silenced or shNT- IEC-Ras34 **(Fig 3.2.2)**. Knockdown of CCTα was confirmed by immunoblot and was approximately 99% **(Fig 3.2.2A)**. Caspase 8 and caspase 3 activation was not observed in CCTα-silenced IEC-Ras34 at any time after detachment **(Fig 3.2.2B and C)** suggesting that the reduced clonogenicity in detached IEC-Ras34 after CCTα knockdown is not a result of caspase activation. As a positive control, anoikis-sensitive IEC-18 were also detached for the same time points and caspase 3/8 activation was observed (results not shown).

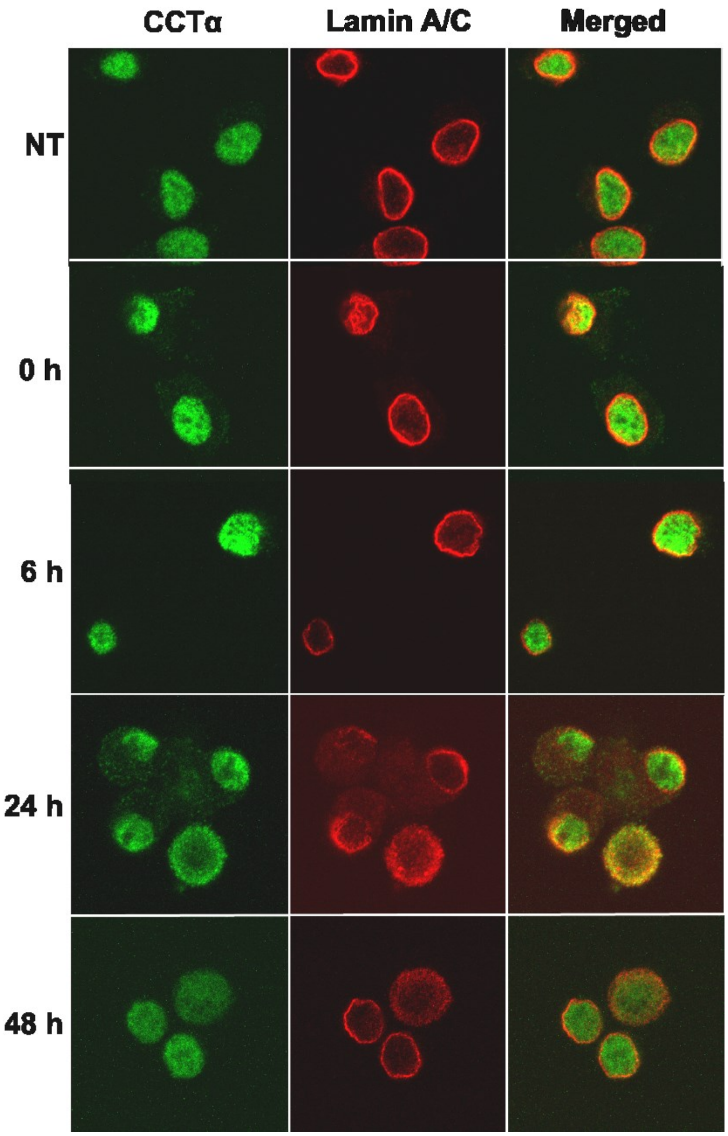

Figure 3.2.1. CCTα is localized to the nucleoplasm in detached IEC-Ras34. Cells were cultured on Seaplaque^{TM} (SP) agarose (1% in α-MEM) for the indicated times, followed by adherence to poly-L-lysine coated coverslips. Cells were fixed, permeabilized and incubated with rabbit anti-CCTα (1:2500) and mouse anti-lamin A/C (1:1500) primary antibodies. Cells were imaged using confocal microscopy.

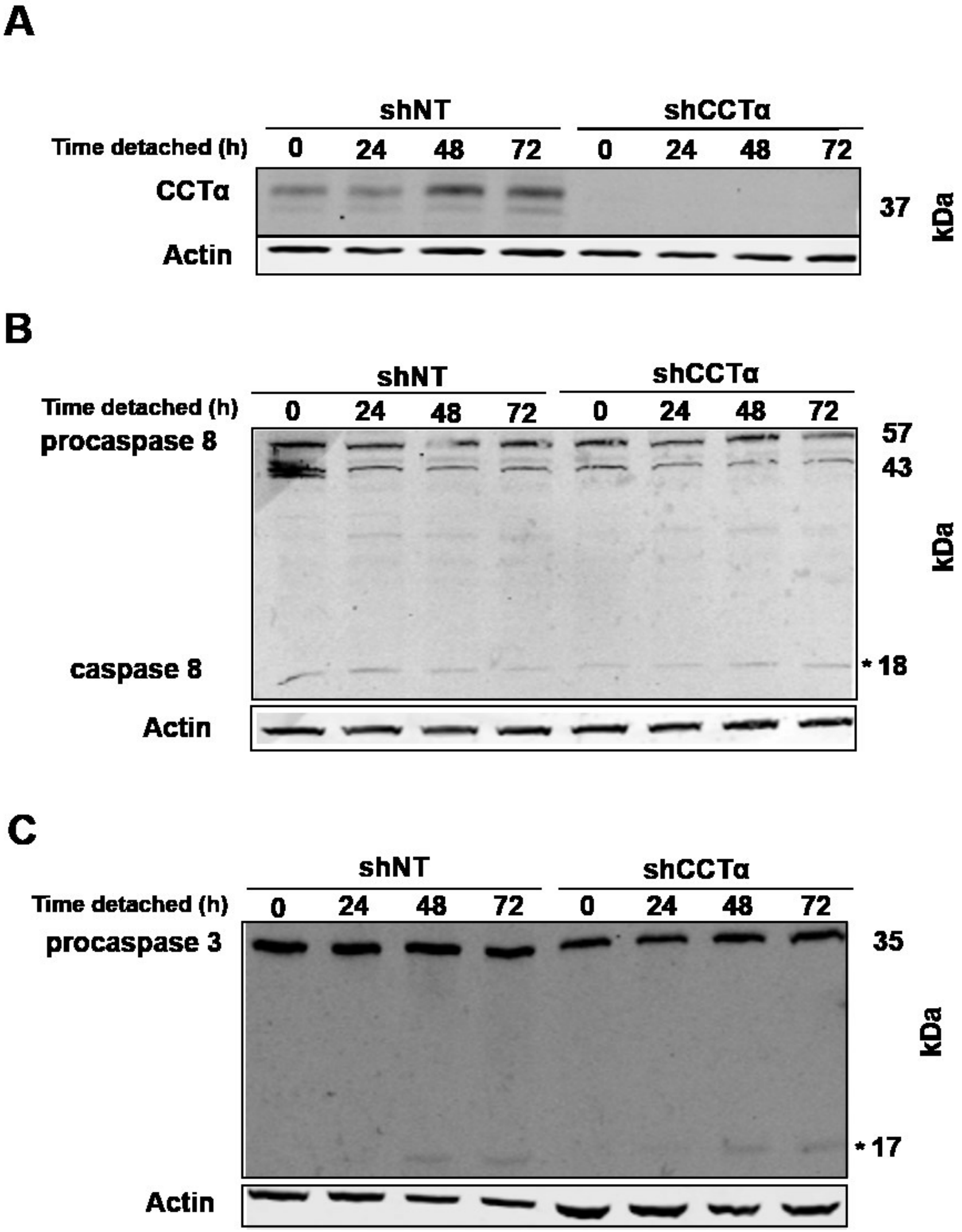

Figure 3.2.2. Knockdown of CCTα does not result in caspase activation upon detachment from an ECM. IEC-Ras34 were infected with virus encoding shRNA against CCTα (shCCTα) or non-targeting control (shNT) and selected with puromycin. Cells were cultured on SP agarose for the indicated times. Cells were lysed in an SDS-PAGE lysis buffer and total cell lysates were immunoblotted against CCTα **(A)**, caspase 8 **(B)** and caspase 3 **(C)**. β-Actin was used as a load control. Immunoblots were visualized using the Odyssey Infrared Imaging System.

PtdCho synthesis is increased after induction of an unfolded protein response (UPR) for proliferation of the ER membranes and to alleviate the ER stress [226]. If CCTα is unavailable for synthesis of PtdCho during an UPR, then an ER stress response could occur, which may explain the reduced clonogenicity when CCTα is silenced in IEC-Ras [186]. To investigate this, changes in signalling through the conserved IRE1α pathway was investigated by measuring total IRE1α expression and JNK activation by phosphorylation. Changes in expression of the chaperone proteins Bip and PDI were also measured **(Fig 3.2.3)**. Again, CCTα knockdown was approximately 99% **(Fig 3.2.3A)**. The expression of IRE1α did not significantly change during detachment in the IEC-Ras34 shNT, but decreased during detachment after CCTα was silenced. It is important to note that the expression of IRE1α in the CCTα-silenced IEC-Ras34 was initially 2-fold higher in the attached cells compared to detached **(Fig 3.2.3B)**. Similarly, JNK activation remained unchanged in detached IEC-Ras34 shNT but decreased in detached CCTα-silenced IEC-Ras34 **(Fig 3.2.3C)**. This could also be attributed to an initial 2-fold higher activation in the attached CCTα-silenced cells. The protein expression of Bip and PDI did not appreciably change during detachment in either IEC-Ras34- shNT or –shCCTα **(Fig 3.2.3D)**. These results suggest that CCTα knockdown may result in an initial ER stress response which diminishes when these cells are cultured in detached conditions. However, measurement of other markers of ER stress such as spliced XBP1 or PERK would help confirm whether a true and sustained ER stress response was occuring.

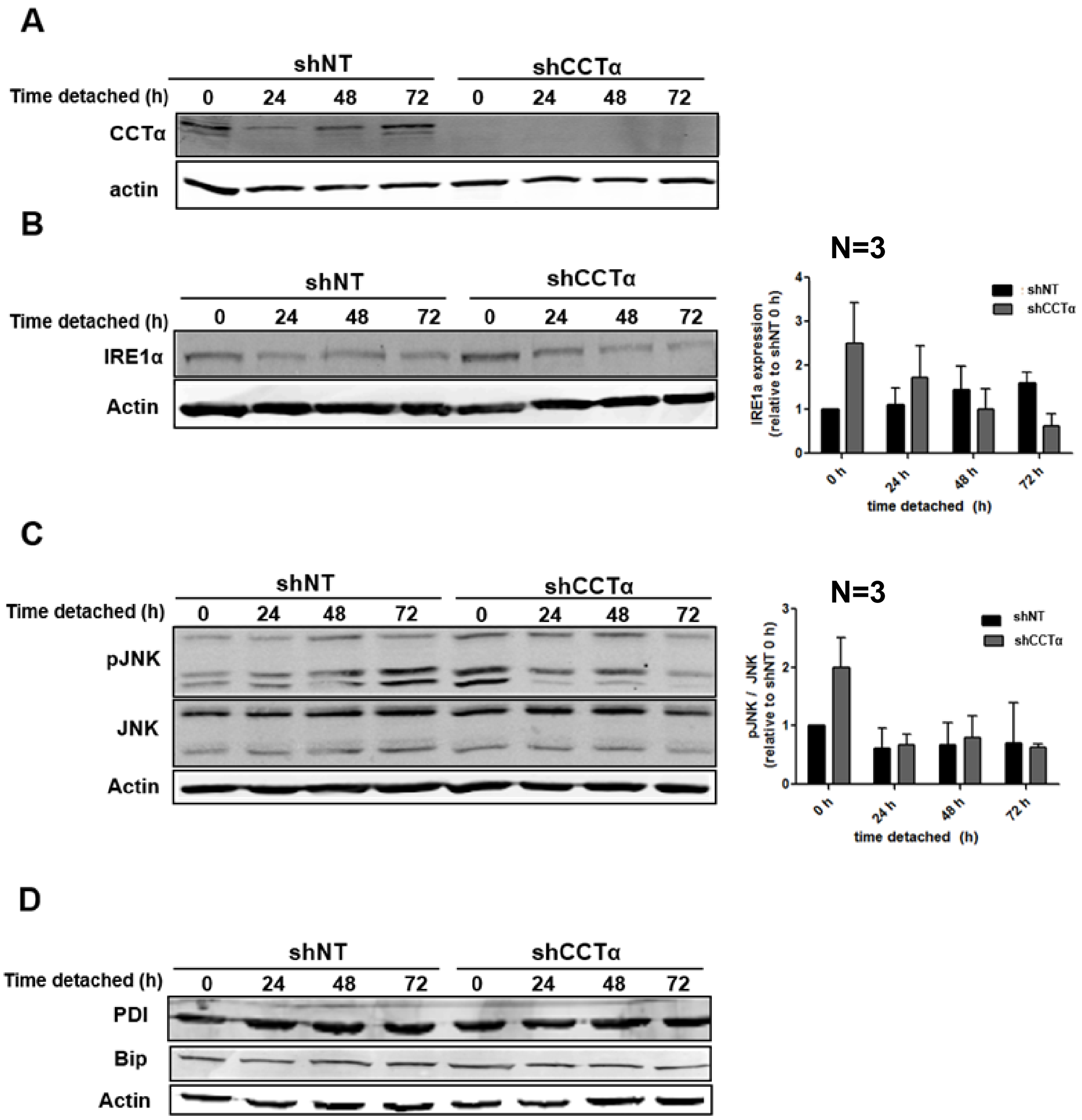

Figure 3.2.3. Effect of CCTα knockdown on the induction of an ER stress response during detachment from an ECM. IEC-Ras34 were infected with virus encoding shRNA against CCTα (shCCTα) or non-targeting control (shNT) and selected with puromycin. Cells were cultured on SP agarose for the indicated times. Cells were lysed in an SDS-PAGE lysis buffer and total cell lysates were immunoblotted against total IRE1α **(A)**, pJNK/JNK **(B)** and, PDI and Bip **(C)**. β-Actin was used as a load control. Immunoblots were visualized using the Odyssey Infrared Imaging System. The values presented are the mean and SEM of 2-3 independent experiments.

3.3 Regulation of LD Formation by CCTα

CCTα-GFP has been reported to localize to the surface of LDs in *D. Melanogaster* (S2 cells), but whether these findings are applicable to endogenous CCTα in mammalian cells was not investigated. Two methods were used to stimulate LD formation depending on the cell type. 3T3-L1 preadipocytes accumulate LDs during differentiation and regulate LD formation in response to various hormonal regulators such as insulin. On the other hand, treatment with oleate or other fatty acids stimulates TAG and CE synthesis and the formation of LDs in most cultured cells. Taken together, LD formation during adipocyte differentiation or oleate treatment provides two mechanisms to study CCTα localization to the surface of expanding LDs. To investigate this, endogenous CCTα localization was analysed by immunofluorescence after differentiation in 3T3-L1 preadipocytes **(Fig 3.3.1)** or after acute oleate treatment in other mammalian cell lines **(Fig 3.3.2)**. To visualize LDs, the neutral lipid dye BODIPY 493/503 was used. Non-differentiated 3T3-L1 preadipocytes had almost no LDs and CCTα was exclusively nuclear. On day 2, there was some evidence for LD formation, with little CCTα exported to the cytoplasm. There were large LDs by day 4 and 7 and CCTα was localized to the cytoplasm and NE only in cells containing LDs. Although readily exported from the nucleus, CCTα did not localize to the surface of LDs during differentiation in 3T3-L1 adipocytes.

Cells treated with oleate to stimulate LD formation included: CHO, HEK 293, HeLa, HepG2, J774A1, IEC-18 and IEC-Ras34 **(Fig 3.3.2)**. CHO had very few LDs at 12 and 24 h and CCTα was mostly nuclear-localized, with minor cytosolic localization **(Fig 3.3.2A)**. HEK 293 also had few LDs, but CCTα associated with the NE, with minor

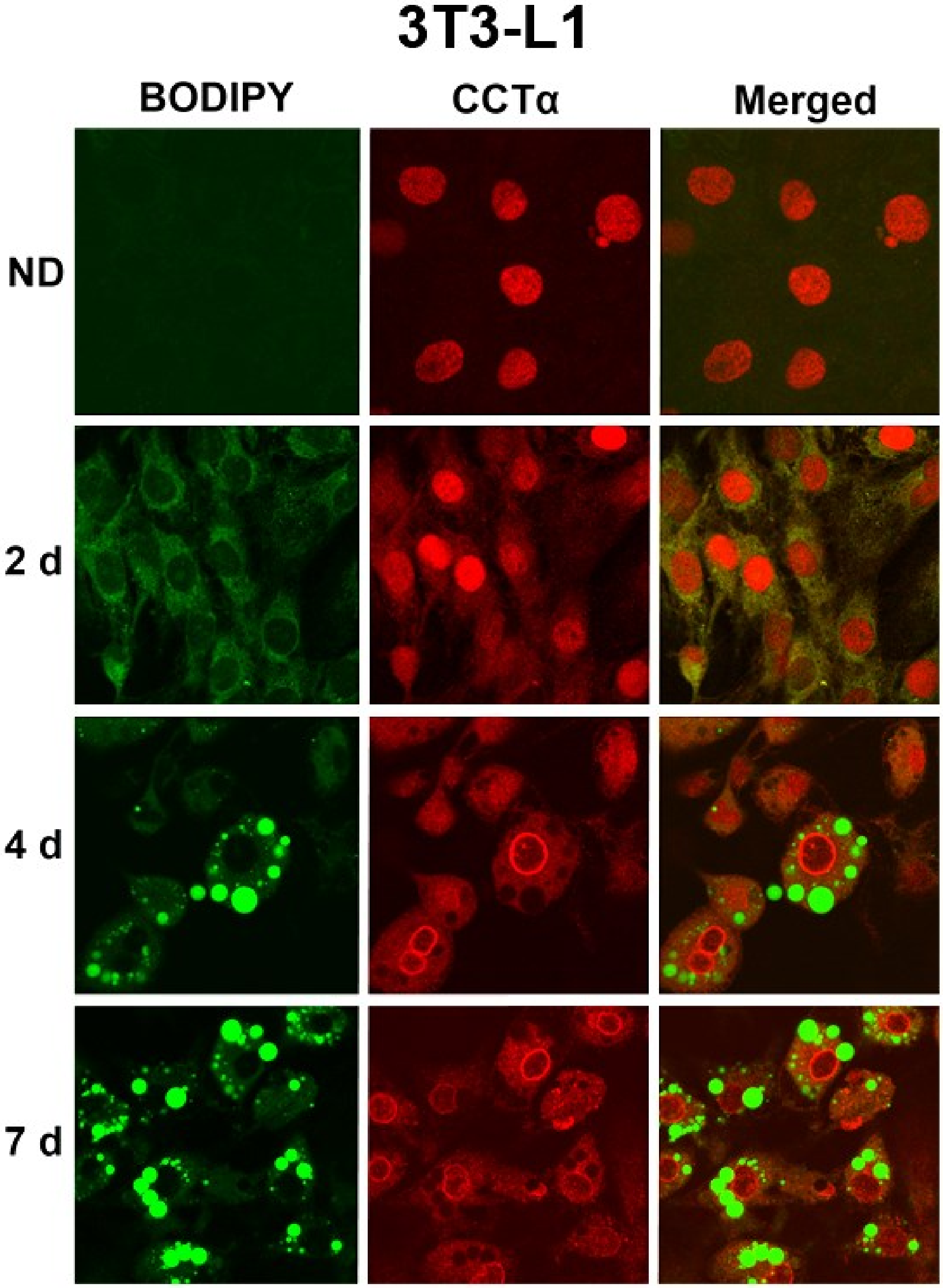

Figure 3.3.1: Localization of endogenous CCTα during LD formation in differentiating 3T3-L1 preadipocytes. Cells were incubated with dexamethasone, insulin and IBMX to induce differentiation. Cells were fixed, permeabilized with saponin and incubated with rabbit anti-CCTα (1:2500) and BODIPY 493/503 (1:1000) and viewed using confocal microscopy.

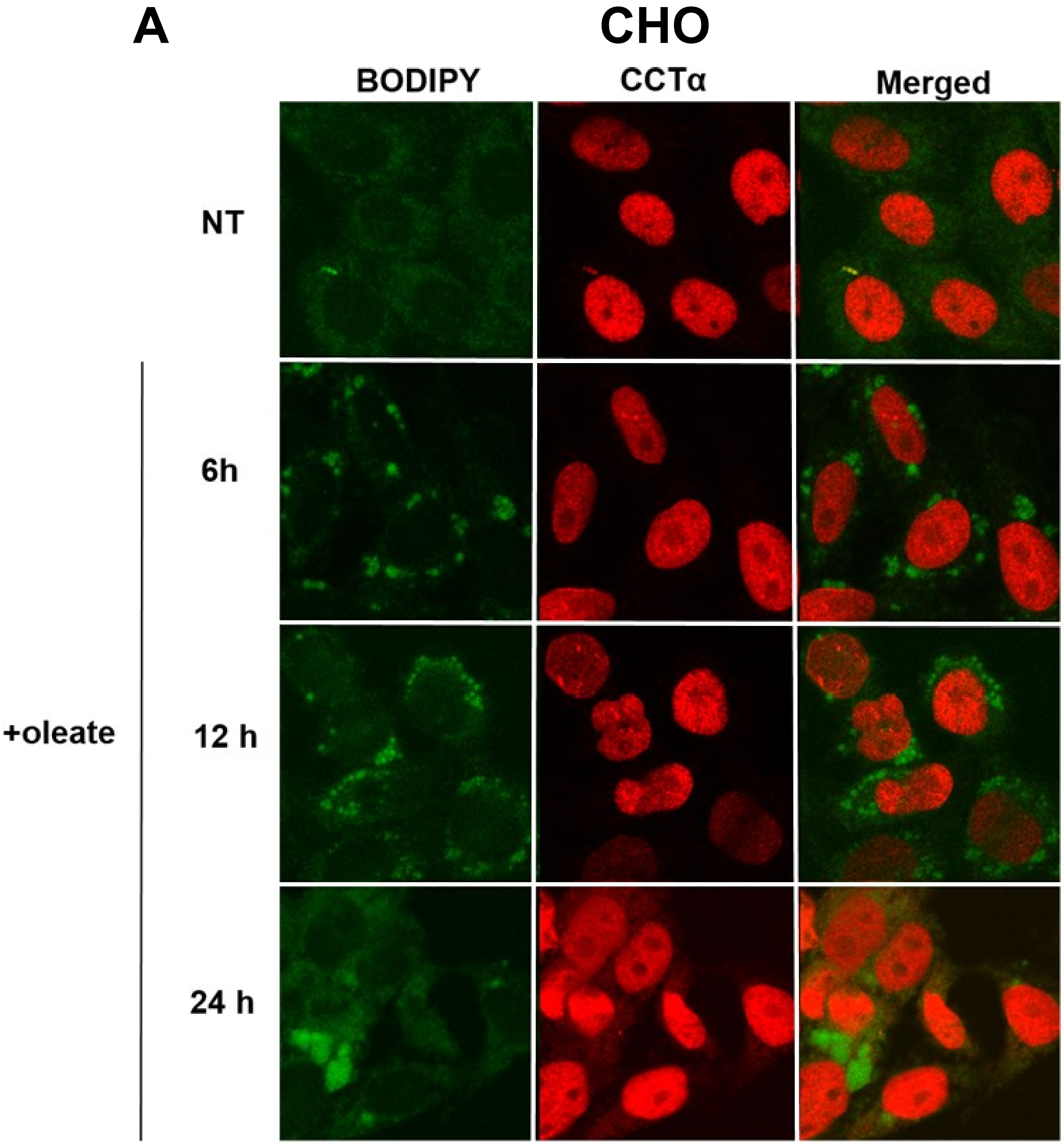

Figure 3.3.2: Localization of endogenous CCTα during LD formation in various mammalian cell lines after acute oleate treatment. Chinese hamster ovary **(A)**, HEK 293 **(B)**, HeLa **(C)**, HepG2 **(D)**, J774A1 **(E)**, IEC-18 **(F)** and IEC-Ras34 **(G)** were treated with 400 µM oleate/BSA for the indicated times. Cells were fixed, permeabilized with saponin and incubated with rabbit anti-CCTα (1:2500) and BODIPY 493/503 (1:1000) and viewed using confocal microscopy.

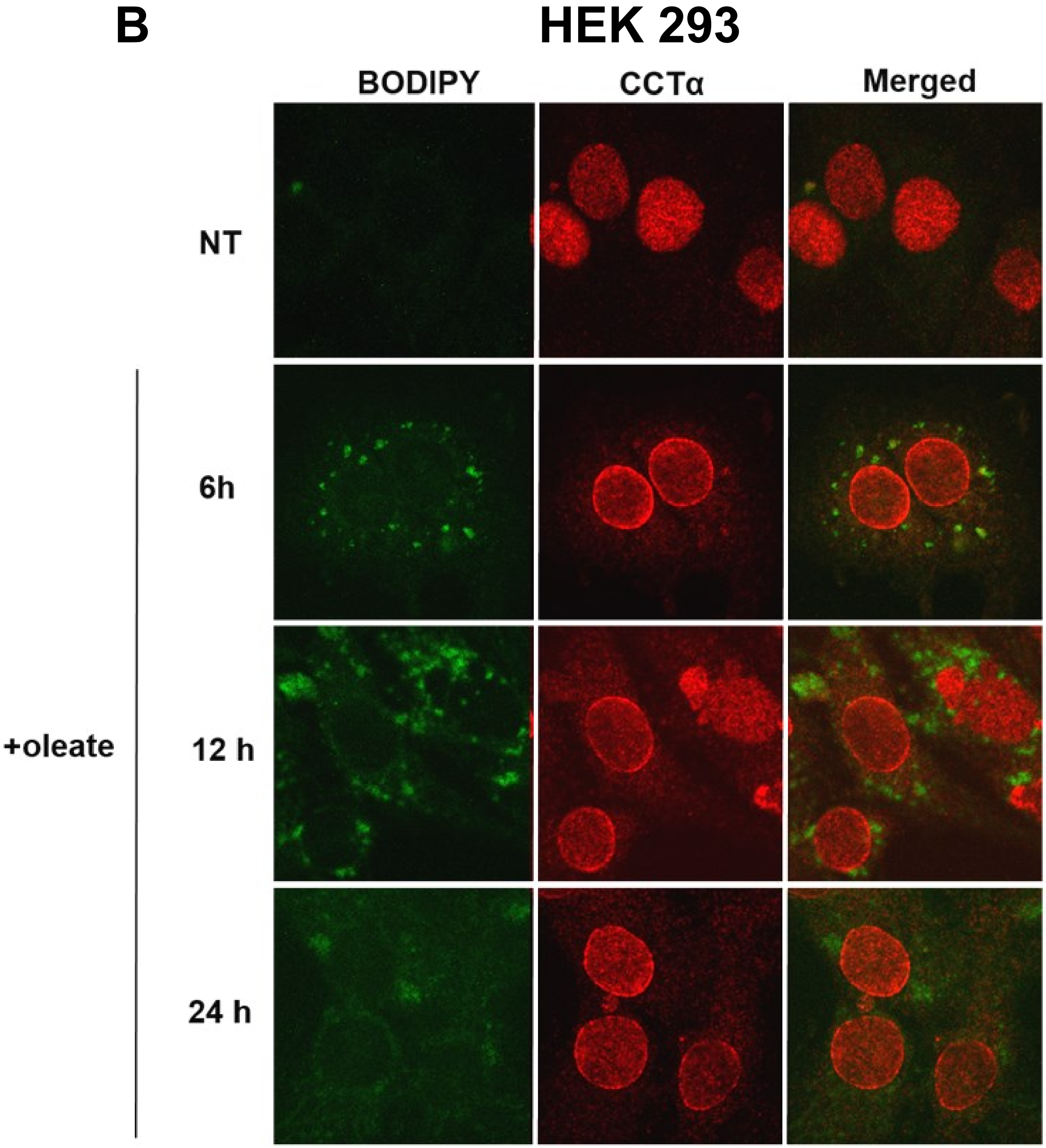
B
HEK 293
BODIPY
CCTα
Merged
NT
6h
12 h
24 h
+oleate

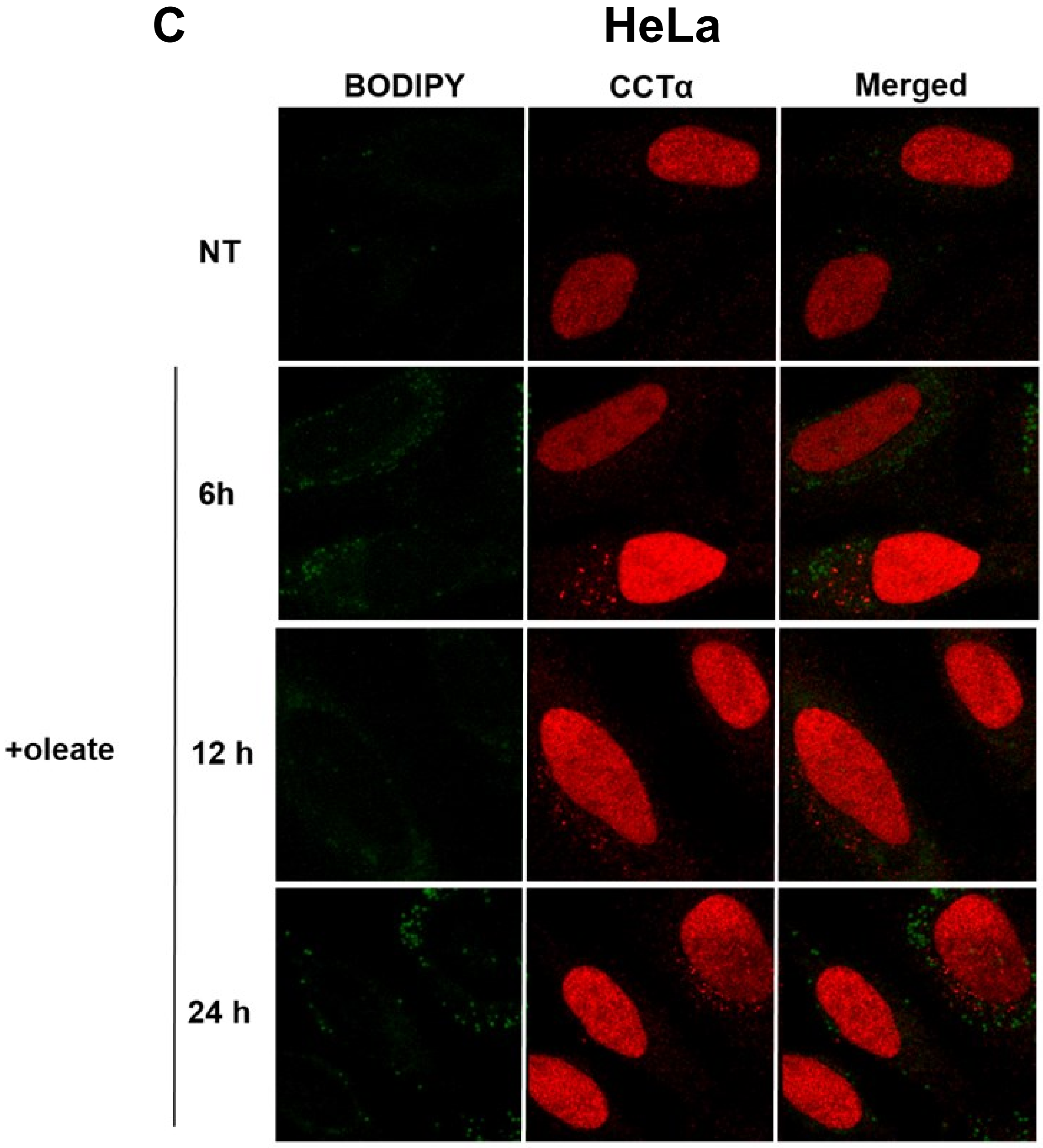
C
HeLa
BODIPY
CCTα
Merged
NT
+oleate
6h
12 h
24 h

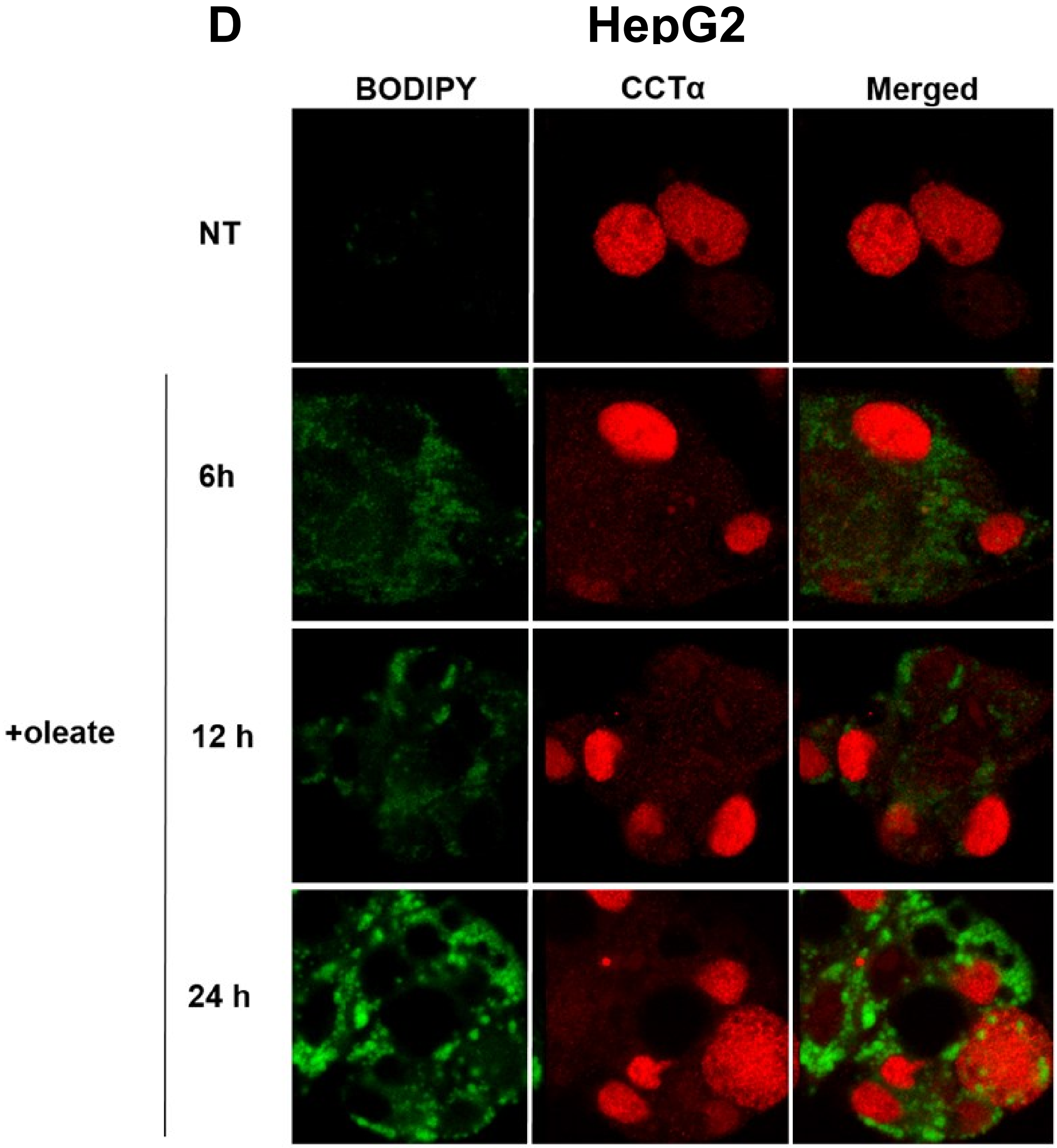
D
HepG2
BODIPY
CCTα
Merged
NT
6h
12 h
24 h
+oleate

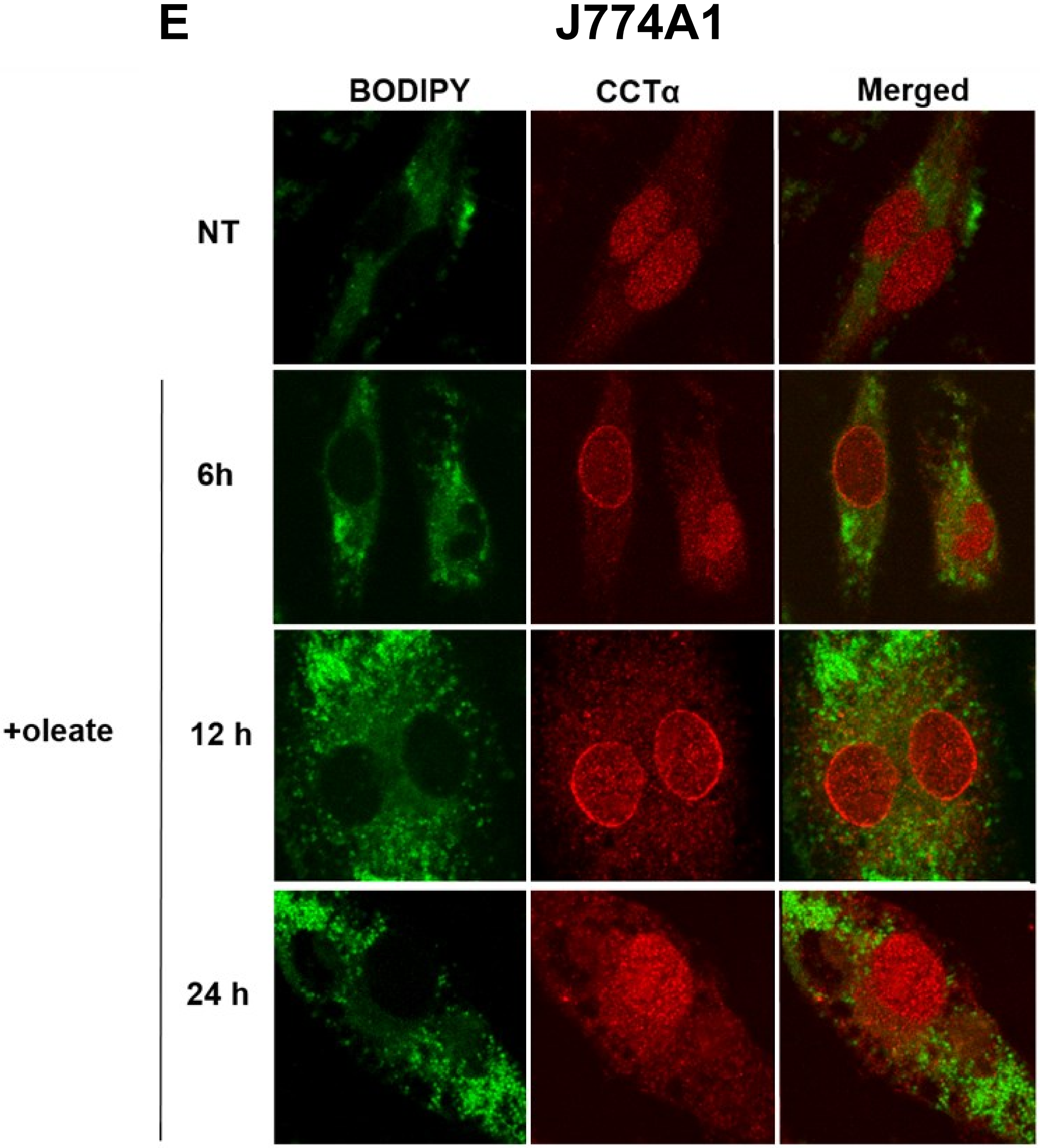
E
J774A1
BODIPY
CCTα
Merged
NT
+oleate
6h
12 h
24 h

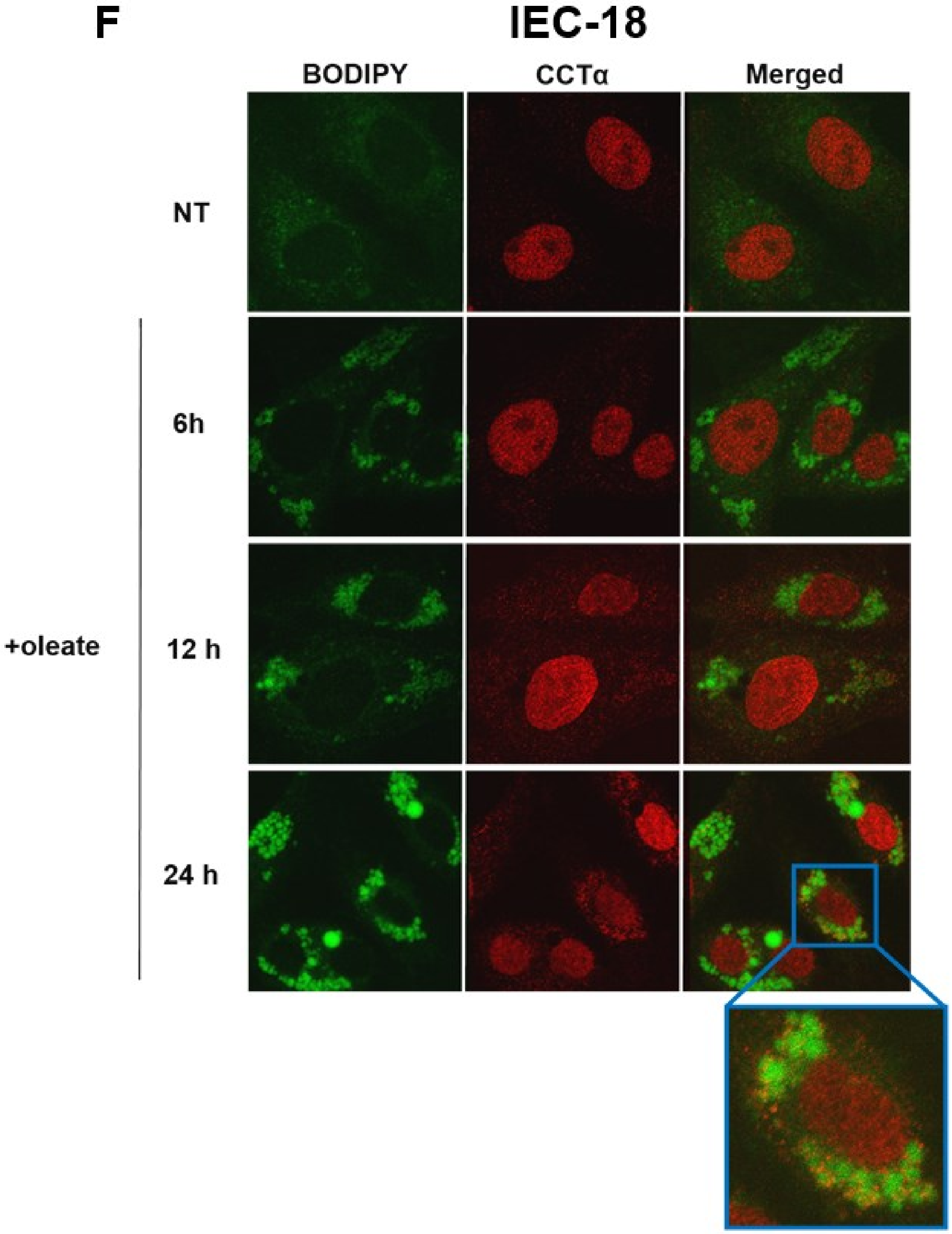
F
IEC-18
BODIPY
CCTα
Merged
NT
+oleate
6h
12 h
24 h

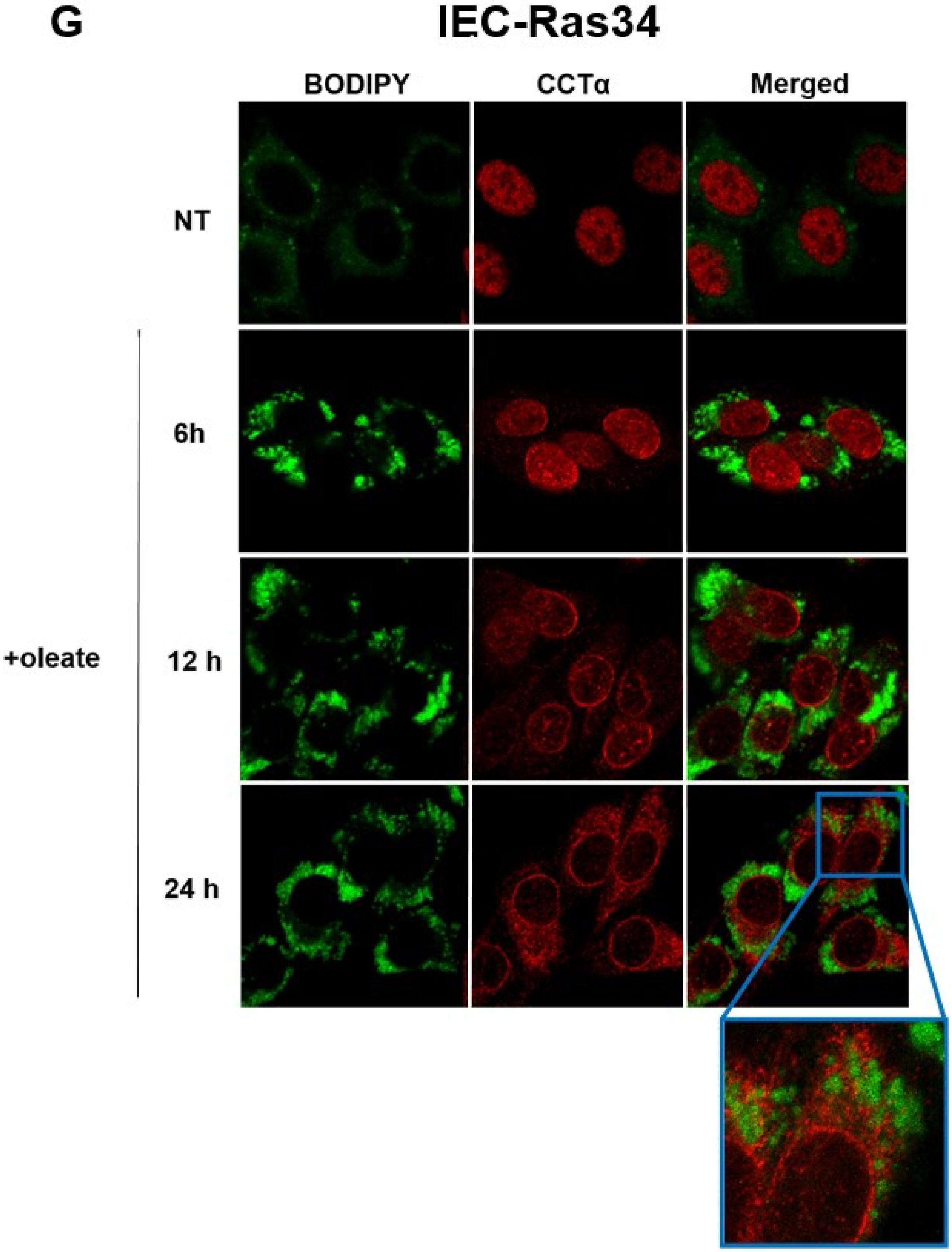
G
IEC-Ras34
BODIPY
CCTα
Merged
NT
+oleate
6h
12 h
24 h

cytosolic localization after 24 h **(Fig 3.3.2B)**. HeLa cells had almost no LDs and CCTα remained nucleoplasmic **(Fig 3.3.2C)**. HepG2 cells had many LDs at 24 h and CCTα was distributed equally between the nucleus and cytosol **(Fig 3.3.2D)**. J774A1 had many small LDs, with CCTα localization at the NE by 6-12 h, followed by extensive export to the cytoplasm by 24 h **(Fig 3.3.2E)**. IEC-18 had many LDs with variable sizes, with some CCTα export but no NE localization by 24 h **(Fig 3.3.2F)**. Finally, IEC-Ras34 had robust LD formation, CCTα associated readily with the NE and was rapidly exported, with almost no nuclear CCTα by 24 h **(Fig 3.3.2G)**. Although CCTα was exported in most cells during oleate treatment, under no circumstance did CCTα localize to the surface of LDs. These results suggest that endogenous CCTα does not localize to the surface of LDs during their formation. However, CCTα was activated during LD formation in IEC-18 and IEC-Ras34, because CCTα was completely dephosphorylated in response to oleate by 12 h (**Fig 3.3.3)**. Phosphorylation was confirmed with an alkaline phosphatase assay (results not shown).

Since CCTα-GFP has been shown to localize to the surface of LDs, it was thought that the fluorescent tag may affect the localization of CCTα. To investigate this, two cell lines from the previous experiment, IEC-18 and IEC-Ras34 were used. Since CCTα-GFP is excited at 488 nm, BODIPY 493/503 could not be used, so the neutral lipid dye DPH was used instead (**Fig 3.3.4)**. In IEC-18 treated with oleate there was LD accumulation and CCTα-GFP localized to the surface of LDs as evidenced by the formation of a green 'ring' around the LDs **(Fig 3.3.4A)**. On the other hand, in IEC-Ras34 treated with oleate there was LD accumulation but CCTα-GFP localized to the NE with very little export

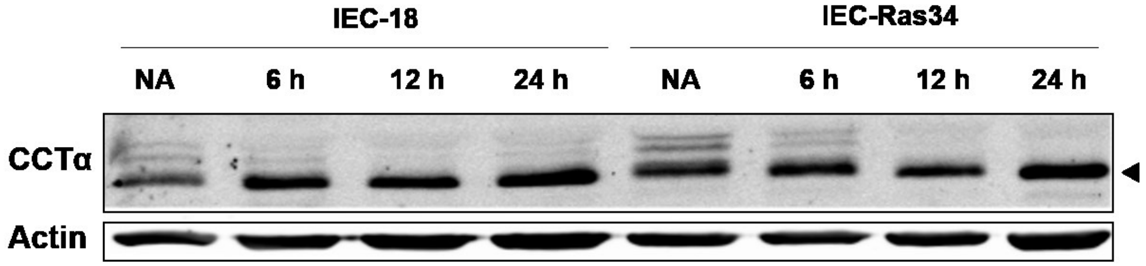

Figure 3.3.3. CCTα is dephosphorylated in IEC-18 and IEC-Ras34 after acute oleate treatment. Cells were treated with 400 μM oleate/BSA for the indicated times. Cells were lysed in an SDS-PAGE lysis buffer and total cell lysates were immunoblotted against CCTα. β-Actin was used as a load control. NA= no addition. The black arrowhead indicates the dephosphorylated form. Immunoblots were visualized using the Odyssey Infrared Imaging System.

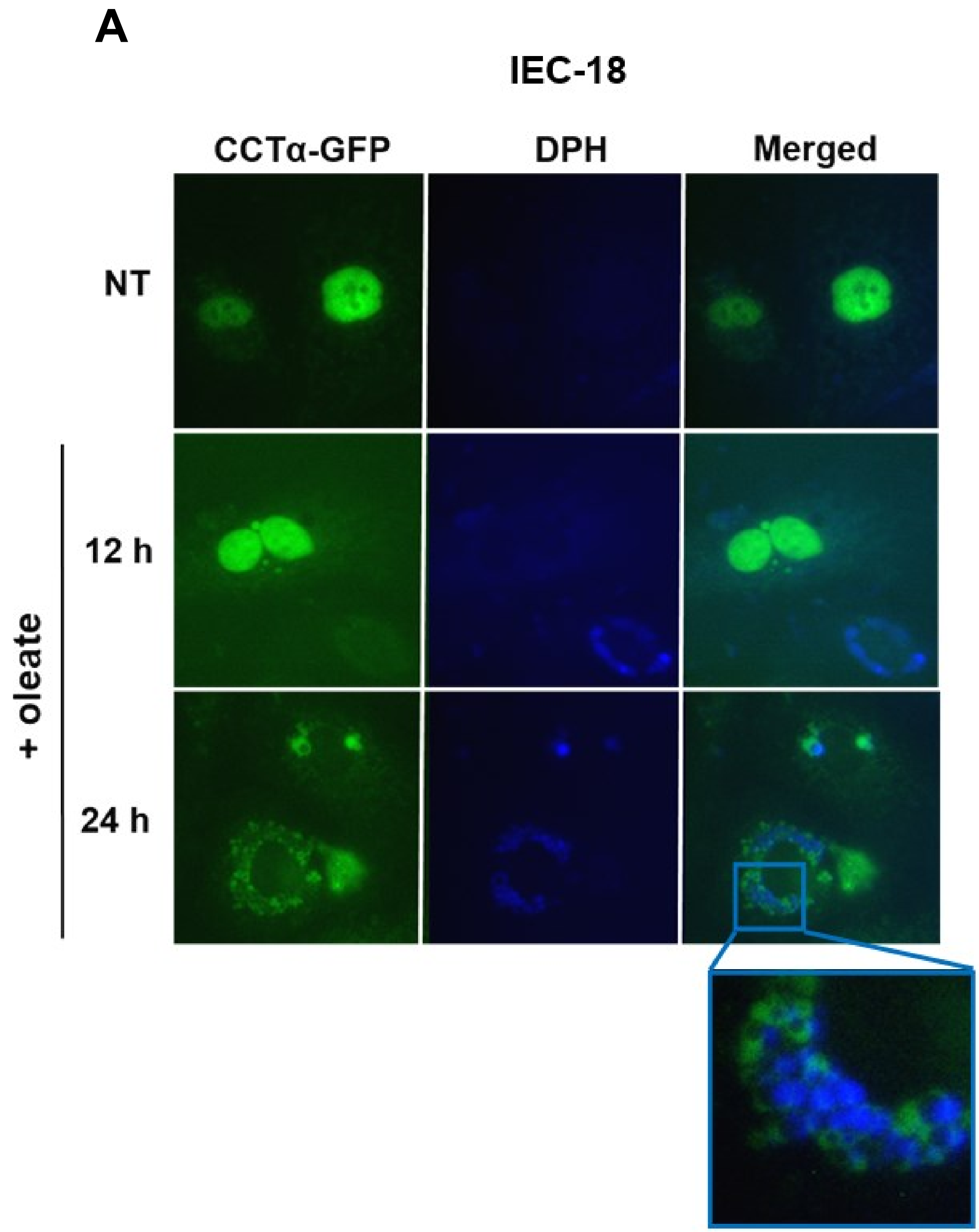

Figure 3.3.4. CCTα-GFP localizes to LDs in IEC-18, but not IEC-Ras34 after acute oleate treatment. IEC-18 **(A)** and IEC-Ras34 **(B)** expressing CCTα-GFP for 24 h were incubated with 400 µM oleate for the indicated times. Cells were fixed, permeabilized with saponin and incubated with DPH (1:1000 in DMSO) and viewed using a Zeiss AxioVert microscope.

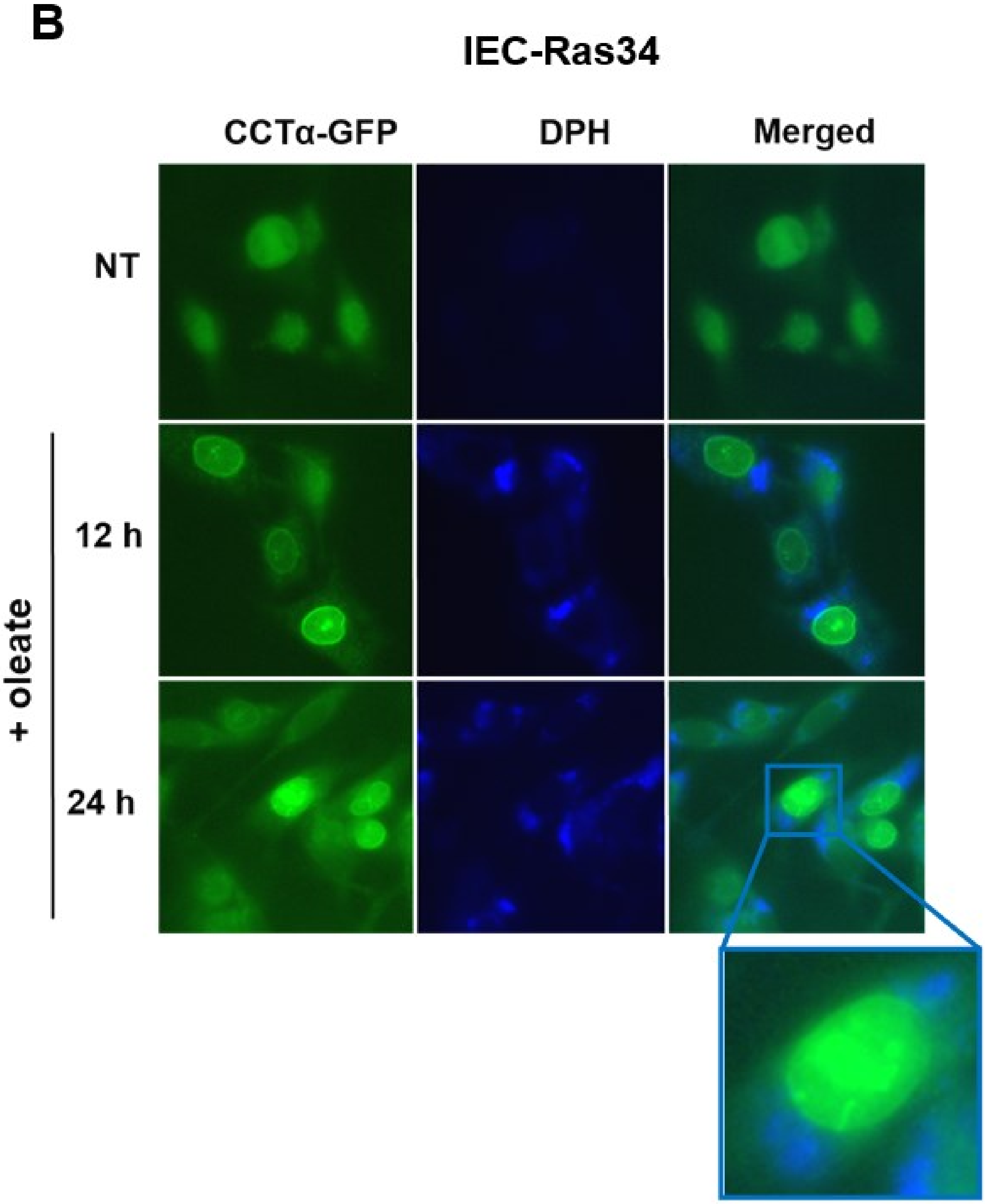
B
IEC-Ras34
CCTα-GFP
DPH
Merged
NT
+ oleate
12 h
24 h

(Fig 3.3.4B). As with endogenous CCTα, there was no localization of CCTα-GFP to the surface of LDs in IEC-Ras34. These results suggest that the GFP tag may affect CCTα localization and may not be a good indicator of LD association by endogenous proteins.

The fluorescent tag GFP is large (approximately 20 kDa) and may influence CCTα localization to the surface of LDs. As a result, a smaller V5/His tagged version of CCTα was used to monitor CCTα localization to the surface of LDs in IEC-18 and IEC-Ras34 **(Fig 3.3.5)**. In IEC-18 there was LD accumulation and CCTα-V5/His was completely cytoplasmic by 24 h **(Fig 3.3.5A)**. However, there was no localization of CCTα-V5/His to the surface of LDs in IEC-18. In IEC-Ras34, CCTα-V5/His localized to the cytoplasm, but not to the surface of LDs as was observed with endogenous CCTα **(Fig 3.3.5B)**. Since CCTα-V5/His behaves similarly to endogenous CCTα, this suggests that the use of fluorescent tags such as GFP may not be ideal for monitoring protein localization to the surface of LDs.

If CCTα is in fact important for synthesis of PtdCho for the formation of LDs, then silencing CCTα should result in compromised LD formation. To investigate this, CCTα was silenced in IEC-18 and IEC-Ras34 with the previously validated shRNA **(Section 3.2)** and LD formation was measured by staining with BODIPY 493/503 and the nuclear marker NPC **(Fig 3.3.6)**. CCTα knockdown was successful and over 90% in both IEC-18 and IEC-Ras34 **(Fig 3.3.6A)**. In CCTα-silenced IEC-18, there were fewer LDs that were larger at 12 h and 24 h suggesting fusion of smaller LDs **(Fig 3.3.6B)**. In CCTα-silenced IEC-Ras34, there was no apparent change in either the number or size of LDs **(Fig 3.3.6C)**. These results suggest that CCTα may have an important role in preventing coalescence of LDs.

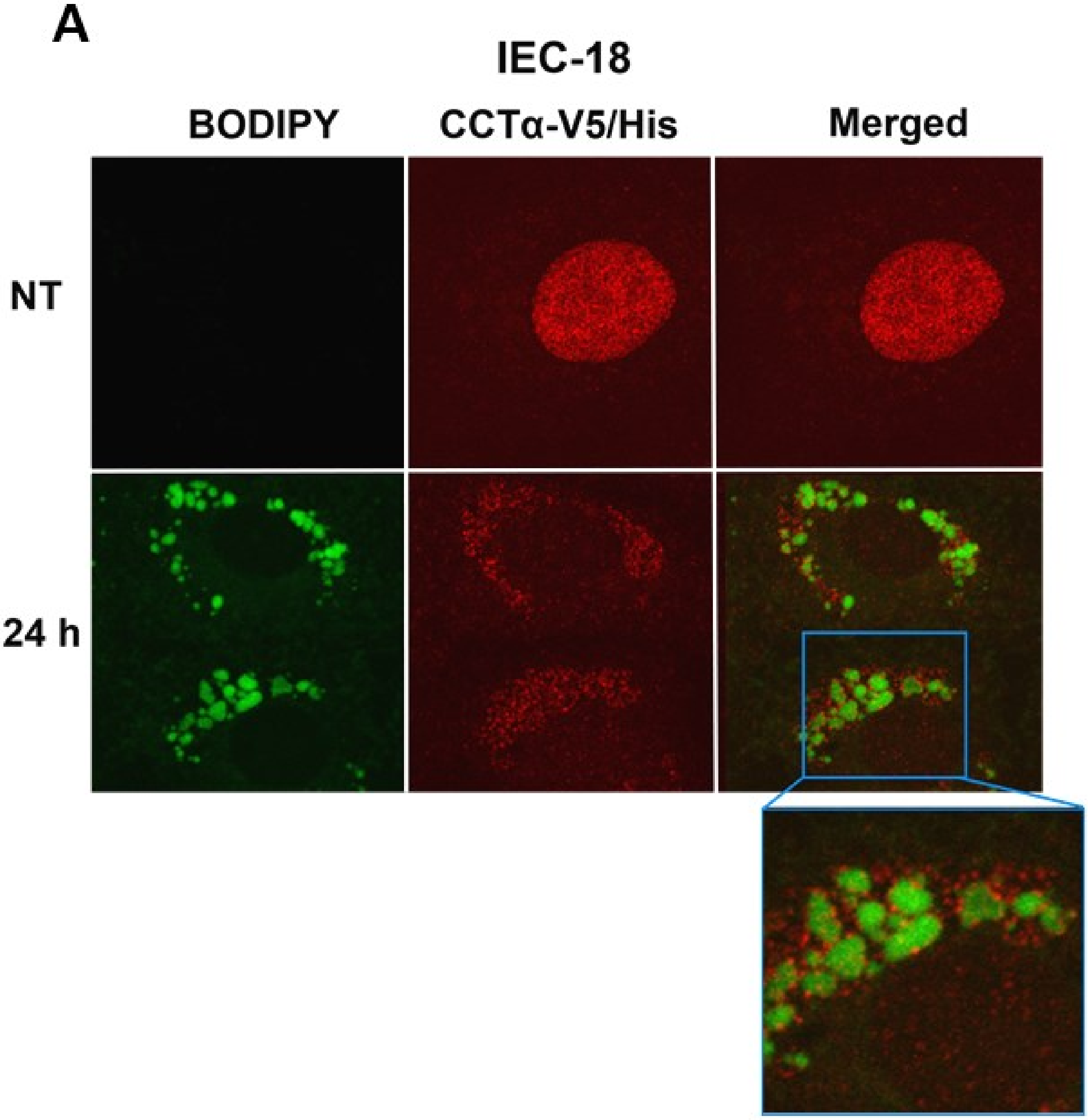

Figure 3.3.5. CCTα V5/His does not localize to LDs in IEC-18 or IEC-Ras after acute oleate treatment. IEC-18 **(A)** and IEC-Ras34 **(B)** expressing CCTα-V5/His for 24 h were incubated with 400 µM oleate/BSA for 24 h. Cells were fixed, permeabilized with saponin and incubated with mouse anti-V5 (1:2000) and BODIPY 493/503 and viewed using confocal microscopy.

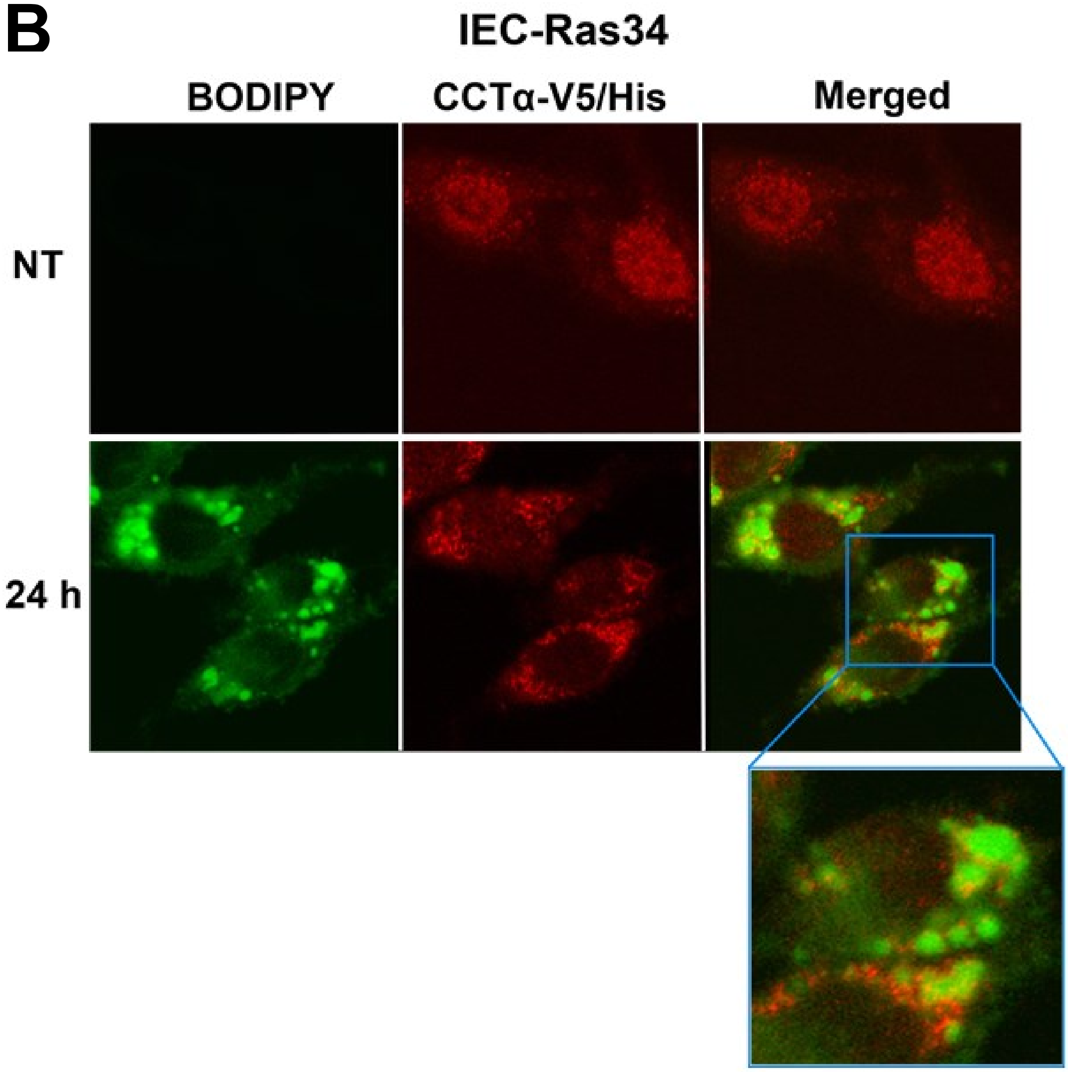
B
IEC-Ras34
BODIPY
CCTα-V5/His
Merged
NT
24 h

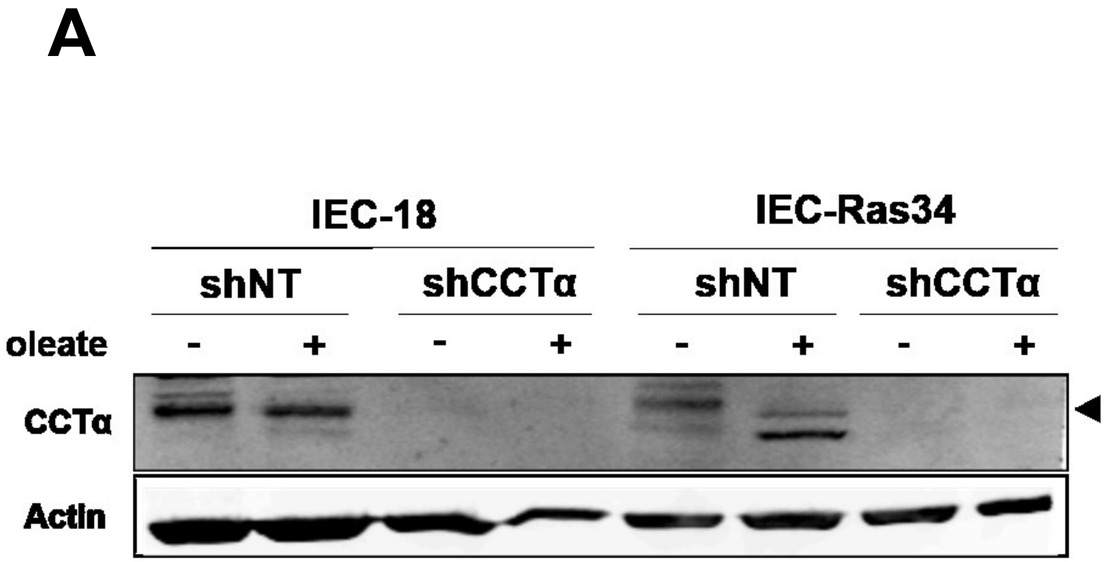

Figure 3.3.6. Effect of CCTα silencing on LD formation in IEC-18 and IEC-Ras34. IEC-18 and IEC-Ras34 were infected with virus encoding shRNA against CCTα (shCCTα) or non-targeting shRNA (shNT) and selected with puromycin. Cells were treated with or without 400 μM oleate/BSA for 24 h. Cells were lysed in an SDS-PAGE lysis buffer and total cell lysates were immunoblotted against CCTα **(A)**. The black arrowhead indicates the dephosphorylated form. IEC-18 **(B)** and IEC-Ras34 **(C)** were fixed, permeabilized with saponin and incubated with mouse anti-NUP62 (NPC; 1:1500), BODIPY 493/503 (1:1000) and viewed using confocal microscopy.

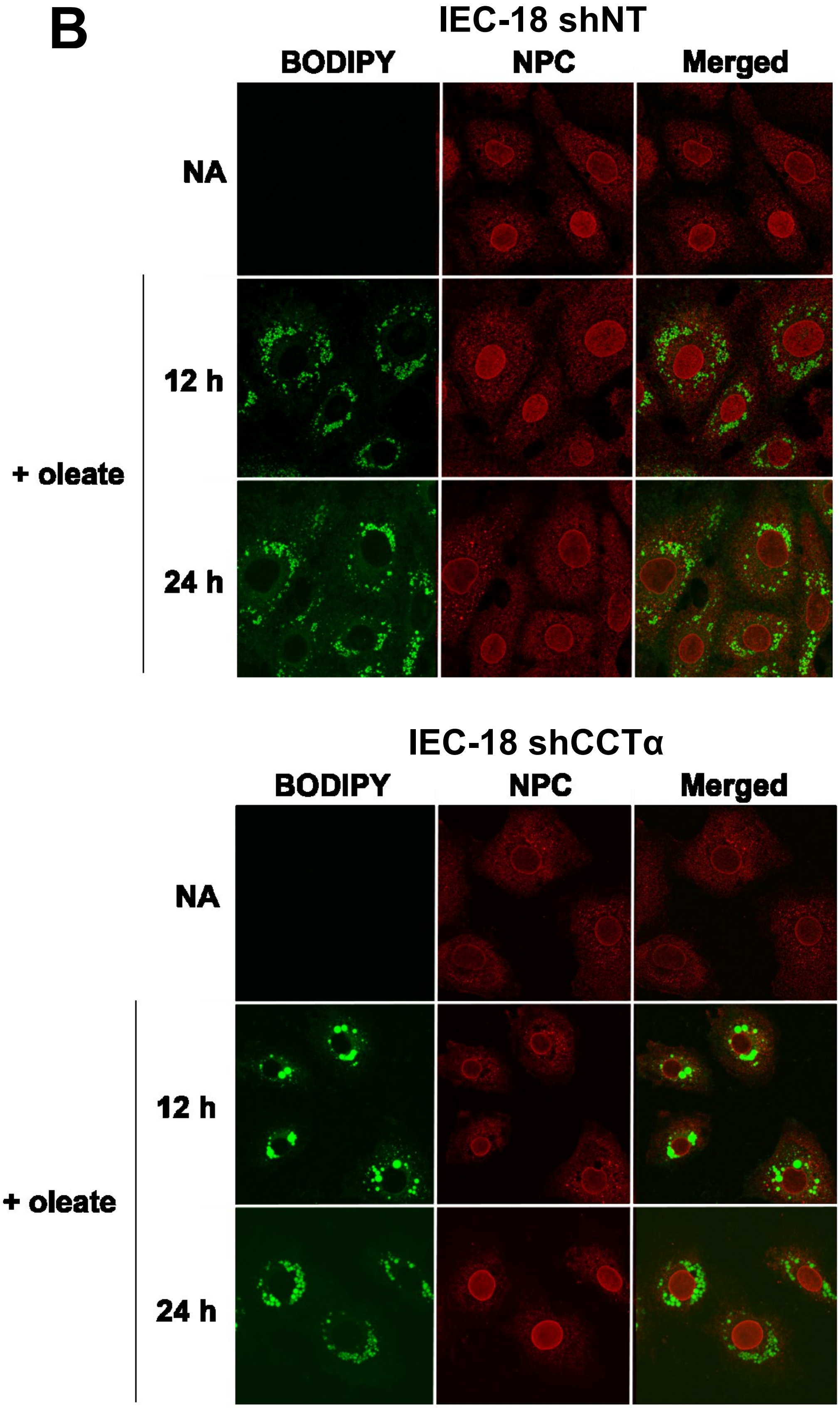
B
IEC-18 shNT
BODIPY
NPC
Merged
NA
12 h
+ oleate
24 h
IEC-18 shCCTα
BODIPY
NPC
Merged
NA
12 h
+ oleate
24 h

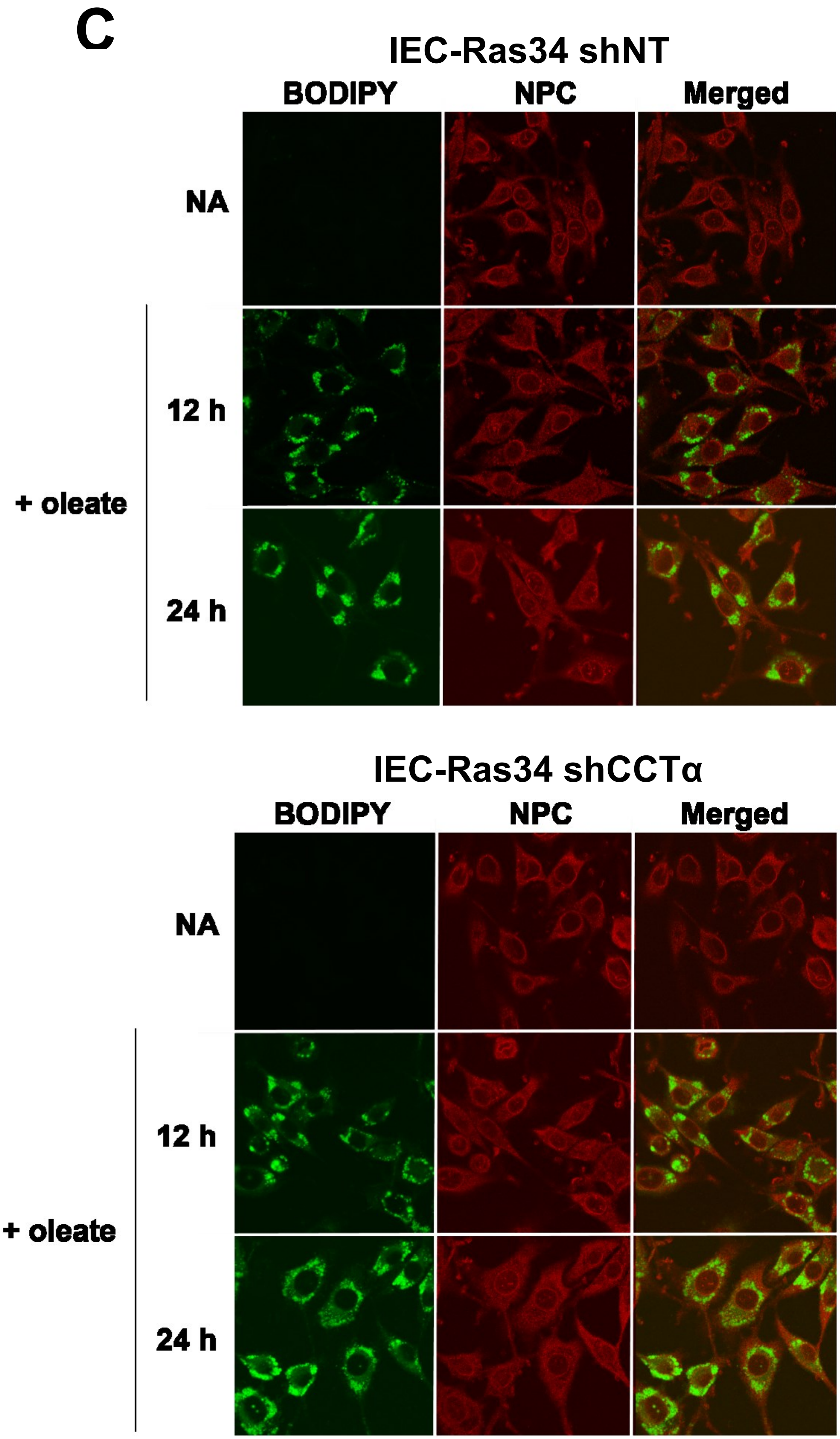
C
IEC-Ras34 shNT
BODIPY
NPC
Merged
NA
12 h
24 h
+ oleate
IEC-Ras34 shCCTα
BODIPY
NPC
Merged
NA
12 h
24 h
+ oleate

Interestingly, oleate appeared to be toxic to CCTα-silenced IEC-18 cells (when viewed under a light microscope) suggesting that the lack of CCTα in these cells compromises LD formation resulting in cellular toxicity and decreased viability. To determine whether cell viability was compromised in CCTα-silenced IEC-18 treated with oleate, an MTT assay was used (**Fig 3.3.7**). Silencing CCTα in the IEC-Ras34 and treating with increasing amounts of oleate (0-400 μM) did not appear to have any cytotoxic effects as the oleate-treated cells had a similar viability as compared to cells that received no oleate. However, this assay should also be completed with other IEC-Ras clones. On the other hand, silencing CCTα in the IEC-18 and treating with increasing concentrations of oleate resulted in a significant 50% decrease in cell viability compared to shNT transduced cells. Taken together, endogenous CCTα is activated during LD formation, but does not localize to LDs. The role of CCTα during LD formation is not exactly clear, but silencing CCTα makes IEC-18 sensitive to oleate, perhaps due to the increased size of LDs as a result of increased LD coalescence.

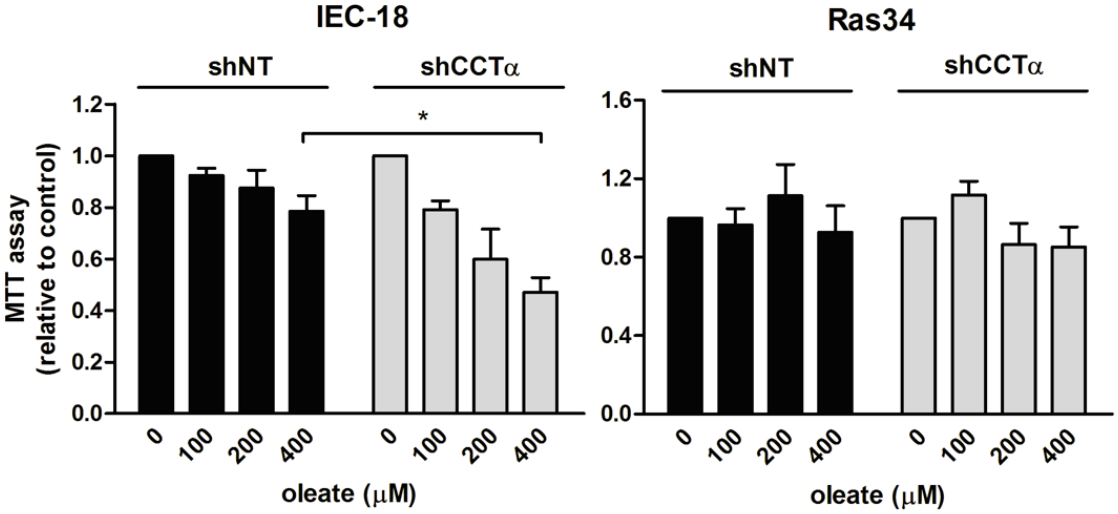

Figure 3.3.7. CCTα-silenced IEC-18 have reduced viability in the presence of increasing amounts of oleate. IEC-18 and IEC-Ras34 were infected with virus encoding shRNA against CCTα (shCCTα) or non-targeting shRNA (shNT) and selected with puromycin. Cells were incubated with increasing concentrations of oleate (0-400 μM) for 24 h and cell viability was measured using the CellTiter 96 AQUEOUS Non-radioactive Cell Proliferation Assay. The values presented are the mean and SEM of three independent experiments. * $P < 0.05$ using a student's *t*-test assuming unequal variances.

CHAPTER 4: DISCUSSION

4.1 High Affinity Choline Transport is Inhibited During Apoptosis

Inhibition of phospholipid synthesis is a common feature of apoptosis and results in perturbations to membrane structure and blocks synthesis of phospholipid-derived secondary messengers. The most abundant phospholipid in eukaryotic cells is PtdCho and synthesis of PtdCho by the CDP-choline pathway is inhibited during apoptosis. In addition, apoptosis is met with increased PtdCho degradation. For example, hydrolysis of PtdCho by phospholipase A1 produces lysoPtdCho - a potent signal for phagocytosis [227]. Inhibition of PtdCho synthesis blocks cell cycle progression resulting in growth arrest and apoptosis. Although we know that the CDP-choline pathway is inhibited during apoptosis, the exact mechanism by which this occurs is unknown. The terminal enzymes in the pathway, CPT and CEPT, are targeted by apoptotic drugs such as farnesol and their inhibition resulted in decreased PtdCho synthesis during apoptosis. However, the substrate for this reaction, CDP-choline, did not accumulate in apoptotic cells and overexpression of CPT did not rescue cells from farnesol-induced apoptosis, suggesting additional targets [228]. On the other hand, CCTα has a cleavage site for effector caspases. Since CCTα expression and activity correlates with cell cycle progression and PtdCho demand, inhibition of CCTα would serve to ablate enzyme activity, resulting in growth arrest and apoptosis. However, since the substrate of CCTα, pChol does not accumulate in apoptotic cells, CK and choline transport activities were also measured.

Previous research in our lab showed that *in vitro* translated CCTα was a substrate for caspases 3, 6, 7, 8 and 9, but only caspase 3 was capable of cleaving CCTα in cultured cells. This was thought to be attributed to a loss of spatial regulatory elements and/or a loss of tertiary structure that occurs in a cell-free system [229]. Nonetheless, we decided to investigate the role of caspase 3 in CCTα regulation and PtdCho synthesis during apoptosis. Since siRNA silencing can diminish, but not totally abolish caspase expression, we used an MCF7 cell model system that completely lacks the caspase 3 gene product. Re-expression of caspase 3 using an adenoviral expression system allowed us to compare caspase 3 -independent and -dependent apoptosis. I chose two agents to induce apoptosis. The first was camptothecin (CMT), which induces apoptosis through the intrinsic pathway by blocking DNA replication. The second was TNFα, which induces apoptosis through the extrinsic pathway by activation of caspase 8. This allowed me to determine whether CCTα regulation and PtdCho synthesis during apoptosis was limited to a particular type of apoptotic program.

Treatment with CMT resulted in the cleavage of PARP, a well-known caspase substrate and is often used as an indicator of successful induction of apoptosis (**Fig 3.1.1)**. Although MCF7 cells lack caspase 3, PARP cleavage was still observed, as was expected since many caspases, such as caspase 7, can still cleave these substrates in the absence of caspase 3. On the other hand, CCTα was cleaved only in MCF7-C3 cells treated with either CMT or TNFα, by removal of the NLS (28 amino acids). Interestingly, treatment with TNFα resulted in ubiquitination of CCTα and reduction in CCTα mRNA expression, which might explain why total CCTα expression in MCF7-C3 cells was almost completely abolished by 24 h [230]. However, CCTα expression was only decreased in the MCF7-C3 cells at 24 h suggesting a caspase 3-dependent mechanism. Very few proteins with a TEED↓ sequence are recognized by caspase 3, which prefers aspartate at the P_4 position [122,123]. Nonetheless, threonine is still tolerated and this result, along with the siRNA knockdown studies involving caspase 3 solidifies the idea that CCTα is a caspase 3 substrate in cultured cells, even if it has a sub-optimal caspase 3 cleavage site.

The removal of the NLS by caspase 3 during apoptosis localizes CCTα to the cytoplasm. CCTα exists predominantly as a soluble nuclear enzyme and removal of the NLS would serve to exclude it from the nucleus. Caspase-cleaved mimics of CCTα are cytoplasmic and have increased activity thought to be a result of close proximity to the other enzymes in the CDP-choline pathway, such as CPT/CEPT [79,193]. Although CCTα is exported from the nucleus and PtdCho synthesis is decreased during FOH-induced apoptosis, this is largely attributed to CPT/CEPT inhibition and DAG depletion, leaving the exact role of CCTα cleavage and mislocalization unanswered. One possible explanation is that blocking CCTα re-entry into the nucleus serves to limit interactions with key nuclear factors. For instance, CCTα is required for the proliferation of the NR and disrupting formation could cause apoptosis independently of PtdCho synthesis [105].

Nonetheless, CCTα was excluded from the nucleus only in cells re-expressing caspase 3 (**Fig 3.1.2)**. Interestingly, CCTα translocated to the nuclear envelope (NE) and was exported from the nucleus independently of caspase-cleavage in response to CMT and TNFα, raising the question as to whether caspase cleavage occurs before or after nuclear export [70]. NE localization of CCTα was not observed in either MCF7 or MCF7-C3 cells treated with CMT (**Fig 3.1.2)**, but MCF7-C3 cells did have reduced staining of the nuclear pore complex (NPC). It is entirely possible that increased cytoplasmic CCTα could be due to a loss of nuclear integrity. Nonetheless, the removal of the NLS is a potential mechanism to keep CCTα excluded from the nucleus in apoptotic cells.

If any of the enzymes of the CDP-choline pathway, including CCTα, are regulated by apoptosis, then there should be a noticeable difference in the flux of [^{3}H]choline through the pathway during a pulse-chase experiment. The benefit of this experiment is two-fold. First, an accumulation or reduction in intermediates or products is indicative of inhibition of a particular enzyme in the pathway. Second, CCTα activity can be inferred based on the conversion of the precursor pChol to the product PtdCho (**Fig 3.1.3**). There was no evidence of CDP-choline accumulation, suggesting that CEPT/CPT activity was unaffected. Interestingly, initial pChol levels after 24 h of CMT treatment were about 50% lower in both cell lines, suggesting inhibition at an early step of the pathway. CCTα activity was also reduced post 24 h CMT treatment in both cell lines by about 50% based on conversion of pChol to PtdCho. This suggests that inhibition of CCTα activity is caspase 3-independent since we also observed reduced activity in cells lacking caspase 3. This observation could be a result of many factors independent of cleavage and nuclear export, including a reduction in the levels of pChol and CTP, as well as cellular acidification that accompanies apoptosis [155]. This would explain why there is increased *in vitro* activity of caspase-cleaved CCTα mimics when soluble and membrane-bound fractions were assayed from CHO-MT58, but not in whole cells [193].

Although CCTα activity is reduced by 50% in MCF7 and MCF7-C3 cells, this was insufficient to explain the decreased incorporation of [^{3}H]choline into pChol during pulse chase **(Fig 3.1.3)** and steady-state experiments. [^{3}H]pChol did not accumulate in apoptotic cells suggesting that an earlier step in the CDP-choline pathway was inhibited.

Although CK had not been previously thought of as a target of apoptotic programs, its roles in proliferation and the cell cycle implicated it as such. In support of this, CKα depletion by RNAi reduced proliferation and induced apoptosis in cancer cells [231]. However, CK activity was unaffected in either MCF7 or MCF7-C3 cells after treatment with CMT (**Fig 3.1.4)**, indicating that CK is not a target of CMT-induced apoptosis. There is one caveat to this experiment; *in vitro* CK activity was assayed under ideal conditions such as pH. Since apoptosis results in acidification and decreased pH in an intact cell, it cannot be definitely concluded that CK is not targeted during apoptosis.

Since most eukaryotic cells are unable to synthesize choline *de novo*, suppression of choline uptake would limit the flux of choline through the pathway, resulting in decreased PtdCho synthesis. This would be sufficient to explain why there is reduced incorporation of [^{3}H]choline into all metabolites along the pathway. It was found that maximal uptake of choline was reduced in both apoptotic MCF7 and MCF7-C3 cells (**Fig 3.1.5)**. This result is in agreement with other studies that show a general suppression of choline input into the pathway during detachment-, farnesol- and chelerythrine-dependent apoptosis [70,187,228], although I am the first to assay uptake directly. Since reduced choline uptake was observed in both MCF7 and MCF7-C3 cells, it can be concluded that blocking choline transport is largely caspase 3-independent. However, there was an even greater inhibition in the cells that re-express caspase 3, suggesting an additional caspase 3-dependent component. The reason for an additional caspase 3-dependent component is not apparent. Although choline uptake was inhibited, the mechanism, or the type of choline transporter(s) inhibited is unknown. Based on HC-3 inhibition studies (**Fig 3.1.6)** it was found that the intermediate or high-affinity choline transporters were targeted during CMT-induced apoptosis, since supplementation with HC-3 in addition to CMT did not result in greater inhibition in MCF7 cells than CMT alone, but did inhibit it further in MCF7-C3 cells. Based on mRNA expression profiles for MCF7 cells, the transporter most likely inhibited is CTL1 [178] and this is in agreement with our findings. However, protein expression of CTL1 by immunoblotting should also be performed to investigate whether there is a concomitant decrease in CTL1 protein expression during apoptosis in MCF7 and MCF7-C3 cells.

The next question was whether a reduction in choline uptake is observed in other forms of apoptosis. I chose to investigate the effect of anoikis on PtdCho synthesis. Understanding how PtdCho synthesis is targeted during detachment in normal cells may provide insight into how PtdCho synthesis is altered in transformed IEC-Ras to promote survival following detachment from the ECM. After 72 h detachment, it was found that IEC-18 had virtually no incorporation of choline into any metabolites in the CDP-choline pathway [187] . However, by 24 h most IEC-18 were dead (~92%) so it is difficult to determine whether decreased PtdCho synthesis preceded anoikis, or whether the decrease was a general phenomenon of cells being dead and no longer metabolically active [232]. Since I posit that inhibition of PtdCho synthesis is a relatively early event in apoptosis, it was worth investigating PtdCho synthesis at earlier time points. Moreover, even at shorter time points, there is evidence of anoikis, such as upregulation of the tumour suppressor Chk2, and cells are still viable [233]. Indeed, there was reduced choline incorporation into all metabolites in the CDP-choline pathway, suggesting inhibition at an earlier step (**Fig 3.1.7**). This result is in agreement with the CMT experiments involving MCF7 cells. Not surprisingly, reduced choline uptake was a result of choline transporter inhibition (**Fig 3.1.8).** One caveat is that a reduction in choline uptake and flux through the pathway could be attributed to the removal of cell surface choline transporters during trypsinization. Therefore, I assayed choline uptake activity immediately after trypsinization and found no difference in attached versus detached IEC-18 (data not shown). Alternatively, a less aggressive method of detachment, such as treatment with EDTA could be used. It would also be interesting to repeat these experiments with the anoikis-resistant IEC-Ras to see whether there is any change in PtdCho synthesis during early detachment or whether choline transport is increased.

Cancer cells have increased synthesis of PtdCho as a result of upregulation of the enzymes in the CDP-choline pathway, such as CK and CCTα. In addition to contributing to PtdCho synthesis, CK has additional roles in survival and proliferation and is required for the generation of pChol, which contributes to mitogenic signalling in addition to PtdCho synthesis [174]. Apoptosis (including anoikis) blocks high-affinity choline uptake, ablating the flux of choline through the pathway. Caspase cleavage and export of CCTα appears to be secondary and overshadowed by pathway inhibition due to decreased choline transport.

4.2 CCTα is Required For Anoikis Resistance in IEC-Ras34

Oncogenic Ras is highly expressed in many tumour types, predominantly in adenocarcinomas of the pancreas (90%), colon (50%) and lung (30%) [234]. Not surprisingly, knockdown of Ras significantly reduced proliferative capacity of such cancers, leading to a less aggressive tumour. However, targeting oncogenic Ras is difficult from a therapeutic standpoint, due to the picomolar affinity for GTP and absence of regulatory sites for allosteric inhibition [235]. As a result, it is often desirable to target the downstream effectors of Ras that are aberrant in various cancers. One such target is MAPK, and pharmacological inhibitors have recently advanced to clinical trials [236].

Ras transformed cells have increased PtdCho synthesis and catabolism, and elevated levels of choline metabolites are often attributed to increased CKα activity [45,237,238]. However, CKα is not rate-limiting suggesting an important role for CCTα in providing PtdCho for Ras transformed cells. Adherent IEC-Ras have increased CCTα expression, but do not have a concomitant increase in PtdCho synthesis, indicating that the bulk of CCTα is inactive. However, upon detachment from an ECM PtdCho synthesis is increased, suggesting that CCTα may be activated [187]. Since activation of CCTα is correlated with membrane association, it was thought that CCTα may localize to membranes during detachment. Interestingly, CCTα remained nucleoplasmic during detachment **(Fig 3.2.1)**. This result agrees with a previous study that showed CCTα undergoing a time-dependent increase in phosphorylation, which is associated with the inactive soluble form [187]. It is possible that CCTα remained nucleoplasmic because of a requirement for interactions with key nuclear factors. For example, CCTα is required for the expansion of the NR by a mechanism that is independent of PtdCho synthesis [105]. CCTα is important for anoikis-resistance of IEC-Ras because silencing CCTα results in anoikis-sensitivity. This increased sensitivity may be due to decreased PtdCho synthesis in the CCTα-silenced cells upon detachment, further suggesting a catalytic primary role for CCTα.

Perturbation in PtdCho metabolism is sufficient to induce an ER unfolded protein response (UPR). For example, PtdCho synthesis was increased in macrophages subjected to free cholesterol loading, or differentiating B-cells in response to lipopolysaccharide

(LPS) [239]. Increased phospholipid synthesis is important for expansion of ER membranes during induction of an UPR, allowing the cell to alleviate the increased ER stress [240]. It follows that if phospholipids such as PtdCho are not available during the induction of an UPR, then the cell is unable to cope with ER stress and will undergo apoptosis. The molecular mechanism linking the UPR to increased PtdCho synthesis is poorly understood. The ER endoribonuclease IRE1α splices XBP1, a transcription factor involved in the expression of genes involved in the ER stress response. XBP1 activation results in a small increase in CCT activity, without a change in protein expression levels [226]. In CCTα-silenced cells, there was an initial increase in the expression of IRE1α (**Fig 3.2.3)**. This suggests that CCTα-silenced cells have increased activation of XBP1, in an attempt to increase activity of any residual CCTα. However, upon detachment, IRE1α expression decreases in CCTα-silenced cells suggesting a decrease in the UPR. Moreover, XBP1 is overexpressed in many cancers and is associated with rapid progression through the cell cycle [241]. The decrease in IRE1α expression (leading to decreased XBP1) could contribute to growth arrest observed in the CCTα-silenced IEC-Ras34 when detached. Moreover, JNK is downstream of IRE1α and follows a similar activation pattern as IRE1α expressing. Since JNK activation is dependent on IRE1α activity, the similar pattern suggests that IRE1α expression and activity are related. These results suggest that CCTα-silenced cells have increased UPR initially, but upon detachment, the UPR response decreases, indicating an inability to cope with increased ER stress, potentially leading to cell death or growth arrest.

4.3 CCTα Does Not Localize to Expanding LDs

CCTα is required for the synthesis of PtdCho on the surface of expanding LDs as identified by an RNAi screen [225]. Interestingly, knockdown of different genes affected LD morphology differently and were categorized based on phenotype. CCTα knockdown resulted in fewer LDs of larger size indicative of coalescence suggesting that PtdCho has an important role in stabilizing growing LDs by regulating size and abundance. Indeed, during LD fusion there is a strong induction of negative membrane curvature that is more easily accommodated when the membranes are enriched in PtdEtn and low in PtdCho [198,214]. Since CCTα is activated in response to localized need of PtdCho at ER and NE membranes, it was thought that CCTα may localize to the surface of LDs in a similar manner to provide PtdCho for expansion of LDs. Krahmer et al. showed that CCTα-GFP localized to the surface of LDs in *Drosophila* S2 cells and was accompanied by increased PtdCho synthesis in response to oleate [218]. It is important to note that the predominant phospholipid in S2 cells is PtdEtn, however knockdown of enzymes involved in PtdEtn synthesis produced no noticeable phenotype [217]. This was interesting because knockdown of PtdCho synthesis genes produced a drastic phenotype despite PtdCho making up a smaller proportion of total phospholipid in these cells [217]. On the other hand, mammalian cells have predominantly PtdCho and less PtdEtn in their membranes, so I wanted to determine whether these results were translatable to a mammalian system [10]. Although our lab has successfully used a GFP tag as a CCTα reporter, it was unknown whether GFP could influence CCTα localization to the surface of LDs [79,105]. GFP is a large protein (238 amino acids) and may influence membrane affinity possibly to the surface of LDs [242]. Therefore, I wanted to determine whether endogenous CCTα localized to the surface of LDs in mammalian cell lines during LD formation.

3T3-L1 preadipocytes are an excellent cell model for studying lipid metabolism. Whereas other cells have the capacity to store TAG and CE in LDs in response to fatty acid stimulation, the main function of adipocytes is to store fat, usually as very large LDs that take up almost the whole cell volume [243]. It was thought that CCTα may localize to the surface of LDs in 3T3-L1 preadipocytes because of the high demand for PtdCho due to rapid accumulation of LDs. However, CCTα localization to the surface of LDs was not observed during 3T3-L1 differentiation **(Fig 3.3.1)**. Fusion of LDs is favourable when membranes are enriched in PtdEtn and low in PtdCho [203]. Therefore, it would be interesting to see whether LDs found in adipocytes with large LDs differ in phospholipid composition compared to LDs found in other cell lines that contain many small LDs. Smaller LDs have a larger surface area, giving them easier access to lipolytic enzymes such as hormone-sensitive lipase, whereas larger LDs would be more suitable for long term storage due to their higher PtdCho content, providing structure and decreased surface area. It would be interesting to determine how cells specifically regulates phospholipid composition of LDs to meet metabolic demand.

Treatment of cells with oleate is a method for stimulating LD formation and I analyzed endogenous CCTα localization during LD formation in multiple cell lines **(Fig 3.3.2)**. As previously mentioned, nuclear CCTα is activated in response to oleate and associates with nuclear and ER membranes via domain M. Following oleate treatment for 12 to 24 h, CCTα translocated to the NE and was exported to the cytosol in all cell lines, but localization to the surface of LDs was not observed. Localization of CCTα to the NE was variable in cells, which was interesting because CCTα export from the nucleus involves association with the NE prior to export. The lack of CCTα localization to the NE in CHO, HeLa, HepG2 and IEC-18 may simply indicate that CCTα may be rapidly exported in these cells, preventing accumulation at the NE. Almost all CCTα was exported in the IEC-Ras34 and correlated with many LDs, whereas CHO and HeLa had very little CCTα export and few LDs. The correlation between LD number and CCTα export suggests that CCTα may play a vital role in the synthesis of PtdCho for LD expansion despite not localizing to the surface of LDs. One possibility is that CCTα is exported and associates with ER membranes to produce CDP-choline for CPT/CEPT. This mechanism seems likely because it couples the two terminal enzymes in the CDP-choline pathway for PtdCho synthesis. However, there was LD formation in cells with nuclear-localized CCTα. This suggests that CCTα was either imported back into the nucleus upon LD formation in these cells, or CCTα functioned entirely within the nucleus, with substrates and products diffusing freely in and out of the nucleus.

I used CCTα tagged with V5/His or GFP to determine whether protein tags affected CCTα localization to the surface of LDs. The V5/His tag is small (3 kDa) and was expected to have minimal impact on protein function. To show this, CCTα-V5/His was expressed in IEC-18 and IEC-Ras34 and its localization analyzed during LD formation. I found that CCTα V5/His behaved similarly to endogenous CCTα in that there was nuclear export with no evidence of it localizing to the surface of LDs **(Fig 3.3.5)**. In addition, CCTα-GFP was expressed in IEC-18 and IEC-Ras34 and its localization analyzed during LD formation. I found that CCTα-GFP localized to the surface of LDs in IEC-18 but not IEC-Ras34, suggesting that the GFP tag may influence

CCTα localization **(Fig 3.3.4)**. A potential reason for why endogenous CCTα did not localize to the surface of LDs is that membrane binding of endogenous CCTα may result in a conformational change or masking of the antibody epitope, preventing recognition during immunohistochemistry. However, we see a similar localization pattern with CCTα-V5/His suggesting that it is not a problem with detection of endogenous CCTα. Alternatively, CCTα localization to the surface of LDs may be specific to certain cells such as S2 cells. However, the most likely reason is that the GFP tag is responsible for targeting CCTα to the surface of LDs. In support of this, it has been previously reported that overexpression of GFP fusion genes resulted in aggregation or mislocalization. [244,245].

CCTα has an important role in LD formation because RNAi silencing in S2 cells resulted in larger LDs [225]. I silenced CCTα in the IEC-18 and IEC-Ras34 to see whether a similar LD phenotype could be achieved in mammalian cells **(Fig 3.3.6)**. In the CCTα-silenced IEC-18 there were fewer LDs of larger size. Interestingly, this was not observed with CCTα-silenced IEC-Ras34, which showed a similar LD size and number compared to control. To confirm these results, knockdown with additional shRNAs against CCTα or rescue assays with different CCTα constructs should be used.

CCTα-silenced IEC-18 grew more slowly and appeared to die when treated with oleate as visualized by light microscopy, suggesting that there was a defect in LD formation resulting in reduced viability. Using an MTT assay to confirm this, I found that CCTα-silenced IEC-18 had reduced viability when treated with increasing concentrations of oleate **(Fig 3.3.7)**. In a physiological context, intestinal cells have a polarized organization consisting of apical and basolateral membranes [246]. This asymmetrical distribution and the presence of highly ordered structures such as tight junctions allows for selective absorption, transport and secretion from the intestinal mucosa. However, isolated intestinal cells grown in culture lose these highly ordered structures and processes, potentially influencing their function [246]. *In vivo,* IEC take up fatty acids from the diet apically, convert them into TAGs to store in LDs or to package into chylomicrons for basolateral secretion [247]. However, recent evidence shows that the main role of enterocyte-specific LDs is to store TAG ultimately destined for chylomicrons [248]. I posit that IEC cultured on dishes lose their polarity and are unable to remove fatty acids as a result of compromised secretion of chylomicrons. As a result, perturbations in the formation of LDs, such as decreased PtdCho synthesis upon CCTα-silencing would lead to an uncontrolled accumulation of fatty acids which may be potentially toxic. Taken together, CCTα is exported from the nucleus or localizes to the NE, but not to the surface of LDs. Nonetheless, CCTα is important for LD homeostasis as silencing CCTα increased sensitivity to oleate. On the other hand, CCTα-silenced IEC-Ras34 did not have reduced viability in the presence of increasing amounts of oleate, so it would be interesting to determine how LD biogenesis and function is regulated in a cancer cell compared to a non-transformed cell.

4.4 Conclusions

PtdCho synthesis is regulated by changes in localization and activity of CCTα. CCTα was cleaved by caspase 3 and exported from the nucleus, but this change in localization contributed minimally to inhibition of the CDP-choline pathway during apoptosis. CCTα remained in the nucleus and was not exported in IEC-Ras34 during detachment from an ECM indicating that the role of CCTα in anoikis-resistance is nuclear and does not require activation through export and association with membranes. The localization of CCTα during LD formation was variable in response to oleate or 3T3-L1 differentiation, with no observed localization to the surface of expanding LDs. Taken together, CCTα localization is an important regulator of enzyme activity.

REFERENCES

1. Levine, Y. and Wilkins, M. (1971). **Structure of oriented lipid bilayers.** *Nature.* **230***(11)*, 69-72

2. Singer, S. J. and Nicolson, G. L. (1972). **The fluid mosaic model of the structure of cell membranes.** *Science.* **175***(23)*, 720-731

3. Dowhan, W. (1997). **Molecular basis for membrane phospholipid diversity: Why are there so many lipids?** *Annu. Rev. Biochem.* **66***(1)*, 199-232

4. Cullis, P. R., Fenske, D. B. and Hope, M. J. (1996). **Physical properties and functional roles of lipids in membranes.** *New comprehensive biochemistry.* **31**, 1-33

5. Fadok, V. A., Bratton, D. L., Frasch, S. C., Warner, M. L. and Henson, P. M. (1998). **The role of phosphatidylserine in recognition of apoptotic cells by phagocytes.** *Cell Death Differ.* **5***(7)*, 551-562

6. Cote, G. G. and Crain, R. C. (1993). **Biochemistry of phosphoinositides.** *Annual review of plant biology.* **44***(1)*, 333-356

7. Blagoveshchenskaya, A., Cheong, F. Y., Rohde, H. M., Glover, G., Knodler, A., Nicolson, T., Boehmelt, G. and Mayinger, P. (2008). **Integration of golgi trafficking and growth factor signaling by the lipid phosphatase SAC1.** *J. Cell Biol.* **180***(4)*, 803-812

8. Zhang, M., Mileykovskaya, E. and Dowhan, W. (2005). **Cardiolipin is essential for organization of complexes III and IV into a supercomplex in intact yeast mitochondria.** *J. Biol. Chem.* **280***(33)*, 29403-29408

9. Kagan, V. E., Tyurin, V. A., Jiang, J., Tyurina, Y. Y., Ritov, V. B., Amoscato, A. A., Osipov, A. N., Belikova, N. A., Kapralov, A. A. and Kini, V. (2005). **Cytochrome c acts as a cardiolipin oxygenase required for release of proapoptotic factors.** *Nature chemical biology.* **1***(4)*, 223-232

10. Colbeau, A., Nachbaur, J. and Vignais, P. (1971). **Enzymac characterization and lipid composition of rat liver subcellular membranes.** *Biochimica et Biophysica Acta (BBA)-Biomembranes.* **249***(2)*, 462-492

11. Van Dijck, P., De Kruijff, B., Verkleij, A., Van Deenen, L. and De Gier, J. (1978). **Comparative studies on the effects of pH and ca< sup> 2 on bilayers of various negatively charged phospholipids and their mixtures with phosphatidylcholine.** *Biochimica et Biophysica Acta (BBA)-Biomembranes.* **512***(1)*, 84-96

12. Nakamura, T., Lin, L. L., Kharbanda, S., Knopf, J. and Kufe, D. (1992). **Macrophage colony stimulating factor activates phosphatidylcholine hydrolysis by cytoplasmic phospholipase A2.** *EMBO J.* **11***(13)*, 4917-4922

13. Monick, M. M., Carter, A. B., Gudmundsson, G., Mallampalli, R., Powers, L. S. and Hunninghake, G. W. (1999). **A phosphatidylcholine-specific phospholipase C regulates activation of p42/44 mitogen-activated protein kinases in lipopolysaccharide-stimulated human alveolar macrophages.** *J. Immunol.* **162***(5)*, 3005-3012

14. Liscovitch, M., Ben-Av, P., Danin, M., Faiman, G., Eldar, H. and Livneh, E. (1993). **Phospholipase D-mediated hydrolysis of phosphatidylcholine: Role in cell signalling.** *J. Lipid Mediat.* **8***(3)*, 177-182

15. Kooijman, E. E., Chupin, V., de Kruijff, B. and Burger, K. N. (2003). **Modulation of membrane curvature by phosphatidic acid and lysophosphatidic acid.** *Traffic.* **4***(3)*, 162-174

16. Foster, D. A. (2007). **Regulation of mTOR by phosphatidic acid?** *Cancer Res.* **67***(1)*, 1-4

17. Li, Z. and Vance, D. E. (2008). **Phosphatidylcholine and choline homeostasis.** *J. Lipid Res.* **49***(6)*, 1187-1194

18. Zhu, X., Song, J., Mar, M., EDWARDS, L. and ZEISEL, S. (2003). **Phosphatidylethanolamine N-methyltransferase (PEMT) knockout mice have hepatic steatosis and abnormal hepatic choline metabolite concentrations despite ingesting a recommended dietary intake of choline.** *Biochem. J.* **370**, 987-993

19. Noga, A. A., Zhao, Y. and Vance, D. E. (2002). **An unexpected requirement for phosphatidylethanolamine N-methyltransferase in the secretion of very low density lipoproteins.** *J. Biol. Chem.* **277***(44)*, 42358-42365

20. Noga, A. A. and Vance, D. E. (2003). **Insights into the requirement of phosphatidylcholine synthesis for liver function in mice.** *J. Lipid Res.* **44***(10)*, 1998-2005

21. Vance, J. E. and Vance, D. E. (2008) Biochemistry of lipids, lipoproteins and membranes. , Elsevier

22. Zinrajh, D., Hörl, G., Jürgens, G., Marc, J., Sok, M. and Cerne, D. (2014). **Increased phosphatidylethanolamine n-methyltransferase gene expression in non-small-cell lung cancer tissue predicts shorter patient survival.** *Oncology Letters.* **7***(6)*, 2175-2179

23. Gibellini, F. and Smith, T. K. (2010). **The kennedy pathway—de novo synthesis of phosphatidylethanolamine and phosphatidylcholine.** *IUBMB Life.* **62***(6)*, 414-428

24. DeLong, C. J., Shen, Y. J., Thomas, M. J. and Cui, Z. (1999). **Molecular distinction of phosphatidylcholine synthesis between the CDP-choline pathway and phosphatidylethanolamine methylation pathway.** *J. Biol. Chem.* **274***(42)*, 29683-29688

25. Seelig, J., MacDonald, P. M. and Scherer, P. G. (1987). **Phospholipid head groups as sensors of electric charge in membranes.** *Biochemistry (N. Y.).* **26***(24)*, 7535-7541

26. Wang, Y., Cao, Z., Newkirk, R. F., Ivy, M. T. and Townsel, J. G. (2001). **Molecular cloning of a cDNA for a putative choline co-transporter from< i> limulus CNS.** *Gene.* **268***(1)*, 123-131

27. Apparsundaram, S., Ferguson, S. and Blakely, R. (2001). **Molecular cloning and characterization of a murine hemicholinium-3-sensitive choline transporter.** *Biochem. Soc. Trans.* **29***(6)*, 711-716

28. Okuda, T. and Haga, T. (2003). **High-affinity choline transporter.** *Neurochem. Res.* **28***(3-4)*, 483-488

29. Michel, V., Yuan, Z., Ramsubir, S. and Bakovic, M. (2006). **Choline transport for phospholipid synthesis.** *Exp. Biol. Med. (Maywood).* **231***(5)*, 490-504

30. GORBOULEV, V., ULZHEIMER, J. C., AKHOUNDOVA, A., ULZHEIMER-TEUBER, I., KARBACH, U., QUESTER, S., BAUMANN, C., LANG, F., BUSCH, A. E. and KOEPSELL, H. (1997). **Cloning and characterization of two human polyspecific organic cation transporters.** *DNA Cell Biol.* **16***(7)*, 871-881

31. Okuda, M., Saito, H., Urakami, Y., Takano, M. and Inui, K. (1996). **cDNA cloning and functional expression of a novel rat kidney organic cation transporter, OCT2.** *Biochem. Biophys. Res. Commun.* **224***(2)*, 500-507

32. Kekuda, R., Prasad, P. D., Wu, X., Wang, H., Fei, Y. J., Leibach, F. H. and Ganapathy, V. (1998). **Cloning and functional characterization of a potential-sensitive, polyspecific organic cation transporter (OCT3) most abundantly expressed in placenta.** *J. Biol. Chem.* **273***(26)*, 15971-15979

33. Grundemann, D., Liebich, G., Kiefer, N., Koster, S. and Schomig, E. (1999). **Selective substrates for non-neuronal monoamine transporters.** *Mol. Pharmacol.* **56***(1)*, 1-10

34. Sala-Rabanal, M., Li, D. C., Dake, G. R., Kurata, H. T., Inyushin, M., Skatchkov, S. N. and Nichols, C. G. (2013). **Polyamine transport by the polyspecific organic cation transporters OCT1, OCT2, and OCT3.** *Molecular pharmaceutics.* **10***(4)*, 1450-1458

35. Ueda, H., Horibe, Y., Kim, K. J. and Lee, V. H. (2000). **Functional characterization of organic cation drug transport in the pigmented rabbit conjunctiva.** *Invest. Ophthalmol. Vis. Sci.* **41***(3)*, 870-876

36. Osredkar, D., Burnik-Papler, T., Pečavar, B., Kralj-Iglič, V. and Kržan, M. (2009). **Kinetic and pharmacological properties of [3H]-histamine transport into cultured type 1 astrocytes from neonatal rats.** *Inflammation Res.* **58***(2)*, 94-102

37. Traiffort, E., Ruat, M., O'Regan, S. and Meunier, F. (2005). **Molecular characterization of the family of choline transporter-like proteins and their splice variants.** *J. Neurochem.* **92***(5)*, 1116-1125

38. Michel, V. and Bakovic, M. (2012). **The ubiquitous choline transporter SLC44A1.** *Central Nervous System Agents in Medicinal Chemistry (Formerly Current Medicinal Chemistry-Central Nervous System Agents).* **12***(2)*, 70-81

39. Yuan, Z., Wagner, L., Poloumienko, A. and Bakovic, M. (2004). **Identification and expression of a mouse muscle-specific CTL1 gene.** *Gene.* **341**, 305-312

40. Nakamura, T., Fujiwara, R., Ishiguro, N., Oyabu, M., Nakanishi, T., Shirasaka, Y., Maeda, T. and Tamai, I. (2010). **Involvement of choline transporter-like proteins, CTL1 and CTL2, in glucocorticoid-induced acceleration of phosphatidylcholine synthesis via increased choline uptake.** *Biological and Pharmaceutical Bulletin.* **33***(4)*, 691-696

41. Ishiguro, N., Oyabu, M., Sato, T., Maeda, T., Minami, H. and Tamai, I. (2008). **Decreased biosynthesis of lung surfactant constituent phosphatidylcholine due to inhibition of choline transporter by gefitinib in lung alveolar cells.** *Pharm. Res.* **25***(2)*, 417-427

42. Aoyama, C., Liao, H. and Ishidate, K. (2004). **Structure and function of choline kinase isoforms in mammalian cells.** *Prog. Lipid Res.* **43***(3)*, 266-281

43. Aoyama, C., Ohtani, A. and Ishidate, K. (2002). **Expression and characterization of the active molecular forms of choline/ethanolamine kinase-α and-β in mouse tissues, including carbon tetrachloride-induced liver.** *Biochem. J.* **363**, 777-784

44. Cuadrado, A., Carnero, A., Dolfi, F., Jimenez, B. and Lacal, J. C. (1993). **Phosphorylcholine: A novel second messenger essential for mitogenic activity of growth factors.** *Oncogene.* **8***(11)*, 2959-2968

45. Ramirez de Molina, A., Banez-Coronel, M., Gutierrez, R., Rodriguez-Gonzalez, A., Olmeda, D., Megias, D. and Lacal, J. C. (2004). **Choline kinase activation is a critical requirement for the proliferation of primary human mammary epithelial cells and breast tumor progression.** *Cancer Res.* **64***(18)*, 6732-6739

46. Wu, G., Aoyama, C., Young, S. G. and Vance, D. E. (2008). **Early embryonic lethality caused by disruption of the gene for choline kinase alpha, the first enzyme in phosphatidylcholine biosynthesis.** *J. Biol. Chem.* **283***(3)*, 1456-1462

47. Wu, G., Sher, R. B., Cox, G. A. and Vance, D. E. (2009). **Understanding the muscular dystrophy caused by deletion of choline kinase beta in mice.** *Biochimica et Biophysica Acta (BBA)-Molecular and Cell Biology of Lipids.* **1791***(5)*, 347-356

48. McMaster, C. R. and M Bell, R. (1997). **CDP-choline: 1, 2-diacylglycerol cholinephosphotransferase.** *Biochimica et Biophysica Acta (BBA)-Lipids and Lipid Metabolism.* **1348***(1)*, 100-110

49. Horibata, Y. and Hirabayashi, Y. (2007). **Identification and characterization of human ethanolaminephosphotransferase1.** *J. Lipid Res.* **48***(3)*, 503-508

50. Yang, W., Moroney, J. V. and Moore, T. S. (2004). **Membrane lipid biosynthesis in< i> chlamydomonas reinhardtii: Ethanolaminephosphotransferase is capable of synthesizing both phosphatidylcholine and phosphatidylethanolamine.** *Arch. Biochem. Biophys.* **430***(2)*, 198-209

51. Henneberry, A. L., Wistow, G. and McMaster, C. R. (2000). **Cloning, genomic organization, and characterization of a human cholinephosphotransferase.** *J. Biol. Chem.* **275***(38)*, 29808-29815

52. Subathra, M., Qureshi, A. and Luberto, C. (2011). **Sphingomyelin synthases regulate protein trafficking and secretion.** *PloS one.* **6***(9)*, e23644

53. Jamil, H., Utal, A. K. and Vance, D. E. (1992). **Evidence that cyclic AMP-induced inhibition of phosphatidylcholine biosynthesis is caused by a decrease in cellular diacylglycerol levels in cultured rat hepatocytes.** *J. Biol. Chem.* **267***(3)*, 1752-1760

54. Sriburi, R., Bommiasamy, H., Buldak, G. L., Robbins, G. R., Frank, M., Jackowski, S. and Brewer, J. W. (2007). **Coordinate regulation of phospholipid biosynthesis and secretory pathway gene expression in XBP-1(S)-induced endoplasmic reticulum biogenesis.** *J. Biol. Chem.* **282***(10)*, 7024-7034

55. Lykidis, A., Murti, K. G. and Jackowski, S. (1998). **Cloning and characterization of a second human CTP:Phosphocholine cytidylyltransferase.** *J. Biol. Chem.* **273***(22)*, 14022-14029

56. Tang, W., Keesler, G. A. and Tabas, I. (1997). **The structure of the gene for murine CTP:Phosphocholine cytidylyltransferase, ctpct. relationship of exon structure to functional domains and identification of transcriptional start sites and potential upstream regulatory elements.** *J. Biol. Chem.* **272***(20)*, 13146-13151

57. Karim, M., Jackson, P. and Jackowski, S. (2003). **Gene structure, expression and identification of a new CTP: Phosphocholine cytidylyltransferase β isoform.** *Biochimica et Biophysica Acta (BBA)-Molecular and Cell Biology of Lipids.* **1633***(1)*, 1-12

58. Lykidis, A., Baburina, I. and Jackowski, S. (1999). **Distribution of CTP:Phosphocholine cytidylyltransferase (CCT) isoforms. identification of a new CCTbeta splice variant.** *J. Biol. Chem.* **274***(38)*, 26992-27001

59. Jackowski, S., Rehg, J. E., Zhang, Y. M., Wang, J., Miller, K., Jackson, P. and Karim, M. A. (2004). **Disruption of CCTbeta2 expression leads to gonadal dysfunction.** *Mol. Cell. Biol.* **24***(11)*, 4720-4733

60. Gunter, C., Frank, M., Tian, Y., Murti, K. G., Rehg, J. E. and Jackowski, S. (2007). **Probucol therapy overcomes the reproductive defect in CTP: Phosphocholine cytidylyltransferase β2 knockout mice.** *Biochimica et Biophysica Acta (BBA)-Molecular and Cell Biology of Lipids.* **1771***(7)*, 845-852

61. Ridsdale, R., Tseu, I., Wang, J. and Post, M. (2001). **CTP:Phosphocholine cytidylyltransferase alpha is a cytosolic protein in pulmonary epithelial cells and tissues.** *J. Biol. Chem.* **276***(52)*, 49148-49155

62. Tseu, I., Ridsdale, R., Liu, J., Wang, J. and Post, M. (2002). **Cell cycle regulation of pulmonary phosphatidylcholine synthesis.** *American journal of respiratory cell and molecular biology.* **26***(4)*, 506-515

63. Tian, Y., Zhou, R., Rehg, J. E. and Jackowski, S. (2007). **Role of phosphocholine cytidylyltransferase alpha in lung development.** *Mol. Cell. Biol.* **27***(3)*, 975-982

64. Henderson, F. C., Miakotina, O. L. and Mallampalli, R. K. (2006). **Proapoptotic effects of P. aeruginosa involve inhibition of surfactant phosphatidylcholine synthesis.** *J. Lipid Res.* **47***(10)*, 2314-2324

65. Yao, Z. M. and Vance, D. E. (1988). **The active synthesis of phosphatidylcholine is required for very low density lipoprotein secretion from rat hepatocytes.** *J. Biol. Chem.* **263***(6)*, 2998-3004

66. Jacobs, R. L., Devlin, C., Tabas, I. and Vance, D. E. (2004). **Targeted deletion of hepatic CTP:Phosphocholine cytidylyltransferase alpha in mice decreases plasma high density and very low density lipoproteins.** *J. Biol. Chem.* **279***(45)*, 47402-47410

67. Wang, Y., MacDonald, J. I. and Kent, C. (1995). **Identification of the nuclear localization signal of rat liver CTP:Phosphocholine cytidylyltransferase.** *J. Biol. Chem.* **270***(1)*, 354-360

68. Fagone, P., Gunter, C., Sage, C. R., Gunn, K. E., Brewer, J. W. and Jackowski, S. (2009). **CTP:Phosphocholine cytidylyltransferase alpha is required for B-cell proliferation and class switch recombination.** *J. Biol. Chem.* **284***(11)*, 6847-6854

69. Dennis, M. K., Taneva, S. G. and Cornell, R. B. (2011). **The intrinsically disordered nuclear localization signal and phosphorylation segments distinguish the membrane affinity of two cytidylyltransferase isoforms.** *J. Biol. Chem.* **286***(14)*, 12349-12360

70. Lagace, T. A., Miller, J. R. and Ridgway, N. D. (2002). **Caspase processing and nuclear export of CTP:Phosphocholine cytidylyltransferase alpha during farnesol-induced apoptosis.** *Mol. Cell. Biol.* **22***(13)*, 4851-4862

71. Lagace, T. and Ridgway, N. (2005). **Induction of apoptosis by lipophilic activators of CTP: Phosphocholine cytidylyltransferase alpha (CCTalpha).** *Biochem. J.* **392**, 449-456

72. Kalmar, G. B., Kay, R. J., LaChance, A. C. and Cornell, R. B. (1994). **Primary structure and expression of a human CTP: Phosphocholine cytidylyltransferase.** *Biochimica et Biophysica Acta (BBA)-Gene Structure and Expression.* **1219***(2)*, 328-334

73. Xie, M., Smith, J. L., Ding, Z., Zhang, D. and Cornell, R. B. (2004). **Membrane binding modulates the quaternary structure of CTP:Phosphocholine cytidylyltransferase.** *J. Biol. Chem.* **279***(27)*, 28817-28825

74. Clement, J. M. and Kent, C. (1999). **CTP: Phosphocholine cytidylyltransferase: Insights into regulatory mechanisms and novel functions.** *Biochem. Biophys. Res. Commun.* **257***(3)*, 643-650

75. Helmink, B. A., Braker, J. D., Kent, C. and Friesen, J. A. (2003). **Identification of lysine 122 and arginine 196 as important functional residues of rat CTP: Phosphocholine cytidylyltransferase alpha.** *Biochemistry (N. Y.).* **42***(17)*, 5043-5051

76. Johnson, J. E. and Cornell, R. B. (1994). **Membrane-binding amphipathic. alpha.-helical peptide derived from CTP: Phosphocholine cytidylyltransferase.** *Biochemistry (N. Y.).* **33***(14)*, 4327-4335

77. Cornell, R. B. and Northwood, I. C. (2000). **Regulation of CTP: Phosphocholine cytidylyltransferase by amphitropism and relocalization.** *Trends Biochem. Sci.* **25***(9)*, 441-447

78. Dunne, S. J., Cornell, R. B., Johnson, J. E., Glover, N. R. and Tracey, A. S. (1996). **Structure of the membrane binding domain of CTP: Phosphocholine cytidylyltransferase.** *Biochemistry (N. Y.).* **35***(37)*, 11975-11984

79. Gehrig, K., Morton, C. C. and Ridgway, N. D. (2009). **Nuclear export of the rate-limiting enzyme in phosphatidylcholine synthesis is mediated by its membrane binding domain.** *J. Lipid Res.* **50***(5)*, 966-976

80. Zidovetzki, R., Laptalo, L. and Crawford, J. (1992). **Effect of diacylglycerols on the activity of cobra venom, bee venom, and pig pancreatic phospholipases A2.** *Biochemistry (N. Y.).* **31***(33)*, 7683-7691

81. Wang, Y. and Kent, C. (1995). **Effects of altered phosphorylation sites on the properties of CTP:Phosphocholine cytidylyltransferase.** *J. Biol. Chem.* **270***(30)*, 17843-17849

82. Wieprecht, M., Wieder, T., Paul, C., Geilen, C. C. and Orfanos, C. E. (1996). **Evidence for phosphorylation of CTP:Phosphocholine cytidylyltransferase by multiple proline-directed protein kinases.** *J. Biol. Chem.* **271***(17)*, 9955-9961

83. Banchio, C., Schang, L. M. and Vance, D. E. (2004). **Phosphorylation of Sp1 by cyclin-dependent kinase 2 modulates the role of Sp1 in CTP:Phosphocholine cytidylyltransferase alpha regulation during the S phase of the cell cycle.** *J. Biol. Chem.* **279***(38)*, 40220-40226

84. MacDonald, J. I. and Kent, C. (1994). **Identification of phosphorylation sites in rat liver CTP: Phosphocholine cytidylyltransferase.** *J. Biol. Chem.* **269***(14)*, 10529-10537

85. Houweling, M., Jamil, H., Hatch, G. M. and Vance, D. E. (1994). **Dephosphorylation of CTP-phosphocholine cytidylyltransferase is not required for binding to membranes.** *J. Biol. Chem.* **269***(10)*, 7544-7551

86. Arnold, R. S., DePaoli-Roach, A. A. and Cornell, R. B. (1997). **Binding of CTP: Phosphocholine cytidylyltransferase to lipid vesicles: Diacylglycerol and enzyme dephosphorylation increase the affinity for negatively charged membranes.** *Biochemistry (N. Y.).* **36***(20)*, 6149-6156

87. Bakovic, M., Waite, K. A. and Vance, D. E. (2000). **Functional significance of Sp1, Sp2, and Sp3 transcription factors in regulation of the murine CTP:Phosphocholine cytidylyltransferase alpha promoter.** *J. Lipid Res.* **41***(4)*, 583-594

88. Banchio, C., Schang, L. M. and Vance, D. E. (2003). **Activation of CTP:Phosphocholine cytidylyltransferase alpha expression during the S phase of the cell cycle is mediated by the transcription factor Sp1.** *J. Biol. Chem.* **278***(34)*, 32457-32464

89. Banchio, C., Lingrell, S. and Vance, D. E. (2007). **Sp-1 binds promoter elements that are regulated by retinoblastoma and regulate CTP:Phosphocholine cytidylyltransferase-alpha transcription.** *J. Biol. Chem.* **282***(20)*, 14827-14835

90. Bakovic, M., Waite, K. and Vance, D. E. (2003). **Oncogenic ha-ras transformation modulates the transcription of the CTP:Phosphocholine cytidylyltransferase alpha gene via p42/44MAPK and transcription factor Sp3.** *J. Biol. Chem.* **278***(17)*, 14753-14761

91. Brown, M. S. and Goldstein, J. L. (1997). **The SREBP pathway: Regulation of cholesterol metabolism by proteolysis of a membrane-bound transcription factor.** *Cell.* **89***(3)*, 331-340

92. Foretz, M., Guichard, C., Ferre, P. and Foufelle, F. (1999). **Sterol regulatory element binding protein-1c is a major mediator of insulin action on the hepatic expression of glucokinase and lipogenesis-related genes.** *Proc. Natl. Acad. Sci. U. S. A.* **96***(22)*, 12737-12742

93. Kast, H. R., Nguyen, C. M., Anisfeld, A. M., Ericsson, J. and Edwards, P. A. (2001). **CTP:Phosphocholine cytidylyltransferase, a new sterol- and SREBP-responsive gene.** *J. Lipid Res.* **42***(8)*, 1266-1272

94. Golfman, L. S., Bakovic, M. and Vance, D. E. (2001). **Transcription of the CTP:Phosphocholine cytidylyltransferase alpha gene is enhanced during the S phase of the cell cycle.** *J. Biol. Chem.* **276***(47)*, 43688-43692

95. Jackowski, S. (1994). **Coordination of membrane phospholipid synthesis with the cell cycle.** *J. Biol. Chem.* **269***(5)*, 3858-3867

96. Goldman, R. D., Gruenbaum, Y., Moir, R. D., Shumaker, D. K. and Spann, T. P. (2002). **Nuclear lamins: Building blocks of nuclear architecture.** *Genes Dev.* **16***(5)*, 533-547

97. Houben, F., Ramaekers, F., Snoeckx, L. and Broers, J. (2007). **Role of nuclear lamina-cytoskeleton interactions in the maintenance of cellular strength.** *Biochimica et Biophysica Acta (BBA)-Molecular Cell Research.* **1773***(5)*, 675-686

98. Goldberg, M., Harel, A. and Gruenbaum, Y. (1999). **The nuclear lamina: Molecular organization and interaction with chromatin.** *Critical Reviews™ in Eukaryotic Gene Expression.* **9***(3-4)*

99. RM Verstraeten, V., V Broers, J., S Ramaekers, F. and M van Steensel, M. (2007). **The nuclear envelope, a key structure in cellular integrity and gene expression.** *Curr. Med. Chem.* **14***(11)*, 1231-1248

100. Fricker, M., Hollinshead, M., White, N. and Vaux, D. (1997). **Interphase nuclei of many mammalian cell types contain deep, dynamic, tubular membrane-bound invaginations of the nuclear envelope.** *J. Cell Biol.* **136***(3)*, 531-544

101. Malhas, A., Goulbourne, C. and Vaux, D. J. (2011). **The nucleoplasmic reticulum: Form and function.** *Trends Cell Biol.* **21***(6)*, 362-373

102. Moir, R. D., Spann, T. P., Lopez-Soler, R. I., Yoon, M., Goldman, A. E., Khuon, S. and Goldman, R. D. (2000). **Review: The dynamics of the nuclear lamins during the cell cycle—relationship between structure and function.** *J. Struct. Biol.* **129***(2)*, 324-334

103. Clubb, B. and Locke, M. (1998). **3T3 cells have nuclear invaginations containing F-actin.** *Tissue and Cell.* **30***(6)*, 684-691

104. Prunuske, A. J. and Ullman, K. S. (2006). **The nuclear envelope: Form and reformation.** *Curr. Opin. Cell Biol.* **18***(1)*, 108-116

105. Gehrig, K., Cornell, R. B. and Ridgway, N. D. (2008). **Expansion of the nucleoplasmic reticulum requires the coordinated activity of lamins and CTP:Phosphocholine cytidylyltransferase alpha.** *Mol. Biol. Cell.* **19***(1)*, 237-247

106. Lagace, T. A. and Ridgway, N. D. (2005). **The rate-limiting enzyme in phosphatidylcholine synthesis regulates proliferation of the nucleoplasmic reticulum.** *Mol. Biol. Cell.* **16***(3)*, 1120-1130

107. Gehrig, K. and Ridgway, N. D. (2011). **CTP: Phosphocholine cytidylyltransferase α (CCTα) and lamins alter nuclear membrane structure without affecting phosphatidylcholine synthesis.** *Biochimica et Biophysica Acta (BBA)-Molecular and Cell Biology of Lipids.* **1811***(6)*, 377-385

108. Shanmugathasan, M. and Jothy, S. (2000). **Apoptosis, anoikis and their relevance to the pathobiology of colon cancer.** *Pathol. Int.* **50***(4)*, 273-279

109. Daleke, D. L. (2003). **Regulation of transbilayer plasma membrane phospholipid asymmetry.** *J. Lipid Res.* **44***(2)*, 233-242

110. Janmey, P. and Kinnunen, P. (2006). **Biophysical properties of lipids and dynamic membranes.** *Trends Cell Biol.* **16***(10)*, 538-546

111. Vernier, P. T., Sun, Y., Marcu, L., Salemi, S., Craft, C. M. and Gundersen, M. A. (2003). **Calcium bursts induced by nanosecond electric pulses.** *Biochem. Biophys. Res. Commun.* **310***(2)*, 286-295

112. Martin, S. J., Reutelingsperger, C. P., McGahon, A. J., Rader, J. A., van Schie, R. C., LaFace, D. M. and Green, D. R. (1995). **Early redistribution of plasma membrane phosphatidylserine is a general feature of apoptosis regardless of the initiating stimulus: Inhibition by overexpression of bcl-2 and abl.** *J. Exp. Med.* **182***(5)*, 1545-1556

113. Fadok, V. A., Voelker, D. R., Campbell, P. A., Cohen, J. J., Bratton, D. L. and Henson, P. M. (1992). **Exposure of phosphatidylserine on the surface of apoptotic lymphocytes triggers specific recognition and removal by macrophages.** *J. Immunol.* **148***(7)*, 2207-2216

114. Tuominen, E. K., Wallace, C. J. and Kinnunen, P. K. (2002). **Phospholipid-cytochrome c interaction: Evidence for the extended lipid anchorage.** *J. Biol. Chem.* **277***(11)*, 8822-8826

115. Ott, M., Robertson, J. D., Gogvadze, V., Zhivotovsky, B. and Orrenius, S. (2002). **Cytochrome c release from mitochondria proceeds by a two-step process.** *Proc. Natl. Acad. Sci. U. S. A.* **99***(3)*, 1259-1263

116. Petrosillo, G., Ruggiero, F. M., Pistolese, M. and Paradies, G. (2001). **Reactive oxygen species generated from the mitochondrial electron transport chain induce cytochrome< i> c dissociation from beef-heart submitochondrial particles via cardiolipin peroxidation. possible role in the apoptosis.** *FEBS Lett.* **509***(3)*, 435-438

117. Vladimirov, Y. A., Demin, E., Proskurnina, E. and Osipov, A. (2009). **Lipoperoxide radical production during oxidation of cardiolipin in the complex with cytochrome c.** *Biochemistry (Moscow) Supplement Series A: Membrane and Cell Biology.* **3***(4)*, 467-477

118. Lutter, M., Fang, M., Luo, X., Nishijima, M., Xie, X. and Wang, X. (2000). **Cardiolipin provides specificity for targeting of tBid to mitochondria.** *Nat. Cell Biol.* **2***(10)*, 754-761

119. Logue, S. and Martin, S. (2008). **Caspase activation cascades in apoptosis.** *Biochem. Soc. Trans.* **36**, 1-9

120. Chen, M. and Wang, J. (2002). **Initiator caspases in apoptosis signaling pathways.** *Apoptosis.* **7***(4)*, 313-319

121. Shiozaki, E. N., Chai, J. and Shi, Y. (2002). **Oligomerization and activation of caspase-9, induced by apaf-1 CARD.** *Proc. Natl. Acad. Sci. U. S. A.* **99***(7)*, 4197-4202

122. Thornberry, N. A., Rano, T. A., Peterson, E. P., Rasper, D. M., Timkey, T., Garcia-Calvo, M., Houtzager, V. M., Nordstrom, P. A., Roy, S., Vaillancourt, J. P., Chapman, K. T. and Nicholson, D. W. (1997). **A combinatorial approach defines specificities of members of the caspase family and granzyme B. functional relationships established for key mediators of apoptosis.** *J. Biol. Chem.* **272***(29)*, 17907-17911

123. McStay, G., Salvesen, G. and Green, D. (2007). **Overlapping cleavage motif selectivity of caspases: Implications for analysis of apoptotic pathways.** *Cell Death & Differentiation.* **15***(2)*, 322-331

124. Bodmer, J., Holler, N., Reynard, S., Vinciguerra, P., Schneider, P., Juo, P., Blenis, J. and Tschopp, J. (2000). **TRAIL receptor-2 signals apoptosis through FADD and caspase-8.** *Nat. Cell Biol.* **2***(4)*, 241-243

125. Hockenbery, D. M., Oltvai, Z. N., Yin, X., Milliman, C. L. and Korsmeyer, S. J. (1993). **Bcl-2 functions in an antioxidant pathway to prevent apoptosis.** *Cell.* **75***(2)*, 241-251

126. Yang, E., Zha, J., Jockel, J., Boise, L. H., Thompson, C. B. and Korsmeyer, S. J. (1995). **Bad, a heterodimeric partner for bcl-x< sub> L and bcl-2, displaces bax and promotes cell death.** *Cell.* **80***(2)*, 285-291

127. Masir, N., Jones, M., Abdul-Rahman, F., Florence, C. S. and Mason, D. Y. (2012). **Variation in BCL2 protein expression in follicular lymphomas without t(14;18) chromosomal translocations.** *Pathology.* **44***(3)*, 228-233

128. Negrini, S., Gorgoulis, V. G. and Halazonetis, T. D. (2010). **Genomic instability—an evolving hallmark of cancer.** *Nature reviews Molecular cell biology.* **11***(3)*, 220-228

129. Hanahan, D. and Weinberg, R. A. (2011). **Hallmarks of cancer: The next generation.** *Cell.* **144***(5)*, 646-674

130. Phelps, R. A., Chidester, S., Dehghanizadeh, S., Phelps, J., Sandoval, I. T., Rai, K., Broadbent, T., Sarkar, S., Burt, R. W. and Jones, D. A. (2009). **A two-step model for colon adenoma initiation and progression caused by APC loss.** *Cell.* **137***(4)*, 623-634

131. Smith, G., Carey, F. A., Beattie, J., Wilkie, M. J., Lightfoot, T. J., Coxhead, J., Garner, R. C., Steele, R. J. and Wolf, C. R. (2002). **Mutations in APC, kirsten-ras, and p53--alternative genetic pathways to colorectal cancer.** *Proc. Natl. Acad. Sci. U. S. A.* **99***(14)*, 9433-9438

132. Frisch, S. M. and Francis, H. (1994). **Disruption of epithelial cell-matrix interactions induces apoptosis.** *J. Cell Biol.* **124***(4)*, 619-626

133. Sjaastad, M. D. and Nelson, W. J. (1997). **Integrin-mediated calcium signaling and regulation of cell adhesion by intracellular calcium.** *Bioessays.* **19***(1)*, 47-55

134. Rosen, K., Shi, W., Calabretta, B. and Filmus, J. (2002). **Cell detachment triggers p38 mitogen-activated protein kinase-dependent overexpression of fas ligand. A novel mechanism of anoikis of intestinal epithelial cells.** *J. Biol. Chem.* **277***(48)*, 46123-46130

135. Karin, M. (1998). **Mitogen-activated protein kinase cascades as regulators of stress responses.** *Ann. N. Y. Acad. Sci.* **851***(1)*, 139-146

136. Valentijn, A. J., Metcalfe, A. D., Kott, J., Streuli, C. H. and Gilmore, A. P. (2003). **Spatial and temporal changes in bax subcellular localization during anoikis.** *J. Cell Biol.* **162***(4)*, 599-612

137. Frisch, S. M., Vuori, K., Kelaita, D. and Sicks, S. (1996). **A role for jun-N-terminal kinase in anoikis; suppression by bcl-2 and crmA.** *J. Cell Biol.* **135***(5)*, 1377-1382

138. Simpson, C. D., Anyiwe, K. and Schimmer, A. D. (2008). **Anoikis resistance and tumor metastasis.** *Cancer Lett.* **272***(2)*, 177-185

139. Colicelli, J. (2004). **Human RAS superfamily proteins and related GTPases.** *Sci. STKE.* **2004***(250)*, RE13

140. Marshall, C. J. (1996). **Ras effectors.** *Curr. Opin. Cell Biol.* **8***(2)*, 197-204

141. Barbacid, M. (1987). **Ras genes.** *Annu. Rev. Biochem.* **56***(1)*, 779-827

142. Yan, J., Roy, S., Apolloni, A., Lane, A. and Hancock, J. F. (1998). **Ras isoforms vary in their ability to activate raf-1 and phosphoinositide 3-kinase.** *J. Biol. Chem.* **273***(37)*, 24052-24056

143. Furth, M. E., Aldrich, T. H. and Cordon-Cardo, C. (1987). **Expression of ras proto-oncogene proteins in normal human tissues.** *Oncogene.* **1***(1)*, 47-58

144. Leon, J., Guerrero, I. and Pellicer, A. (1987). **Differential expression of the ras gene family in mice.** *Mol. Cell. Biol.* **7***(4)*, 1535-1540

145. Koera, K., Nakamura, K., Nakao, K., Miyoshi, J., Toyoshima, K., Hatta, T., Otani, H., Aiba, A. and Katsuki, M. (1997). **K-ras is essential for the development of the mouse embryo.** *Oncogene.* **15***(10)*, 1151-1159

146. Campbell, S. L., Khosravi-Far, R., Rossman, K. L., Clark, G. J. and Der, C. J. (1998). **Increasing complexity of ras signaling.** *Oncogene.* **17***(11)*, 1395-1413

147. Khwaja, A., Rodriguez-Viciana, P., Wennstrom, S., Warne, P. H. and Downward, J. (1997). **Matrix adhesion and ras transformation both activate a phosphoinositide 3-OH kinase and protein kinase B/akt cellular survival pathway.** *EMBO J.* **16***(10)*, 2783-2793

148. McFall, A., Ulku, A., Lambert, Q. T., Kusa, A., Rogers-Graham, K. and Der, C. J. (2001). **Oncogenic ras blocks anoikis by activation of a novel effector pathway independent of phosphatidylinositol 3-kinase.** *Mol. Cell. Biol.* **21***(16)*, 5488-5499

149. Reginato, M. J., Mills, K. R., Paulus, J. K., Lynch, D. K., Sgroi, D. C., Debnath, J., Muthuswamy, S. K. and Brugge, J. S. (2003). **Integrins and EGFR coordinately regulate the pro-apoptotic protein bim to prevent anoikis.** *Nat. Cell Biol.* **5***(8)*, 733-740

150. Frankel, A., Rosen, K., Filmus, J. and Kerbel, R. S. (2001). **Induction of anoikis and suppression of human ovarian tumor growth in vivo by down-regulation of bcl-X(L).** *Cancer Res.* **61***(12)*, 4837-4841

151. Rosen, K., Rak, J., Leung, T., Dean, N. M., Kerbel, R. S. and Filmus, J. (2000). **Activated ras prevents downregulation of bcl-X(L) triggered by detachment from the extracellular matrix. A mechanism of ras-induced resistance to anoikis in intestinal epithelial cells.** *J. Cell Biol.* **149***(2)*, 447-456

152. Liu, Z., Li, H., Derouet, M., Filmus, J., LaCasse, E. C., Korneluk, R. G., Kerbel, R. S. and Rosen, K. V. (2005). **Ras oncogene triggers up-regulation of cIAP2 and XIAP in intestinal epithelial cells: Epidermal growth factor receptor-dependent and -independent mechanisms of ras-induced transformation.** *J. Biol. Chem.* **280***(45)*, 37383-37392

153. Yoo, B. H., Wu, X., Li, Y., Haniff, M., Sasazuki, T., Shirasawa, S., Eskelinen, E. L. and Rosen, K. V. (2010). **Oncogenic ras-induced down-regulation of autophagy mediator beclin-1 is required for malignant transformation of intestinal epithelial cells.** *J. Biol. Chem.* **285***(8)*, 5438-5449

154. Vander Heiden, M. G., Cantley, L. C. and Thompson, C. B. (2009). **Understanding the warburg effect: The metabolic requirements of cell proliferation.** *Science.* **324***(5930)*, 1029-1033

155. Gottlob, K., Majewski, N., Kennedy, S., Kandel, E., Robey, R. B. and Hay, N. (2001). **Inhibition of early apoptotic events by akt/PKB is dependent on the first committed step of glycolysis and mitochondrial hexokinase.** *Genes Dev.* **15***(11)*, 1406-1418

156. Christofk, H. R., Vander Heiden, M. G., Harris, M. H., Ramanathan, A., Gerszten, R. E., Wei, R., Fleming, M. D., Schreiber, S. L. and Cantley, L. C. (2008). **The M2 splice isoform of pyruvate kinase is important for cancer metabolism and tumour growth.** *Nature.* **452***(7184)*, 230-233

157. Elstrom, R. L., Bauer, D. E., Buzzai, M., Karnauskas, R., Harris, M. H., Plas, D. R., Zhuang, H., Cinalli, R. M., Alavi, A., Rudin, C. M. and Thompson, C. B. (2004). **Akt stimulates aerobic glycolysis in cancer cells.** *Cancer Res.* **64***(11)*, 3892-3899

158. Bauer, D. E., Hatzivassiliou, G., Zhao, F., Andreadis, C. and Thompson, C. B. (2005). **ATP citrate lyase is an important component of cell growth and transformation.** *Oncogene.* **24***(41)*, 6314-6322

159. Young, C. D. and Anderson, S. M. (2008). **Sugar and fat-that's where it's at: Metabolic changes in tumors.** *Breast Cancer Res.* **10***(1)*, 202

160. Kuhajda, F. P. (2000). **Fatty-acid synthase and human cancer: New perspectives on its role in tumor biology.** *Nutrition.* **16***(3)*, 202-208

161. Menendez, J. A. and Lupu, R. (2007). **Fatty acid synthase and the lipogenic phenotype in cancer pathogenesis.** *Nature Reviews Cancer.* **7***(10)*, 763-777

162. Swinnen, J. V., Van Veldhoven, P. P., Timmermans, L., De Schrijver, E., Brusselmans, K., Vanderhoydonc, F., Van de Sande, T., Heemers, H., Heyns, W. and Verhoeven, G. (2003). **Fatty acid synthase drives the synthesis of phospholipids partitioning into detergent-resistant membrane microdomains.** *Biochem. Biophys. Res. Commun.* **302***(4)*, 898-903

163. Liang, G., Yang, J., Horton, J. D., Hammer, R. E., Goldstein, J. L. and Brown, M. S. (2002). **Diminished hepatic response to fasting/refeeding and liver X receptor agonists in mice with selective deficiency of sterol regulatory element-binding protein-1c.** *J. Biol. Chem.* **277***(11)*, 9520-9528

164. Horton, J. D., Shah, N. A., Warrington, J. A., Anderson, N. N., Park, S. W., Brown, M. S. and Goldstein, J. L. (2003). **Combined analysis of oligonucleotide microarray data from transgenic and knockout mice identifies direct SREBP target genes.** *Proc. Natl. Acad. Sci. U. S. A.* **100***(21)*, 12027-12032

165. Thupari, J. N., Pinn, M. L. and Kuhajda, F. P. (2001). **Fatty acid synthase inhibition in human breast cancer cells leads to malonyl-CoA-induced inhibition of fatty acid oxidation and cytotoxicity.** *Biochem. Biophys. Res. Commun.* **285***(2)*, 217-223

166. Pelech, S. L., Pritchard, P. H., Brindley, D. N. and Vance, D. E. (1983). **Fatty acids promote translocation of CTP:Phosphocholine cytidylyltransferase to the endoplasmic reticulum and stimulate rat hepatic phosphatidylcholine synthesis.** *J. Biol. Chem.* **258***(11)*, 6782-6788

167. Cornell, R. and Vance, D. E. (1987). **Translocation of CTP: Phosphocholine cytidylyltransferase from cytosol to membranes in HeLa cells: Stimulation by fatty acid, fatty alcohol, mono-and diacylglycerol.** *Biochimica et Biophysica Acta (BBA)-Lipids and Lipid Metabolism.* **919***(1)*, 26-36

168. De Schrijver, E., Brusselmans, K., Heyns, W., Verhoeven, G. and Swinnen, J. V. (2003). **RNA interference-mediated silencing of the fatty acid synthase gene attenuates growth and induces morphological changes and apoptosis of LNCaP prostate cancer cells.** *Cancer Res.* **63***(13)*, 3799-3804

169. Zhou, W., Simpson, P. J., McFadden, J. M., Townsend, C. A., Medghalchi, S. M., Vadlamudi, A., Pinn, M. L., Ronnett, G. V. and Kuhajda, F. P. (2003). **Fatty acid synthase inhibition triggers apoptosis during S phase in human cancer cells.** *Cancer Res.* **63***(21)*, 7330-7337

170. Menendez, J. A., Mehmi, I., Atlas, E., Colomer, R. and Lupu, R. (2004). **Novel signaling molecules implicated in tumor-associated fatty acid synthase-dependent breast cancer cell proliferation and survival: Role of exogenous dietary fatty acids, p53-p21WAF1/CIP1, ERK1/2 MAPK, p27KIP1, BRCA1, and NF-κB.** *Int. J. Oncol.* **24***(3)*, 591-608

171. Aboagye, E. O. and Bhujwalla, Z. M. (1999). **Malignant transformation alters membrane choline phospholipid metabolism of human mammary epithelial cells.** *Cancer Res.* **59***(1)*, 80-84

172. Exton, J. H. (1998). **Phospholipid-Derived second messengers.** *Comprehensive Physiology.*

173. Daly, P. F., Lyon, R. C., Faustino, P. J. and Cohen, J. S. (1987). **Phospholipid metabolism in cancer cells monitored by 31P NMR spectroscopy.** *J. Biol. Chem.* **262***(31)*, 14875-14878

174. Glunde, K., Ackerstaff, E., Mori, N., Jacobs, M. A. and Bhujwalla, Z. M. (2006). **Choline phospholipid metabolism in cancer: Consequences for molecular pharmaceutical interventions.** *Molecular pharmaceutics.* **3***(5)*, 496-506

175. Yamashita, S., Yamashita, J., Sakamoto, K., Inada, K., Nakashima, Y., Murata, K., Saishoji, T., Nomura, K. and Ogawa, M. (1993). **Increased expression of membrane-associated phospholipase A2 shows malignant potential of human breast cancer cells.** *Cancer.* **71***(10)*, 3058-3064

176. Kassis, J., Moellinger, J., Lo, H., Greenberg, N. M., Kim, H. G. and Wells, A. (1999). **A role for phospholipase C-gamma-mediated signaling in tumor cell invasion.** *Clin. Cancer Res.* **5***(8)*, 2251-2260

177. Bjorkoy, G., Overvatn, A., Diaz-Meco, M. T., Moscat, J. and Johansen, T. (1995). **Evidence for a bifurcation of the mitogenic signaling pathway activated by ras and phosphatidylcholine-hydrolyzing phospholipase C.** *J. Biol. Chem.* **270***(36)*, 21299-21306

178. Eliyahu, G., Kreizman, T. and Degani, H. (2007). **Phosphocholine as a biomarker of breast cancer: Molecular and biochemical studies.** *International journal of cancer.* **120***(8)*, 1721-1730

179. Inazu, M., Yamada, T., Kubota, N. and Yamanaka, T. (2013). **Functional expression of choline transporter-like protein 1 (CTL1) in small cell lung carcinoma cells: A target molecule for lung cancer therapy.** *Pharmacological Research.* **76**, 119-131

180. Glunde, K., Shah, T., Winnard, P. T.,Jr, Raman, V., Takagi, T., Vesuna, F., Artemov, D. and Bhujwalla, Z. M. (2008). **Hypoxia regulates choline kinase expression through hypoxia-inducible factor-1 alpha signaling in a human prostate cancer model.** *Cancer Res.* **68***(1)*, 172-180

181. Hernandez-Alcoceba, R., Saniger, L., Campos, J., Nunez, M. C., Khaless, F., Gallo, M. A., Espinosa, A. and Lacal, J. C. (1997). **Choline kinase inhibitors as a novel approach for antiproliferative drug design.** *Oncogene.* **15***(19)*, 2289-2301

182. Yalcin, A., Clem, B., Makoni, S., Clem, A., Nelson, K., Thornburg, J., Siow, D., Lane, A., Brock, S. and Goswami, U. (2009). **Selective inhibition of choline kinase simultaneously attenuates MAPK and PI3K/AKT signaling.** *Oncogene.* **29***(1)*, 139-149

183. Ramírez de Molina, A., Gallego-Ortega, D., Sarmentero-Estrada, J., Lagares, D., Gómez del Pulgar, T., Bandrés, E., García-Foncillas, J. and Lacal, J. C. (2008). **Choline kinase as a link connecting phospholipid metabolism and cell cycle regulation: Implications in cancer therapy.** *Int. J. Biochem. Cell Biol.* **40***(9)*, 1753-1763

184. Ghosh, A., Akech, J., Mukherjee, S. and Das, S. K. (2002). **Differential expression of cholinephosphotransferase in normal and cancerous human mammary epithelial cells.** *Biochem. Biophys. Res. Commun.* **297***(4)*, 1043-1048

185. Ros, S., Santos, C. R., Moco, S., Baenke, F., Kelly, G., Howell, M., Zamboni, N. and Schulze, A. (2012). **Functional metabolic screen identifies 6-phosphofructo-2-kinase/fructose-2,6-biphosphatase 4 as an important regulator of prostate cancer cell survival.** *Cancer. Discov.* **2***(4)*, 328-343

186. Bayet-Robert, M., Morvan, D., Chollet, P. and Barthomeuf, C. (2010). **Pharmacometabolomics of docetaxel-treated human MCF7 breast cancer cells provides evidence of varying cellular responses at high and low doses.** *Breast Cancer Res. Treat.* **120***(3)*, 613-626

187. Arsenault, D. J., Yoo, B. H., Rosen, K. V. and Ridgway, N. D. (2013). **Ras-induced up-regulation of CTP:Phosphocholine cytidylyltransferase alpha contributes to malignant transformation of intestinal epithelial cells.** *J. Biol. Chem.* **288***(1)*, 633-643

188. Yen, C. L., Mar, M. H. and Zeisel, S. H. (1999). **Choline deficiency-induced apoptosis in PC12 cells is associated with diminished membrane phosphatidylcholine and sphingomyelin, accumulation of ceramide and diacylglycerol, and activation of a caspase.** *FASEB J.* **13***(1)*, 135-142

189. Miquel, K., Pradines, A., Terce, F., Selmi, S. and Favre, G. (1998). **Competitive inhibition of choline phosphotransferase by geranylgeraniol and farnesol inhibits phosphatidylcholine synthesis and induces apoptosis in human lung adenocarcinoma A549 cells.** *J. Biol. Chem.* **273***(40)*, 26179-26186

190. Araki, W. and Wurtman, R. J. (1997). **Control of membrane phosphatidylcholine biosynthesis by diacylglycerol levels in neuronal cells undergoing neurite outgrowth.** *Proc. Natl. Acad. Sci. U. S. A.* **94***(22)*, 11946-11950

191. Wright, M. M., Henneberry, A. L., Lagace, T. A., Ridgway, N. D. and McMaster, C. R. (2001). **Uncoupling farnesol-induced apoptosis from its inhibition of phosphatidylcholine synthesis.** *J. Biol. Chem.* **276***(27)*, 25254-25261

192. Cui, Z., Houweling, M., Chen, M. H., Record, M., Chap, H., Vance, D. E. and Terce, F. (1996). **A genetic defect in phosphatidylcholine biosynthesis triggers apoptosis in chinese hamster ovary cells.** *J. Biol. Chem.* **271***(25)*, 14668-14671

193. Morton, C. C., Aitchison, A. J., Gehrig, K. and Ridgway, N. D. (2013). **A mechanism for suppression of the CDP-choline pathway during apoptosis.** *J. Lipid Res.* **54***(12)*, 3373-3384

194. Thiele, C. and Spandl, J. (2008). **Cell biology of lipid droplets.** *Curr. Opin. Cell Biol.* **20***(4)*, 378-385

195. Brasaemle, D. L. and Wolins, N. E. (2012). **Packaging of fat: An evolving model of lipid droplet assembly and expansion.** *J. Biol. Chem.* **287***(4)*, 2273-2279

196. Walther, T. C. and Farese, R. V.,Jr. (2012). **Lipid droplets and cellular lipid metabolism.** *Annu. Rev. Biochem.* **81**, 687-714

197. Daniel, J., Maamar, H., Deb, C., Sirakova, T. D. and Kolattukudy, P. E. (2011). **Mycobacterium tuberculosis uses host triacylglycerol to accumulate lipid droplets and acquires a dormancy-like phenotype in lipid-loaded macrophages.** *PLoS pathogens.* **7***(6)*, e1002093

198. Bartz, R., Zehmer, J. K., Zhu, M., Chen, Y., Serrero, G., Zhao, Y. and Liu, P. (2007). **Dynamic activity of lipid droplets: Protein phosphorylation and GTP-mediated protein translocation.** *Journal of proteome research.* **6***(8)*, 3256-3265

199. Chanderbhan, R., Noland, B. J., Scallen, T. J. and Vahouny, G. V. (1982). **Sterol carrier protein2. delivery of cholesterol from adrenal lipid droplets to mitochondria for pregnenolone synthesis.** *J. Biol. Chem.* **257***(15)*, 8928-8934

200. Krahmer, N., Farese Jr, R. V. and Walther, T. C. (2013). **Balancing the fat: Lipid droplets and human disease.** *EMBO molecular medicine.* **5***(7)*, 973-983

201. Fujimoto, T., Ohsaki, Y., Cheng, J., Suzuki, M. and Shinohara, Y. (2008). **Lipid droplets: A classic organelle with new outfits.** *Histochem. Cell Biol.* **130***(2)*, 263-279

202. Kuerschner, L., Moessinger, C. and Thiele, C. (2008). **Imaging of lipid biosynthesis: How a neutral lipid enters lipid droplets.** *Traffic.* **9***(3)*, 338-352

203. Thiam, A. R., Farese Jr, R. V. and Walther, T. C. (2013). **The biophysics and cell biology of lipid droplets.** *Nature Reviews Molecular Cell Biology.* **14***(12)*, 775-786

204. Walther, T. C. and Farese Jr, R. V. (2009). **The life of lipid droplets.** *Biochimica et Biophysica Acta (BBA)-Molecular and Cell Biology of Lipids.* **1791***(6)*, 459-466

205. Ploegh, H. L. (2007). **A lipid-based model for the creation of an escape hatch from the endoplasmic reticulum.** *Nature.* **448***(7152)*, 435-438

206. Szymanski, K. M., Binns, D., Bartz, R., Grishin, N. V., Li, W. P., Agarwal, A. K., Garg, A., Anderson, R. G. and Goodman, J. M. (2007). **The lipodystrophy protein seipin is found at endoplasmic reticulum lipid droplet junctions and is important for droplet morphology.** *Proc. Natl. Acad. Sci. U. S. A.* **104***(52)*, 20890-20895

207. Brasaemle, D. L., Levin, D. M., Adler-Wailes, D. C. and Londos, C. (2000). **The lipolytic stimulation of 3T3-L1 adipocytes promotes the translocation of hormone-sensitive lipase to the surfaces of lipid storage droplets.** *Biochimica et Biophysica Acta (BBA)-Molecular and Cell Biology of Lipids.* **1483***(2)*, 251-262

208. Greenberg, A. S., Shen, W. J., Muliro, K., Patel, S., Souza, S. C., Roth, R. A. and Kraemer, F. B. (2001). **Stimulation of lipolysis and hormone-sensitive lipase via the extracellular signal-regulated kinase pathway.** *J. Biol. Chem.* **276***(48)*, 45456-45461

209. Donaldson, J. G. and Jackson, C. L. (2011). **ARF family G proteins and their regulators: Roles in membrane transport, development and disease.** *Nature reviews Molecular cell biology.* **12***(6)*, 362-375

210. Wendel, A. A., Lewin, T. M. and Coleman, R. A. (2009). **Glycerol-3-phosphate acyltransferases: Rate limiting enzymes of triacylglycerol biosynthesis.** *Biochimica et Biophysica Acta (BBA)-Molecular and Cell Biology of Lipids.* **1791***(6)*, 501-506

211. Bozza, P. T. and Viola, J. P. (2010). **Lipid droplets in inflammation and cancer.** *Prostaglandins, Leukotrienes and Essential Fatty Acids (PLEFA).* **82***(4)*, 243-250

212. Beller, M., Riedel, D., Jansch, L., Dieterich, G., Wehland, J., Jackle, H. and Kuhnlein, R. P. (2006). **Characterization of the drosophila lipid droplet subproteome.** *Mol. Cell. Proteomics.* **5***(6)*, 1082-1094

213. Stone, S. J., Levin, M. C., Zhou, P., Han, J., Walther, T. C. and Farese, R. V.,Jr. (2009). **The endoplasmic reticulum enzyme DGAT2 is found in mitochondria-associated membranes and has a mitochondrial targeting signal that promotes its association with mitochondria.** *J. Biol. Chem.* **284***(8)*, 5352-5361

214. Tauchi-Sato, K., Ozeki, S., Houjou, T., Taguchi, R. and Fujimoto, T. (2002). **The surface of lipid droplets is a phospholipid monolayer with a unique fatty acid composition.** *J. Biol. Chem.* **277***(46)*, 44507-44512

215. Fei, W., Shui, G., Zhang, Y., Krahmer, N., Ferguson, C., Kapterian, T. S., Lin, R. C., Dawes, I. W., Brown, A. J. and Li, P. (2011). **A role for phosphatidic acid in the formation of "supersized" lipid droplets.** *PLoS genetics.* **7***(7)*, e1002201

216. Adeyo, O., Horn, P. J., Lee, S., Binns, D. D., Chandrahas, A., Chapman, K. D. and Goodman, J. M. (2011). **The yeast lipin orthologue Pah1p is important for biogenesis of lipid droplets.** *J. Cell Biol.* **192***(6)*, 1043-1055

217. Saito, H., Kawagishi, A., Tanaka, M., Tanimoto, T., Okada, S., Komatsu, H. and Handa, T. (1999). **Coalescence of lipid emulsions in floating and freeze–thawing processes: Examination of the coalescence transition state theory.** *J. Colloid Interface Sci.* **219***(1)*, 129-134

218. Krahmer, N., Guo, Y., Wilfling, F., Hilger, M., Lingrell, S., Heger, K., Newman, H. W., Schmidt-Supprian, M., Vance, D. E. and Mann, M. (2011). **Phosphatidylcholine synthesis for lipid droplet expansion is mediated by localized activation of CTP: Phosphocholine cytidylyltransferase.** *Cell metabolism.* **14***(4)*, 504-515

219. Levine, T. and Loewen, C. (2006). **Inter-organelle membrane contact sites: Through a glass, darkly.** *Curr. Opin. Cell Biol.* **18***(4)*, 371-378

220. Toulmay, A. and Prinz, W. A. (2011). **Lipid transfer and signaling at organelle contact sites: The tip of the iceberg.** *Curr. Opin. Cell Biol.* **23***(4)*, 458-463

221. Dawson, R. M. (1973). **The exchange of phospholipids between cell membranes.** *Subcell. Biochem.* **2***(1)*, 69-89

222. Lev, S. (2010). **Non-vesicular lipid transport by lipid-transfer proteins and beyond.** *Nature Reviews Molecular Cell Biology.* **11***(10)*, 739-750

223. Pol, A., Gross, S. P. and Parton, R. G. (2014). **Review: Biogenesis of the multifunctional lipid droplet: Lipids, proteins, and sites.** *J. Cell Biol.* **204***(5)*, 635-646

224. Horl, G., Wagner, A., Cole, L. K., Malli, R., Reicher, H., Kotzbeck, P., Kofeler, H., Hofler, G., Frank, S., Bogner-Strauss, J. G., Sattler, W., Vance, D. E. and Steyrer, E. (2011). **Sequential synthesis and methylation of phosphatidylethanolamine promote lipid droplet biosynthesis and stability in tissue culture and in vivo.** *J. Biol. Chem.* **286***(19)*, 17338-17350

225. Guo, Y., Walther, T. C., Rao, M., Stuurman, N., Goshima, G., Terayama, K., Wong, J. S., Vale, R. D., Walter, P. and Farese, R. V. (2008). **Functional genomic screen reveals genes involved in lipid-droplet formation and utilization.** *Nature.* **453***(7195)*, 657-661

226. Sriburi, R., Jackowski, S., Mori, K. and Brewer, J. W. (2004). **XBP1: A link between the unfolded protein response, lipid biosynthesis, and biogenesis of the endoplasmic reticulum.** *J. Cell Biol.* **167***(1)*, 35-41

227. Atsumi, G., Murakami, M., Kojima, K., Hadano, A., Tajima, M. and Kudo, I. (2000). **Distinct roles of two intracellular phospholipase A2s in fatty acid release in the cell death pathway. proteolytic fragment of type IVA cytosolic phospholipase A2alpha inhibits stimulus-induced arachidonate release, whereas that of type VI Ca2+-independent phospholipase A2 augments spontaneous fatty acid release.** *J. Biol. Chem.* **275***(24)*, 18248-18258

228. Anthony, M. L., Zhao, M. and Brindle, K. M. (1999). **Inhibition of phosphatidylcholine biosynthesis following induction of apoptosis in HL-60 cells.** *J. Biol. Chem.* **274***(28)*, 19686-19692

229. Germain, M., Affar, E. B., D'Amours, D., Dixit, V. M., Salvesen, G. S. and Poirier, G. G. (1999). **Cleavage of automodified poly(ADP-ribose) polymerase during apoptosis. evidence for involvement of caspase-7.** *J. Biol. Chem.* **274***(40)*, 28379-28384

230. Mallampalli, R. K., Ryan, A. J., Salome, R. G. and Jackowski, S. (2000). **Tumor necrosis factor-alpha inhibits expression of CTP:Phosphocholine cytidylyltransferase.** *J. Biol. Chem.* **275***(13)*, 9699-9708

231. Glunde, K., Raman, V., Mori, N. and Bhujwalla, Z. M. (2005). **RNA interference-mediated choline kinase suppression in breast cancer cells induces differentiation and reduces proliferation.** *Cancer Res.* **65***(23)*, 11034-11043

232. Liu, Z., Li, H., Wu, X., Yoo, B., Yan, S., Stadnyk, A., Sasazuki, T., Shirasawa, S., LaCasse, E. and Korneluk, R. (2006). **Detachment-induced upregulation of XIAP and cIAP2 delays anoikis of intestinal epithelial cells.** *Oncogene.* **25***(59)*, 7680-7690

233. Yoo, B. H., Berezkin, A., Wang, Y., Zagryazhskaya, A. and Rosen, K. V. (2012). **Tumor suppressor protein kinase Chk2 is a mediator of anoikis of intestinal epithelial cells.** *International Journal of Cancer.* **131***(2)*, 357-366

234. Bos, J. L. (1989). **Ras oncogenes in human cancer: A review.** *Cancer Res.* **49***(17)*, 4682-4689

235. Ostrem, J. M., Peters, U., Sos, M. L., Wells, J. A. and Shokat, K. M. (2013). **K-ras (G12C) inhibitors allosterically control GTP affinity and effector interactions.** *Nature.* **503***(7477)*, 548-551

236. English, J. M. and Cobb, M. H. (2002). **Pharmacological inhibitors of MAPK pathways.** *Trends Pharmacol. Sci.* **23***(1)*, 40-45

237. Ratnam, S. and Kent, C. (1995). **Early increase in choline kinase activity upon induction of the H-< i> ras oncogene in mouse fibroblast cell lines.** *Arch. Biochem. Biophys.* **323***(2)*, 313-322

238. Teegarden, D., Taparowsky, E. J. and Kent, C. (1990). **Altered phosphatidylcholine metabolism in C3H10T1/2 cells transfected with the harvey-ras oncogene.** *J. Biol. Chem.* **265***(11)*, 6042-6047

239. Rush, J. S., Sweitzer, T., Kent, C., Decker, G. L. and Waechter, C. J. (1991). **Biogenesis of the endoplasmic reticulum in activated B lymphocytes: Temporal relationships between the induction of protein N-glycosylation activity and the biosynthesis of membrane protein and phospholipid.** *Arch. Biochem. Biophys.* **284***(1)*, 63-70

240. Schuck, S., Prinz, W. A., Thorn, K. S., Voss, C. and Walter, P. (2009). **Membrane expansion alleviates endoplasmic reticulum stress independently of the unfolded protein response.** *J. Cell Biol.* **187***(4)*, 525-536

241. Romero-Ramirez, L., Cao, H., Nelson, D., Hammond, E., Lee, A. H., Yoshida, H., Mori, K., Glimcher, L. H., Denko, N. C., Giaccia, A. J., Le, Q. T. and Koong, A. C. (2004). **XBP1 is essential for survival under hypoxic conditions and is required for tumor growth.** *Cancer Res.* **64***(17)*, 5943-5947

242. Tsien, R. Y. (1998). **The green fluorescent protein.** *Annu. Rev. Biochem.* **67***(1)*, 509-544

243. Rizzatti, V., Boschi, F., Pedrotti, M., Zoico, E., Sbarbati, A. and Zamboni, M. (2013). **Lipid droplets characterization in adipocyte differentiated 3T3-L1 cells: Size and optical density distribution.** *Eur. J. Histochem.* **57***(3)*, e24

244. Lisenbee, C. S., Karnik, S. K. and Trelease, R. N. (2003). **Overexpression and mislocalization of a Tail-Anchored GFP redefines the identity of peroxisomal ER.** *Traffic.* **4***(7)*, 491-501

245. Huh, W., Falvo, J. V., Gerke, L. C., Carroll, A. S., Howson, R. W., Weissman, J. S. and O'Shea, E. K. (2003). **Global analysis of protein localization in budding yeast.** *Nature.* **425***(6959)*, 686-691

246. Versantvoort, C. H., Ondrewater, R. C., Duizer, E., Van de Sandt, Johannes JM, Gilde, A. J. and Groten, J. P. (2002). **Monolayers of IEC-18 cells as an in vitro model for screening the passive transcellular and paracellular transport across the intestinal barrier: Comparison of active and passive transport with the human colon carcinoma caco-2 cell line.** *Environ. Toxicol. Pharmacol.* **11***(3)*, 335-344

247. Tso, P. and Balint, J. A. (1986). **Formation and transport of chylomicrons by enterocytes to the lymphatics.** *Am. J. Physiol.* **250***(6 Pt 1)*, G715-26

248. Mardani, M., Rezapour, S. and Higgins, J. A. (2011). **Investigation of the assembly of chylomicrons in hamster enterocytes using pluronic-L81 acid as a probe.** *Acta Med. Iran.* **49***(6)*, 341-351